Tsutomu HORI and Manami HORI
(Nagasaki Institute of Applied Science, Japan) July 2023, pp. 1~104

Theoretical Hydrostatics of Floating Bodies
— New Developments on the Center of Buoyancy, the Metacentric Radius and the Hydrostatic Stability —

by Tsutomu HORI † and Manami HORI ††

Summary

This paper presents new developments in the fundamental theory for the hydrostatics of floating bodies, such as a ship. In it, we show that a proof that the center of buoyancy is equal to the center of hydrostatic pressure, a new derivation of the metacenter radius, and theoretical treatments of the hydrostatic stability of floating bodies based on the above two new theories.

In Chapter 1, we prove that "the center of buoyancy of a ship is equal to the center of hydrostatic pressure". This subject is an unsolved problem in physics and naval architecture, even though the buoyancy taught by Archimedes' principle can be obtained clearly by the surface integral of hydrostatic pressure. As a breakthrough, we dared to create the left-right asymmetric pressure field by inclining the ship with heel angle θ. In that state, the force and moment due to hydrostatic pressure were calculated correctly with respect to the tilted coordinate system fixed to the floating body. By doing so, we succeeded in determining the center of pressure for the shape of rectangular and arbitrary cross-sections. Then, by setting the heel angle θ to zero, it was proved that the center of hydrostatic pressure is equal to the well-known center of buoyancy, *i.e.*, the centroid of the cross-sectional area under the water surface in the upright state. Furthermore, we show an extension to the center of buoyancy for a 3-D floating body.

In Chapter 2, we develop a new theory on the derivation of the transverse metacentric radius which governs the hydrostatic stability of ships. As a new development in its derivation process, it was shown that the direction of movement of the center of buoyancy due to lateral inclination of ship is the direction of the half angle $\frac{\theta}{2}$ of the heel angle θ. By finding it, we were able to derive a metacentric radius worthy of its name by showing that the metacentric radius correctly represents the radius centered on the metacenter, which is the center of inclination.

---

† *Professor Emeritus*, HORI's Laboratory of Ship Waves and Hydrostatic Stability, Nagasaki Institute of Applied Science, Japan

†† *Jewel Manami HORI of Five Stars JP,* Daughter of †

viXra : 2307.0154 *Classical Physics*
Submitted : 28 July 2023 (Ver. 1)
Replaced : 3 November 2023 (Ver. 2 : Four Appendices are added.)
Replaced : 20 December 2023 (Ver. 3)
Replaced : 15 February 2024 (Ver. 4)

E-mail : milky-jun_0267.h@mxb.cncm.ne.jp
HomePage : http://www2.cncm.ne.jp/~milky-jun_0267.h/HORI-Lab/ *(in Japanese)*

Theoretical Hydrostatics of Floating Bodies
— New Developments on the Center of Buoyancy, the Metacentric Radius and the Hydrostatic Stability —

by Tsutomu HORI and Manami HORI

In Chapters 3 and 4, theoretical treatments on the hydrostatic stability of ships are presented. As the simplest hull form, a columnar ship with rectangular cross-section, which is made of homogeneous squared timber with arbitrary breadth and arbitrary material, is chosen. In Chapter 3, the conditions under which the ship is stable in the upright state with horizontal deck are analyzed by means of ship's hydrostatics. And in Chapter 4, the stable attitude in an inclined state of the ship, which is not stable in the upright state with horizontal deck, is analyzed. By doing so, the dependence of the stable conditions and of the inclined attitude on the breadth and material of the ship will be clarified.

In Appendices, we prove that the center of hydrostatic pressure is equal to the well-known center of buoyancy for four shapes separately which are a triangular prism and a semi-submerged circular cylinder as floating bodies, and a submerged circular cylinder and an arbitrary shaped submerged body as submerged bodies.

We would like to report all of you smart readers about the new developments on the theoretical hydrostatics of floating bodies.

Keywords

Center of Buoyancy, Hydrostatic Pressure, Archimedes' Principle, Surface Integral, Gauss's Integral Theorem, Inclined Ship, Heel Angle, Metacentric Radius, Hydrostatic Stability, Floating Bodies, Stable Conditions, Upright State, Stable Attitude, Inclined State

Theoretical Hydrostatics of Floating Bodies
— New Developments on the Center of Buoyancy, the Metacentric Radius and the Hydrostatic Stability —

by Tsutomu HORI and Manami HORI

Contents

Theoretical Hydrostatics of Floating Bodies
— New Developments on the Center of Buoyancy, the Metacentric Radius and the Hydrostatic Stability — *by Tsutomu HORI and Manami HORI*

Appendices

Chapter 1
Proof that the Center of Buoyancy is Equal to the Center of Pressure by means of the Surface Integral of Hydrostatic Pressure

In this Chapter 1, we prove that "the center of buoyancy of a ship is equal to the center of hydrostatic pressure". This subject is an unsolved problem in physics and naval architecture, even though the buoyancy taught by Archimedes' principle[(1)] can be obtained clearly by the surface integral of hydrostatic pressure. Then we thought that the reason why the vertical position of the center of pressure could not be determined was that the horizontal force would be zero due to equilibrium in the upright state.

As a breakthrough, we dared to assume the left-right asymmetric pressure field by inclining the ship with heel angle θ. In that state, the force and moment due to hydrostatic pressure were calculated correctly with respect to the tilted coordinate system fixed to the floating body. By doing so, we succeeded in determining the center of pressure.

Then, by setting the heel angle θ to zero in order to make it upright state, it was proved that the center of hydrostatic pressure is equal to the well-known center of buoyancy, *i.e.*, the centroid of the cross-sectional area under the water surface.

Specifically, the above proof is first shown for a rectangular cross-section, and then for an arbitrary shape of floating body by applying Gauss's integral theorem. Furthermore, we show an extension to the center of buoyancy for a 3-D floating body.

1.1 Introduction

It is a well-known fact in physics and naval architecture that the position of "Center of Buoyancy" acting on a ship is equal to the center of the volume of the geometric shape under the water surface.

The buoyancy taught by Archimedes' principle[(1)] is clearly obtained by the surface integral of the hydrostatic pressure, but the position of the center of buoyancy is described in every textbook (on physics[(2)], fluid dynamics[(3),(4)], hydraulics[(5)], naval architecture[(6),(7-a),(7-b),(8-a),(9-a),(10),(11-a)] and nautical mechanics[(12-a)], *etc.*) as the center of gravity where the volume under the water surface is replaced by water. There is no explanation that it is the center of pressure due to hydrostatic pressure[(13),(14)].

Recently, Komatsu[(15)] raised the issue of "the center of buoyancy ≠ the center of pressure?" at 2007 in Japan, and it was actively discussed by Seto[(16),(17)], Suzuki[(18)], Yoshimura and Yasukawa[(19)], Komatsu[(20)], Yabushita and Watanabe[(21)] and others in research committees and academic meetings of the Japan Society of Naval Architects and Ocean Engineers (hereinafter abbreviated as *JASNAOE*). At the same time, in Europe, the problem was studied in detail by Mégel and Kliava[(22),(23)] in terms of potential energy. However, no one was able to solve this issue.

On the other hand, it is also an indisputable fact that the well-known center of buoyancy (*i.e.* the volume center of the underwater portion) is correct from the viewpoint of ship's stability (that is to say, the positioning of the metacenter by calculating the metacentric radius $\overline{BM}$, as shown in Chapters 2 and 3).

In response to this unsolved problem, we considered that the reason why the vertical center of pressure could not be determined was because the horizontal forces equilibrated to zero in the upright state. To solve this problem, Hori[24),(25)] dared to create the left-right asymmetric pressure field by inclining the ship with heel angle θ, and attempted in 2018 to integrate the hydrostatic pressure acting on the ship surface. Then, the forces and moments acting on the inclined ship were calculated correctly with respect to a tilted coordinate system fixed to the ship. In this case, both orthogonal components of the force acting on the ship are not zero. Therefore, it was shown that the center of pressure at the inclined state can be determined. By setting the heel angle θ to zero, we proved that the center of hydrostatic pressure coincides with the centroid of cross-sectional area under the water surface in the upright state, *i.e.*, the well-known center of buoyancy. First, a columnar ship with the rectangular cross-section[24)] was proved. And then an arbitrary cross-sectional shape[25)] was proved and published in the Journal "*NAVIGATION*" of Japan Institute of Navigation (hereinafter abbreviated as *JIN*).

For this problem, Yabushita[26)] showed that the center of buoyancy is the center of pressure by tilting the direction of gravity from the vertical direction in his text book. Later, Yabushita *et al.*[27)] showed that the same conclusion can be obtained by tilting only the coordinate system, not by tilting the floating body or direction of gravity [2nd half of 28)]. Furthermore, Suzuki[29)] gave a detailed examination of Hori's theory[24)]. On the other hand, Komatsu[30)] performed an analysis in which only the vertical buoyant component was extracted from the hydrostatic pressure acting on the surface of the laterally inclined floating body, as shown by Hori[24)]. As a result, he claimed that the center of action of buoyancy is different from the well-known center of buoyancy. Also, Yabushita[31)] *et al.* attempted an elaborate analysis in terms of the potential energy of buoyancy, which is adopted by Mégel and Kliava[22),(23)], and showed that the height of the center of buoyancy is equal to the conventional position of the center of buoyancy. In this way, as many researchers are studying this issue with various approaches, the discussions have deepened in *JASNAOE*.

To sublate these discussions, we have illustrated that "the center of buoyancy is equal to the center of pressure" for a semi-submerged circular cylinder [1st half of 28)] and a submerged circular cylinder[32)] which does not change its shape under the water even if it is inclined, and for a triangular prism[33)], using the same method[34)]. The proofs for these three shapes and the arbitrary shaped submerged body below were later published on viXra.org[35),(36)] in English, and are written in Appendix A.2, A.3, A.4 and A.5 of present paper.

In order to put an end to the above discussions, we proved that "the center of buoyancy = the center of pressure" for a submerged body with arbitrary shape [1st half of 37)] using Gauss's integral theorem in 2021. Furthermore, it was published in the same journal "*NAVIGATION*" of *JIN* that it is easier to prove for a floating body with arbitrary shape [2nd half of 37)] than author's previous paper[25)] by using Gauss's theorem in the same way[38)].

We subsequently summarized the proofs in English for the case of the rectangular cross-section[24)], which is the easiest to understand, and for the floating body of arbitrary cross-sectional shape [2nd half of 37)] by applying Gauss's integral theorem. And we published them on this *viXra.org*[39)] and in the bulletin of our university, *Nagasaki Institute of Applied Science*[40)]. Furthermore, we showed an extension to the center of buoyancy for a 3-D floating body.

In this Chapter 1, we will describe them consistently.

1. 2 Positioning of the Center of Hydrostatic Pressure C_P Acting on the Inclined Rectangular Cross-Section

Fig. 1.1 shows a two-dimensional rectangular cross−section[24), 1st half of (39),(40)] of breadth $2b$ and depth $f+h$ (draft f and freeboard h) with a heel angle θ to the starboard side. The origin o is set at the center of the bottom surface, and the coordinate system fixed to the floating body is $o-\eta\zeta$ and the coordinate system fixed to the space is $o-yz$. Here, the z-axis of the latter is directed vertically upwards.

In the figure, atmospheric pressure is shown as a dashed vector, hydrostatic pressure as a solid vector, each pressure as a thin vector, and each force as a thick vector. All these vectors act perpendicularly to the surface of the floating body.

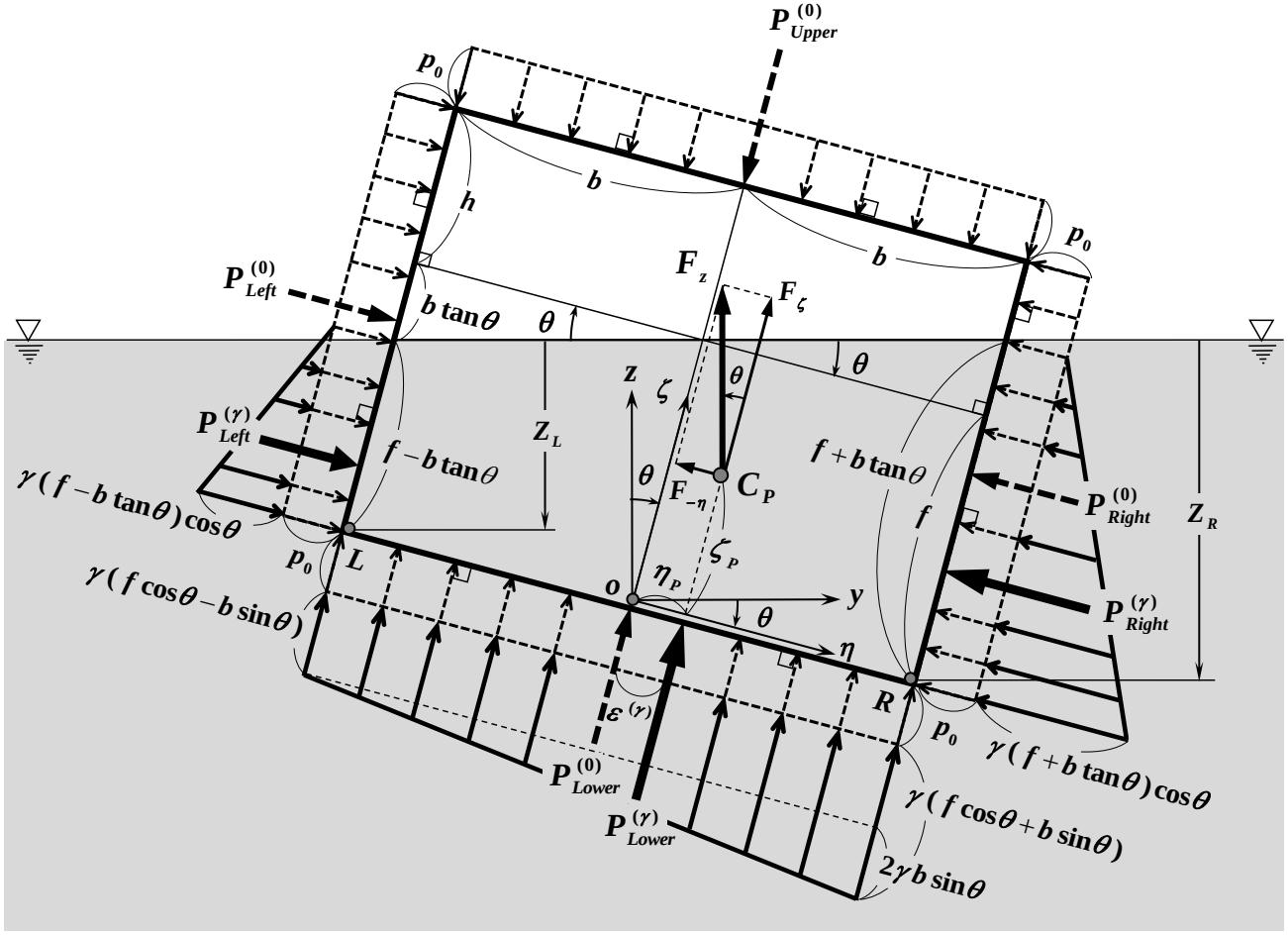

Fig. 1.1 Hydrostatic pressure and the center of pressure acting on the inclined rectangular cross-section.

1.2.1 Forces due to hydrostatic pressure acting on four surfaces around an inclined cross-section

When the floating body is inclined laterally by heel angle θ, the left-right asymmetric pressure field is created. Then, as shown in Fig. 1.1, the water depths Z_L and Z_R under the still water surface at the bottom points of port L and starboard R are expressed respectively in the form :

$$\left.\begin{aligned} Z_L &= (f - b\tan\theta)\cos\theta \\ Z_R &= (f + b\tan\theta)\cos\theta \end{aligned}\right\} \quad \cdots\cdots(1.1)$$

Let's calculate the forces P_{Left} acting on the port side (indicated by the subscript "*Left*") and P_{Right} acting on the starboard side (indicated by the subscript "*Right*"). P_{Left} is calculated by superimposing $P_{Left}^{(0)}$, which is obtained by the integrating the uniformly distributed atmospheric pressure acting on the port side, and $P_{Left}^{(\gamma)}$, which is obtained by the integrating the triangularly distributed hydrostatic pressure acting on the submerged area. Similarly, P_{Right} is calculated by superimposing $P_{Right}^{(0)}$ and $P_{Right}^{(\gamma)}$ on the starboard side. Therefore, if the atmospheric pressure is p_0 and the specific weight of water is γ, the above P_{Left} and P_{Right} can be written respectively by using the water depths Z_L and Z_R in Eq. (1.1) as follows :

$$\left.\begin{aligned} P_{Left} &= P_{Left}^{(0)} + P_{Left}^{(\gamma)} \\ &= p_0(f+h) + \frac{1}{2}\gamma Z_L (f - b\tan\theta) \\ &= p_0(f+h) + \frac{1}{2}\gamma (f - b\tan\theta)^2 \cos\theta \\ P_{Right} &= P_{Right}^{(0)} + P_{Right}^{(\gamma)} \\ &= p_0(f+h) + \frac{1}{2}\gamma Z_R (f + b\tan\theta) \\ &= p_0(f+h) + \frac{1}{2}\gamma (f + b\tan\theta)^2 \cos\theta \end{aligned}\right\} \quad \cdots\cdots(1.2)$$

The force P_{Upper} acting on the upper deck (indicated by the subscript "*Upper*") is obtained only by $P_{Upper}^{(0)}$ due to the atmospheric pressure of uniform distribution. And the force P_{Lower} acting on the bottom (indicated by the subscript "*Lower*") is obtained by superimposing $P_{Lower}^{(0)}$ due to the atmospheric pressure and $P_{Lower}^{(\gamma)}$ due to the hydrostatic pressure of trapezoidal distribution. Therefore, each of P_{Upper} and P_{Lower} can be written by using Z_L and Z_R as follows :

$$\left.\begin{aligned} P_{Upper} &= P_{Upper}^{(0)} \\ &= 2p_0 b \\ P_{Lower} &= P_{Lower}^{(0)} + P_{Lower}^{(\gamma)} \\ &= 2p_0 b + \frac{\gamma Z_L + \gamma Z_R}{2} \cdot 2b \\ &= 2p_0 b + 2\gamma f b \cos\theta \end{aligned}\right\} \quad \cdots\cdots(1.3)$$

1.2.2 Combined Forces $F_{-\eta}$ and F_{ζ} in the $-\eta$ and ζ directions

The combined forces $F_{-\eta}$ and F_{ζ} acting in the $-\eta$ (in the direction of the negative axis of η) and ζ directions fixed on the floating body can be obtained by using P_{Left}, P_{Right} in Eq. (1.2) and P_{Upper}, P_{Lower} in Eq. (1.3) as follows :

$$\left.\begin{aligned} F_{-\eta} &= P_{Right} - P_{Left} = P^{(\gamma)}_{Right} - P^{(\gamma)}_{Left} \\ &= 2\gamma f b \sin\theta \\ F_{\zeta} &= P_{Lower} - P_{Upper} = P^{(\gamma)}_{Lower} \\ &= 2\gamma f b \cos\theta \end{aligned}\right\} \quad \cdots\cdots(1.4)$$

Here, it can be seen that $F_{-\eta}$ is obliquely leftward, and F_{ζ} is obliquely upward. And for the both forces, the atmospheric pressure p_0 is canceled out.

1.2.3 Forces F_{-y} and F_z converted in the $-y$ and z directions

The horizontal component F_{-y} and the vertical component F_z acting on the floating body can be calculated by transforming the coordinates of the both forces $F_{-\eta}$ and F_{ζ} in Eq. (1.4) as follows :.

$$\left.\begin{aligned} F_{-y} &= F_{-\eta}\cos\theta - F_{\zeta}\sin\theta \\ &= 2\gamma f b(\sin\theta\cdot\cos\theta - \cos\theta\cdot\sin\theta) = 0 \\ F_z &= F_{\zeta}\cos\theta + F_{-\eta}\sin\theta \\ &= 2\gamma f b(\cos^2\theta + \sin^2\theta) = 2\gamma f b \end{aligned}\right\} \quad \cdots\cdots(1.5)$$

Here, it can be seen that the horizontal component F_{-y} does not act as a combined force due to pressure integration, even when the floating body is laterally inclined and the pressure field is left-right asymmetric. On the other hand, the vertical component F_z can be written as :

$$\begin{aligned} F_z &= \gamma\cdot(2b\cdot f) \\ &= \gamma\cdot(\textit{Area of the trapezoid under water surface}) \\ &= \textit{Buoyancy} \end{aligned} \quad \cdots\cdots(1.6)$$

By the above equation, F_z is the buoyancy exactly as taught by Archimedes' principle[1].

1.2.4 Moments M_{η} and M_{ζ} due to hydrostatic pressure in the η and ζ directions

First, we calculate the moment M_{η} due to the forces in the η direction. The counterclockwise moment M_{η} around the origin o due to $P^{(0)}_{Right}$, $P^{(0)}_{Left}$ and $P^{(\gamma)}_{Right}$, $P^{(\gamma)}_{Left}$ can be obtained by using Eq. (1.2). As shown in Fig. 1.1, the former is multiplied by the lever up to the action point of the pressure distributed uniformly, and the latter is multiplied by the lever of the pressure distributed triangularly, so that the moment M_{η} is can be calculated as follows :

$$\begin{aligned} M_{\eta} &= P^{(0)}_{Rigrt}\cdot\frac{f+h}{2} + P^{(\gamma)}_{Right}\cdot\frac{f+b\tan\theta}{3} - \left(P^{(0)}_{Left}\cdot\frac{f+h}{2} + P^{(\gamma)}_{Left}\cdot\frac{f-b\tan\theta}{3}\right) \\ &= \frac{1}{6}\gamma\left\{Z_R(f+b\tan\theta)^2 - Z_L(f-b\tan\theta)^2\right\} \\ &= \gamma b\sin\theta\left(f^2 + \frac{b^2}{3}\tan^2\theta\right) \end{aligned} \quad \cdots\cdots(1.7)$$

Here, the terms for atmospheric pressure p_0 is canceled out, as in the case of the forces in Eq. (1.4).

Next, let us consider calculating the moment M_ζ due to the forces in the ζ direction. To do this, we need to find the distance $\varepsilon^{(\gamma)}$ from origin o to the action point of $P_{Lower}^{(\gamma)}$. Here, the hydrostatic pressure of the trapezoidal distribution of acting on the bottom surface is decomposed into the uniform distribution and the triangular distribution. Since only the pressure of the triangular distribution contributes to the moment around origin o shown in Fig. 1.1, the distance $\varepsilon^{(\gamma)}$ can be determined by using Eq. (1.3) as follows :

$$\varepsilon^{(\gamma)} = \frac{\frac{1}{2}\cdot 2b\cdot 2\gamma b\sin\theta\cdot\left(b-\frac{2b}{3}\right)}{P_{Lower}^{(\gamma)}} = \frac{\frac{2}{3}\gamma b^3\sin\theta}{2\gamma f b\cos\theta} = \frac{b^2}{3f}\tan\theta \quad \cdots\cdots\cdots\cdots (1.8)$$

Therefore, the counterclockwise moment M_ζ around the origin o due to the forces $P_{Lower}^{(0)}$, $P_{Lower}^{(\gamma)}$ and $P_{Upper}^{(0)}$ acting in the ζ direction can also be calculated as :

$$\begin{aligned} M_\zeta &= P_{Lower}^{(0)}\times 0 + P_{Lower}^{(\gamma)}\cdot\varepsilon^{(\gamma)} - P_{Upper}^{(0)}\times 0 \\ &= P_{Lower}^{(\gamma)}\cdot\varepsilon^{(\gamma)} = \frac{2}{3}\gamma b^3\sin\theta \end{aligned} \quad \cdots\cdots\cdots\cdots (1.9)$$

As a result, M_ζ is obtained as the numerator in Eq. (1.8), and does not depend on p_0, like M_η in Eq. (1.7),.

1.2.5 Positioning of the center of hydrostatic pressure C_P for a rectangular cross-section

Consider the determination of the position of the center of hydrostatic pressure C_P acting on the floating body with a rectangular cross-section.

The counterclockwise moments M_η and M_ζ about origin o calculated in the previous section can be written by the combined forces $F_{-\eta}$ and F_ζ acting on $C_P(\eta_P, \zeta_P)$, as below. In doing so, it is based on the hydraulic method used by Ohgushi[9-a] for an example problem of the rolling gate.

$$\left.\begin{aligned} M_\eta &= F_{-\eta}\cdot\zeta_P \\ M_\zeta &= F_\zeta\cdot\eta_P \end{aligned}\right\} \quad \cdots\cdots\cdots\cdots (1.10)$$

Therefore, the distances η_P and ζ_P in the η and ζ directions from the origin o to the center of pressure C_P can be determined respectively by using $F_{-\eta}$, F_ζ of Eq. (1.4) in Section 1.2.2 and M_η, M_ζ of Eqs. (1.7), (1.9) in Section 1.2.4, as follows :

Chapter 1 : Proof that the Center of Buoyancy is Equal to the Center of Pressure by means of the Surface Integral of Hydrostatic Pressure

$$\left.\begin{aligned}
\eta_P &= \frac{M_\zeta}{F_\zeta} \\
&= \frac{P_{Lower}^{(\gamma)} \cdot \varepsilon^{(\gamma)}}{P_{Lower}^{(\gamma)}} = \varepsilon^{(\gamma)} = \frac{b^2}{3f}\tan\theta \quad \left(= \eta_G \right]_{\text{Eq. (A.1.5)}} \Big) \\
\zeta_P &= \frac{M_\eta}{F_{-\eta}} \\
&= \frac{\gamma b \sin\theta \left(f^2 + \dfrac{b^2}{3}\tan^2\theta \right)}{2\gamma f b \sin\theta} \\
&= \frac{f}{2} + \frac{b^2}{6f}\tan^2\theta \quad \left(= \zeta_G \right]_{\text{Eq. (A.1.5)}} \Big)
\end{aligned}\right\} \cdots\cdots\cdots\cdots\cdots\cdots (1.11)$$

As shown in the Appendix A.1, this result (η_P, ζ_P) coincides with the result (η_G, ζ_G) of Eq. (A.1.5), in which the centroid of the trapezoidal region under the water surface is geometrically determined by calculating the areal moment. Hence, it is correct and equal to the well-known position of the center of buoyancy.

Then, the specific weight γ of water have been cancelled out in the denominator and numerator of Eq. (1.11) respectively. And η_P is obtained as the action point $\varepsilon^{(\gamma)}$ calculated by Eq. (1.8), on which the force $P_{Lower}^{(\gamma)}$ acts.

Here, it should be noted that the position ζ_P of the center of pressure in the ζ - direction could be determined because the zero factor $\sin\theta$ at the heel angle $\theta \to 0$ was offset in the denominator and numerator, as shown in the 2nd part of Eq. (1.11). If we start and calculate as an upright state $\theta = 0$, both the denominator $F_{-\eta}$ and the numerator M_η are zero in equilibrium, so the fraction will be indeterminate forms and ζ_P cannot be determined.

To clarify this result, let's determine the center of pressure C_P in the upright state by setting the heel angle to $\theta \to 0$. Then, since the $\eta\zeta$ - coordinates tilted and fixed on the floating body coincide with the yz - coordinates fixed in space, the Eq. (1.11) becomes as :

$$\left.\begin{aligned}
(\eta_P, \zeta_P)\big]_{\theta\to 0} &= (y_P, z_P) = \left(0, \frac{f}{2}\right) \\
\therefore\ C_P &= B
\end{aligned}\right\} \cdots\cdots\cdots\cdots\cdots\cdots\cdots\cdots (1.12)$$

Here, it can be obtained that the center of pressure is equal to rectangular centroid. This proves that the center of hydrostatic pressure C_P coincides with the well-known "Center of Buoyancy, B" for the rectangular cross - section.

1.3 Positioning of the Center of Hydrostatic Pressure C_P Acting on the Inclined Floating Body with an Arbitrary Form

In this section, we apply the same method as used in the previous Section 1.2, in which a rectangular shape is inclined laterally, to the floating body with an arbitrary form[37), 2nd half of (39),(40)]. It is shown that the position of the center of pressure can be more easily determined by integrating the hydrostatic pressure using Gauss's integral theorem than author's previous paper[25)].

Fig. 1.2 shows a transverse section of an arbitrarily shaped floating body with a heel angle θ to the starboard side. The origin o is placed in the center of the still water surface, and the coordinate system fixed to the floating body and tilted is $o\text{-}\eta\zeta$, and the coordinate system fixed to space is $o\text{-}yz$. Here,

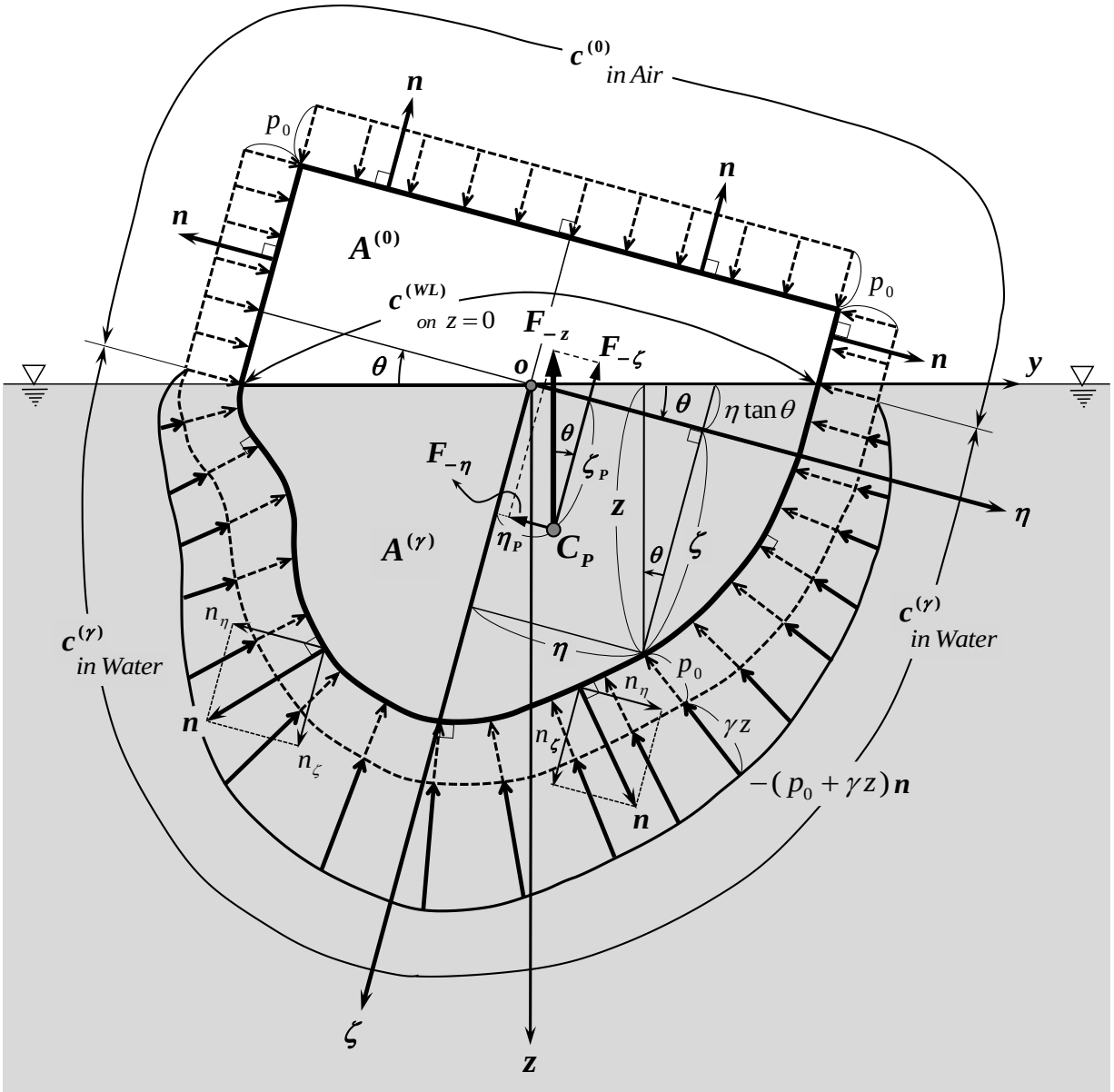

Fig. 1.2 Hydrostatic pressure and the center of pressure acting on the inclined floating body with arbitrary form.

the z - axis of the latter is vertically downwards, and the opposite direction to that of Fig. 1.1.

Also, $\boldsymbol{n}$ is the outward unit normal vector standing on the surface of the floating body, and is written as follows :

$$\boldsymbol{n} = n_\eta \boldsymbol{j} + n_\zeta \boldsymbol{k} \quad \cdots\cdots(1.13)$$

Here, n_η and n_ζ are the directional cosines in the η and ζ coordinates fixed to the body, and $\boldsymbol{j}$ and $\boldsymbol{k}$ are the basic vectors in the η and ζ directions, similarly.

In the figure, the atmospheric pressure is shown as a dashed vector, the hydrostatic pressure as a solid vector, same as in Fig. 1.1. And all of the vectors act in the $-\boldsymbol{n}$ direction perpendicular to the floating body surface.

As shown in Fig. 1.2, the water depth z on the surface (η, ζ) of the floating body is written as :

$$\begin{aligned} z(\eta,\zeta) &= (\zeta + \eta \tan\theta)\cos\theta \\ &= \zeta\cos\theta + \eta\sin\theta \end{aligned} \quad \cdots\cdots(1.14)$$

Here, as in Sction 1.2, if the atmospheric pressure is written as p_0 and the specific weight of water is written as γ , the hydrostatic pressure $p(\eta, \zeta)$ can be obtained for positive and negative z as follows :

$$p(\eta,\zeta) = \begin{cases} p_0 & (for\ z<0\ ;\ c^{(0)}\ in\ Air) \\ p_0 + \gamma z(\eta,\zeta) & (for\ z\geq 0\ ;\ c^{(\gamma)}\ in\ Water) \end{cases} \quad \cdots\cdots(1.15)$$

1.3.1 Components $F_{-\eta}$ and $F_{-\zeta}$ of the total force due to hydrostatic pressure in the $-\eta$ and $-\zeta$ directions acting on the floating body

The total force $\boldsymbol{F}$ acting on the floating body is calculated by pressure integration over the circumference of the body surface $c^{(0)} + c^{(\gamma)}$ with the line element $d\ell$, as follows :

$$\begin{aligned} \boldsymbol{F} &= -\oint_{c^{(0)}+c^{(\gamma)}} p(\eta,\zeta)\,\boldsymbol{n}\,d\ell \\ &= F_{-\eta}(-\boldsymbol{j}) + F_{-\zeta}(-\boldsymbol{k}) \end{aligned} \quad \cdots\cdots(1.16)$$

The $-\eta$ directional component $F_{-\eta}$ and the $-\zeta$ directional component $F_{-\zeta}$ of the above total force $\boldsymbol{F}$ can be obtained by integrating the $-\eta$ and $-\zeta$ components of the hydrostatic pressure $p(\eta, \zeta)$ in Eq. (1.15). Here, the integral path is written as $c^{(0)}$ for the aerial part of the floating body and as $c^{(\gamma)}$ for the underwater part, as shown in Fig. 1.2. Then, $F_{-\eta}$ and $F_{-\zeta}$ are respectively calculated by summing the integrals along the two paths : $c^{(0)}$, where the atmospheric pressure p_0 acts, and $c^{(\gamma)}$, where the hydrostatic pressure $p_0 + \gamma z$ acts, as follows :

$$\left.\begin{aligned} F_{-\eta} &= \oint_{c^{(0)}+c^{(\gamma)}} p(\eta,\zeta)\, n_\eta\, d\ell \\ &= \int_{c^{(0)}} p_0 n_\eta\, d\ell + \int_{c^{(\gamma)}} (p_0+\gamma z)\, n_\eta\, d\ell \\ &= \oint_{c^{(0)}+c^{(\gamma)}} p_0 n_\eta\, d\ell + \gamma \int_{c^{(\gamma)}} z n_\eta\, d\ell \\ F_{-\zeta} &= \oint_{c^{(0)}+c^{(\gamma)}} p(\eta,\zeta)\, n_\zeta\, d\ell \\ &= \int_{c^{(0)}} p_0 n_\zeta\, d\ell + \int_{c^{(\gamma)}} (p_0+\gamma z)\, n_\zeta\, d\ell \\ &= \oint_{c^{(0)}+c^{(\gamma)}} p_0 n_\zeta\, d\ell + \gamma \int_{c^{(\gamma)}} z n_\zeta\, d\ell \end{aligned}\right\} \quad \cdots\cdots(1.17)$$

Both results are obtained by summing the line integral over the entire circumference $c^{(0)}+c^{(\gamma)}$ of the floating body about p_0 and it over the underwater surface $c^{(\gamma)}$ of the body about γz.

Here, because of $z=0$ on the still water surface (y-axis), the equality relation is not broken even if the integral term for the path $c^{(WL)}$ on the still water surface is added to the second term, as shown in Fig. 1.2. As a result, it can be expressed as a contour integral of $c^{(\gamma)}+c^{(WL)}$ under the water surface. Therefore, $F_{-\eta}$ and $F_{-\zeta}$ can be written as the sum of the contour integral of the two paths, respectively, as follows :

$$\left.\begin{aligned} F_{-\eta} &= \oint_{c^{(0)}+c^{(\gamma)}} p_0 n_\eta\, d\ell + \gamma \int_{c^{(\gamma)}} z n_\eta\, d\ell + \gamma \int_{c^{(WL)}} z n_\eta\, d\ell \\ &= \oint_{c^{(0)}+c^{(\gamma)}} p_0 n_\eta\, d\ell + \gamma \oint_{c^{(\gamma)}+c^{(WL)}} z n_\eta\, d\ell \\ F_{-\zeta} &= \oint_{c^{(0)}+c^{(\gamma)}} p_0 n_\zeta\, d\ell + \gamma \int_{c^{(\gamma)}} z n_\zeta\, d\ell + \gamma \int_{c^{(WL)}} z n_\zeta\, d\ell \\ &= \oint_{c^{(0)}+c^{(\gamma)}} p_0 n_\zeta\, d\ell + \gamma \oint_{c^{(\gamma)}+c^{(WL)}} z n_\zeta\, d\ell \end{aligned}\right\} \quad \cdots\cdots(1.18)$$

Therefore, the following two-dimensional (η-ζ plane) Gauss's integral theorem, in which n_η and n_ζ are the directional cosines of the outward unit normal vector in η and ζ directions, can be applied to the contour integrals of the above Eq. (1.18), respectively.

$$\left.\begin{aligned} \oint_c u(\eta,\zeta)\, n_\eta\, d\ell &= \iint_A \frac{\partial u}{\partial \eta}\, dA \\ \oint_c v(\eta,\zeta)\, n_\zeta\, d\ell &= \iint_A \frac{\partial v}{\partial \zeta}\, dA \end{aligned}\right\} \quad \cdots\cdots(1.19)$$

Then, both $F_{-\eta}$ and $F_{-\zeta}$ can be converted to the area integral, in which the area of the aerial part of the floating body is denoted as $A^{(0)}$ and the area of the underwater part as $A^{(\gamma)}$. As a result of the calculation, both forces can be expressed only in terms of the area integral of underwater $A^{(\gamma)}$, as follows :

$$\left.\begin{aligned} F_{-\eta} &= \iint_{A^{(0)}+A^{(\gamma)}} \frac{\partial p_0}{\partial \eta}\, dA + \gamma \iint_{A^{(\gamma)}} \frac{\partial z}{\partial \eta}\, dA \\ &= \gamma \iint_{A^{(\gamma)}} \frac{\partial z}{\partial \eta}\, dA \\ F_{-\zeta} &= \iint_{A^{(0)}+A^{(\gamma)}} \frac{\partial p_0}{\partial \zeta}\, dA + \gamma \iint_{A^{(\gamma)}} \frac{\partial z}{\partial \zeta}\, dA \\ &= \gamma \iint_{A^{(\gamma)}} \frac{\partial z}{\partial \zeta}\, dA \end{aligned}\right\} \cdots\cdots (1.20)$$

This is the result of finding that the area integral with respect to p_0 in the 1st term of the above equation vanishes because the integrand becomes zero.

Furthermore, using Eq. (1.14) for water depth z, the both forces $F_{-\eta}$ and $F_{-\zeta}$ in Eq. (1.20) can be calculated as below. Then, each of the 1st term of integrand for $A^{(\gamma)}$ in the following equation will become zero and vanish.

$$\left.\begin{aligned} F_{-\eta} &= \gamma \iint_{A^{(\gamma)}} \frac{\partial(\zeta \cos\theta + \eta \sin\theta)}{\partial \eta}\, dA \\ &= \gamma \sin\theta \iint_{A^{(\gamma)}} dA = \gamma A^{(\gamma)} \sin\theta \\ F_{-\zeta} &= \gamma \iint_{A^{(\gamma)}} \frac{\partial(\eta \sin\theta + \zeta \cos\theta)}{\partial \zeta}\, dA \\ &= \gamma \cos\theta \iint_{A^{(\gamma)}} dA = \gamma A^{(\gamma)} \cos\theta \end{aligned}\right\} \cdots\cdots (1.21)$$

It can be seen that both are determined by the area $A^{(\gamma)}$ of the floating body under the still water surface and the heel angle θ, and do not depend on the atmospheric pressure p_0.

In addition, $F_{-\eta}$ and $F_{-\zeta}$ are obtained as $-\eta$ and $-\zeta$ directional components of the buoyancy $\gamma A^{(\gamma)}$, as shown by F_{-z} of Eq. (1.22) in the next section, respectively.

1.3.2 Forces F_{-y} and F_{-z} converted in $-y$ and $-z$ directions

The horizontal component ($-y$ direction) F_{-y} and the vertical component ($-z$ direction) F_{-z} acting on the floating body can be obtained by transforming the coordinates of the both forces $F_{-\eta}$ and $F_{-\zeta}$ in Eq. (1.21) of the previous section, as follows :

$$\left.\begin{aligned} F_{-y} &= F_{-\eta} \cos\theta - F_{-\zeta} \sin\theta \\ &= \gamma A^{(\gamma)} (\sin\theta \cdot \cos\theta - \cos\theta \cdot \sin\theta) \\ &= 0 \\ F_{-z} &= F_{-\zeta} \cos\theta + F_{-\eta} \sin\theta \\ &= \gamma A^{(\gamma)} (\cos^2\theta + \sin^2\theta) \\ &= \gamma A^{(\gamma)} \;\; (= \mathit{Buoyancy}) \end{aligned}\right\} \cdots\cdots (1.22)$$

Here, it can be seen that the horizontal component F_{-y} does not act as a combined force due to pressure integration, even when the floating body is laterally inclined and is left-right asymmetric. On the other hand, since the vertical component F_{-z} is the product of the specific weight γ of water and the cross-sectional area $A^{(\gamma)}$ of the floating body under the water surface, it is the buoyancy itself generated vertically upward, as taught by Archimedes' principle (1). This situation is similar to Eq. (1.5) for the rectangular cross-section in Section 1.2.

1.3.3 Moments M_η and M_ζ due to hydrostatic pressure in the η and ζ directions

In this section, we shall calculate the total counterclockwise moment M_o around the origin o due to hydrostatic pressure acting on the surface of the floating body. It can be calculated by superimposing the clockwise moment M_η due to the pressure component in the direction $-\eta$ and the counterclockwise moment M_ζ in the direction $-\zeta$, as follows :

$$M_o = -M_\eta + M_\zeta \quad \cdots\cdots (1.23)$$

Here, M_η and M_ζ can be calculated by multiplying the integrand in Eq. (1.17) by ζ or η as the moment lever respectively, in the following form :

$$\left.\begin{aligned} M_\eta &= \oint_{c^{(0)}+c^{(\gamma)}} p(\eta,\zeta)\,\zeta\, n_\eta\, d\ell \\ &= \int_{c^{(0)}} p_0\,\zeta\, n_\eta\, d\ell + \int_{c^{(\gamma)}} (p_0+\gamma z)\,\zeta\, n_\eta\, d\ell \\ M_\zeta &= \oint_{c^{(0)}+c^{(\gamma)}} p(\eta,\zeta)\,\eta\, n_\zeta\, d\ell \\ &= \int_{c^{(0)}} p_0\,\eta\, n_\zeta\, d\ell + \int_{c^{(\gamma)}} (p_0+\gamma z)\,\eta\, n_\zeta\, d\ell \end{aligned}\right\} \quad \cdots\cdots (1.24)$$

Now, as in the case of forces $F_{-\eta}$ and $F_{-\zeta}$ in Eq. (1.18), let's connect the path $c^{(0)}$ and $c^{(\gamma)}$ with respect to p_0 and add a term for the path $c^{(WL)}$ on the still water surface with respect to γz where the integral value become zero as shown in Fig. 1.2. Then, M_η and M_ζ can be expressed as the sum of the contour integrals of the two paths, respectively, as follows :

$$\left.\begin{aligned} M_\eta &= \oint_{c^{(0)}+c^{(\gamma)}} p_0\,\zeta\, n_\eta\, d\ell + \gamma\int_{c^{(\gamma)}} z\,\zeta\, n_\eta\, d\ell + \gamma\int_{c^{(WL)}} z\,\zeta\, n_\eta\, d\ell \\ &= p_0\oint_{c^{(0)}+c^{(\gamma)}} \zeta\, n_\eta\, d\ell + \gamma\oint_{c^{(\gamma)}+c^{(WL)}} z\,\zeta\, n_\eta\, d\ell \\ M_\zeta &= \oint_{c^{(0)}+c^{(\gamma)}} p_0\,\eta\, n_\zeta\, d\ell + \gamma\int_{c^{(\gamma)}} z\,\eta\, n_\zeta\, d\ell + \gamma\int_{c^{(WL)}} z\,\eta\, n_\zeta\, d\ell \\ &= p_0\oint_{c^{(0)}+c^{(\gamma)}} \eta\, n_\zeta\, d\ell + \gamma\oint_{c^{(\gamma)}+c^{(WL)}} z\,\eta\, n_\zeta\, d\ell \end{aligned}\right\} \quad \cdots\cdots (1.25)$$

Therefore, we can apply Gauss's integral theorem in Eq. (1.19) to the above contour integrals, as in the case of forces $F_{-\eta}$ and $F_{-\zeta}$ in Section 1.3.1, and convert them into area integrals. Furthermore,

using Eq. (1.14) for the water depth z, the moments M_η and M_ζ in Eq. (1.25) can be written, respectively, as follows :

$$\left.\begin{aligned} M_\eta &= p_0 \iint_{A^{(0)}+A^{(\gamma)}} \frac{\partial \zeta}{\partial \eta}\, dA + \gamma \iint_{A^{(\gamma)}} \frac{\partial (z\zeta)}{\partial \eta}\, dA \\ &= \gamma \iint_{A^{(\gamma)}} \frac{\partial (\zeta^2 \cos\theta + \eta\zeta \sin\theta)}{\partial \eta}\, dA \\ &= \gamma \sin\theta \iint_{A^{(\gamma)}} \zeta\, dA \\ M_\zeta &= p_0 \iint_{A^{(0)}+A^{(\gamma)}} \frac{\partial \eta}{\partial \zeta}\, dA + \gamma \iint_{A^{(\gamma)}} \frac{\partial (z\eta)}{\partial \zeta}\, dA \\ &= \gamma \iint_{A^{(\gamma)}} \frac{\partial (\eta^2 \sin\theta + \zeta\eta \cos\theta)}{\partial \zeta}\, dA \\ &= \gamma \cos\theta \iint_{A^{(\gamma)}} \eta\, dA \end{aligned}\right\} \quad \cdots\cdots\cdots\cdots\cdots\cdots\cdots\cdots\cdots\cdots (1.26)$$

Here, both moments are proportional to the areal moments of the submerged area $A^{(\gamma)}$ of the floating body about the η-axis or ζ-axis, respectively. This is the result that integrands in the terms for p_0 and the 1st term for $A^{(\gamma)}$ in the above equations become zero and vanished.

1.3.4 Positioning of the center of hydrostatic pressure C_P for the floating body with an arbitrary form

In order to locate the center of pressure C_P in o-$\eta\zeta$ coordinate system fixed to the body, the similar hydraulic method[9-a] as used for rectangular cross-section in Section 1.2.5 is applied.

Since the forces $F_{-\eta}$ and $F_{-\zeta}$ due to the hydrostatic pressure obtained in Section 1.3.1 act on the center of pressure $C_P(\eta_P, \zeta_P)$, the clockwise moment M_η and the counterclockwise moment M_ζ obtained in Section 1.3.3 can be expressed respectively same as Eq. (1.10) in Section 1.2.5, as follows :

$$\left.\begin{aligned} M_\eta &= F_{-\eta}\, \zeta_P \\ M_\zeta &= F_{-\zeta}\, \eta_P \end{aligned}\right\} \quad \cdots\cdots\cdots\cdots\cdots\cdots\cdots\cdots\cdots\cdots\cdots\cdots\cdots\cdots\cdots\cdots\cdots\cdots (1.27)$$

Here, the total counterclockwise moment M_o around the origin o in Eq. (1.23) can be calculated as :

$$M_o = -F_{-\eta}\, \zeta_P + F_{-\zeta}\, \eta_P \quad \cdots\cdots\cdots\cdots\cdots\cdots\cdots\cdots\cdots\cdots\cdots\cdots\cdots\cdots\cdots\cdots\cdots\cdots (1.28)$$

Then, the moment M_{C_P} around the point C_P, at which $F_{-\eta}$ and $F_{-\zeta}$ act, is computed as follows, and becomes zero.

$$M_{C_P} = -F_{-\eta} \times 0 + F_{-\zeta} \times 0 = 0 \quad \cdots\cdots\cdots\cdots\cdots\cdots\cdots\cdots\cdots\cdots\cdots\cdots\cdots\cdots\cdots\cdots\cdots\cdots (1.29)$$

This correctly indicates that C_P is the center of hydrostatic pressure for the floating body.

Therefore, the unknown coordinate (η_P, ζ_P) of this center of pressure C_P can be determined by Eq. (1.27). Here, the η-coordinate, η_P, can be determined by using the 2nd part of Eq. (1.21) for $F_{-\zeta}$ and the 2nd part of Eq. (1.26) for M_ζ, as follows :

$$\eta_P = \frac{M_\zeta}{F_{-\zeta}} = \frac{\gamma \cos\theta \iint_{A^{(\gamma)}} \eta \, dA}{\gamma A^{(\gamma)} \cos\theta}$$
$$= \frac{1}{A^{(\gamma)}} \iint_{A^{(\gamma)}} \eta \, dA \left(= \eta_G \right) \quad \cdots\cdots (1.30)$$

Further, the ζ-coordinate, ζ_P, can be determined by using the 1st part of Eq. (1.21) for $F_{-\eta}$ and the 1st part of Eq. (1.26) for M_η, as follows :

$$\zeta_P = \frac{M_\eta}{F_{-\eta}} = \frac{\gamma \sin\theta \iint_{A^{(\gamma)}} \zeta \, dA}{\gamma A^{(\gamma)} \sin\theta}$$
$$= \frac{1}{A^{(\gamma)}} \iint_{A^{(\gamma)}} \zeta \, dA \left(= \zeta_G \right) \quad \cdots\cdots (1.31)$$

As a result, both the specific weight γ of water and the heel angle θ have been cancelled out in the denominator and numerator respectively, so that η_P and ζ_P are obtained in the following simple geometrical format. It is a form in which the areal moment about the ζ-axis and it about the η-axis are each divided by the area $A^{(\gamma)}$ of the submerged portion. This shows that the center of pressure (η_P, ζ_P) of the floating body in the inclined state clearly coincides with the centroid (η_G, ζ_G) of the submerged area $A^{(\gamma)}$, that is, the well-known center of buoyancy.

Considering the above, ζ_P of vertical component can be obtained by offsetting the zero factor $\sin\theta$ at the heel angle $\theta \to 0$ with the denominator and numerator, as shown in Eq. (1.31). Here, if we start the calculation as the upright state $\theta = 0$, both the denominator $F_{-\eta}$ and the numerator M_η are in equilibrium and become zero, so the fraction becomes indeterminate forms and ζ_P cannot be determined. This is the reason why we were able to determine the position of the center of pressure in the ζ direction as $\zeta_P = \zeta_G$ by inclining the floating body laterally.

On the other hand, in the calculation of η_P in Eq. (1.30), even if the heel angle is $\theta = 0$ from the beginning, the denominator $F_{-\zeta}$ takes a finite value as the cosine component of the buoyancy. Therefore, the horizontal component η_P can be determined as $\eta_P = \eta_G$, if we start and calculate as the upright state.

These situations described above are exactly the same as in Eq. (1.11) of Section 1.2.5 for a rectangular cross-section.

As a final step, let's find the center of pressure in the upright state by setting the heel angle to $\theta \to 0$, in order to make this result clearer. Then, since the $\eta\zeta$-coordinates tilted and fixed on the floating body coincide with the yz-coordinates fixed in space, the Eqs. (1.30) and (1.31) become as :

$$\left.\begin{aligned} (y_P, z_P) &= \left(\frac{1}{A^{(\gamma)}} \iint_{A^{(\gamma)}} y \, dA \, , \, \frac{1}{A^{(\gamma)}} \iint_{A^{(\gamma)}} z \, dA \right) = (y_G, z_G) \\ \therefore \; C_P &= B \end{aligned}\right\} \quad \cdots\cdots (1.32)$$

Therefore, this proves that the center of hydrostatic pressure C_P coincides with the well-known "Center of Buoyancy, B" for the floating body.

In addition, the reason why the consequence of z_P shown in Eq. (1.32) could be derived more easily than the author's previous paper[25] is that Gauss's integral theorem was applied to an inclined $o-\eta\zeta$ coordinate system fixed to a floating body.

1.3.5 Extension to the center of buoyancy for a 3-D floating body

In the previous section, we were able to show that the center of hydrostatic pressure $C_P(y_P, z_P)$ in the cross-section, *i.e.*, yz-plane, of a floating body for the upright state is equal to its centroid $G(y_G, z_G)$ of the underwater area, *i.e.,* the well-known center of buoyancy B.

As shown in Fig. 1.3, the cross-sectional area under the water surface in the longitudinal direction x is $A^{(\gamma)}(x)$, the y-coordinate of the center of buoyancy in the horizontal direction are $y_P(x)$, and the z-coordinate in the vertical direction are $z_P(x)$. The position of the center of buoyancy $B(X_B, Y_B, Z_B)$ for a 3-dimensional floating body, such as a ship, is determined by dividing the volume integral $A^{(\gamma)}(x)\,dx$ of the moment with x as the lever for X_B, with $y_P(x)$ for Y_B and with $z_P(x)$ for Z_B from the stern (*After Perpendicular : A.P.*) to the bow (*Fore Perpendicular : F.P.*) in the x direction respectively, by the underwater volume $V^{(\gamma)}$, as follows :

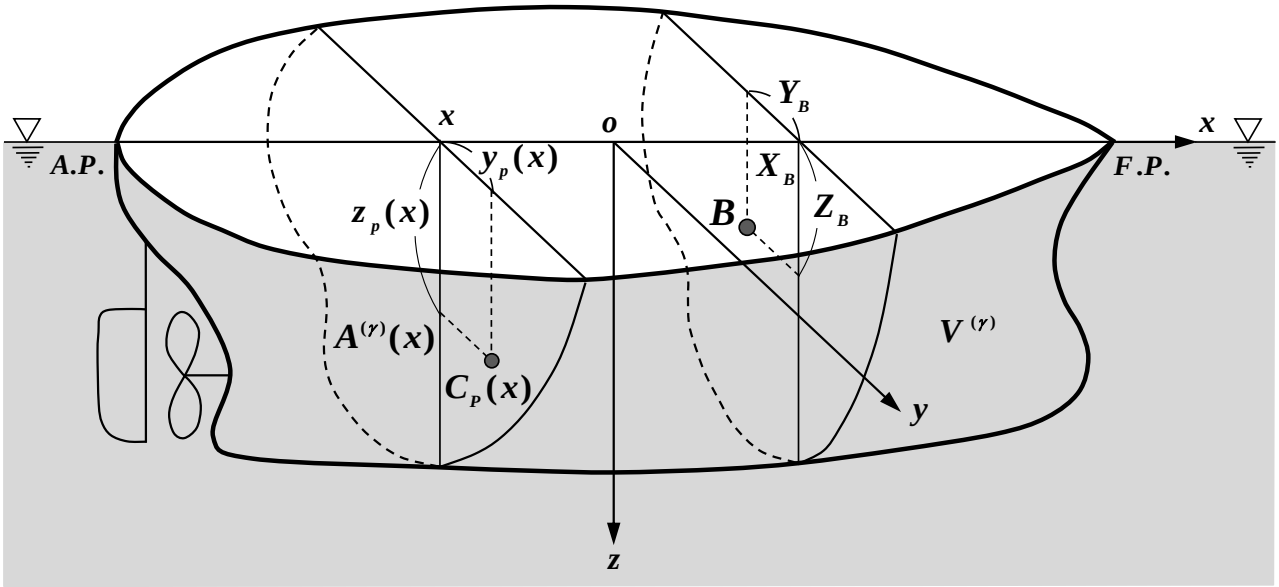

Fig. 1.3 Center of buoyancy of the 3-D floating body $B(X_B, Y_B, Z_B)$ and of the cross-section $C_P(y_P(x), z_P(x))$ for the upright state.

$$\left.\begin{aligned} X_B &= \frac{\int_{A.P.}^{F.P.} x \cdot A^{(\gamma)}(x)\,dx}{\int_{A.P.}^{F.P.} A^{(\gamma)}(x)\,dx} = \frac{1}{V^{(\gamma)}} \int_{A.P.}^{F.P.} x \cdot A^{(\gamma)}(x)\,dx \\ Y_B &= \frac{\int_{A.P.}^{F.P.} y_P(x) \cdot A^{(\gamma)}(x)\,dx}{\int_{AP}^{FP} A^{(\gamma)}(x)\,dx} = \frac{1}{V^{(\gamma)}} \int_{A.P.}^{F.P.} y_P(x) \cdot A^{(\gamma)}(x)\,dx \\ Z_B &= \frac{\int_{A.P.}^{F.P.} z_P(x) \cdot A^{(\gamma)}(x)\,dx}{\int_{A.P.}^{F.P.} A^{(\gamma)}(x)\,dx} = \frac{1}{V^{(\gamma)}} \int_{A.P.}^{F.P.} z_P(x) \cdot A^{(\gamma)}(x)\,dx \end{aligned}\right\} \cdots\cdots\cdots\cdots\cdots\cdots (1.33)$$

The three equations above are nothing more than correctly determining the xyz-coordinates of the volume centroid of the geometric shape of the underwater portion of the 3-D floating body.

1.4 Conclusions

In this chapter, we elucidated an unsolved problem in physics and naval architecture by proving that "the center of hydrostatic pressure is equal to the well-known center of buoyancy of a ship".

To solve this problem, we dared to assume the left-right asymmetric pressure field by inclining the ship with heel angle. In that state, the force and moment due to hydrostatic pressure were calculated correctly with respect to the tilted coordinate system fixed to the floating body. By doing so, we succeeded in determining the center of hydrostatic pressure. Finally, by setting the heel angle to zero, the result of the upright state was obtained and the proof was clarified.

As for the shape of the floating body, the simplest rectangular cross-section was proved first, and then the arbitrary cross-sectional shape was proved by applying Gauss's integral theorem. And we showed an extension to the center of buoyancy for a 3-D floating body.

As a postscript, in Appendices A.2, A.3, A.4 and A.5, we also provide separate proofs for following four shapes. The triangular prism [2nd half of (35)] and semi-submerged circular cylinder [1st half of (35)] shown in A.2 and A.3 are included in the proof of arbitrary shaped floating body in Section 1.3, but since they are two typical cross-sectional shapes along with rectangles in Section 1.2, they are written. Furthermore, as the proofs for submerged bodies, in A.4 and A.5, the submerged circuler cylinder [1st half of (36)] and arbitrary shaped submerged body [2nd half of (36)] are described, so please read them if you are interested.

Chapter 2
New Theory on the Derivation of Metacentric Radius Governing the Hydrostatic Stability of Ships

In this Chapter 2, we develop a new theory on the derivation of the transverse metacentric radius which governs the hydrostatic stability of ships.

As a new development in its derivation process, it was shown that the direction of movement of the center of buoyancy due to lateral inclination of ship is the direction of the half angle $\frac{\theta}{2}$ of the heel angle θ. By finding it, we were able to derive a metacentric radius worthy of its name by showing that the metacentric radius correctly represents the radius centered on the metacenter, which is the center of inclination.

2. 1 Introduction

The transverse metacentric radius $\overline{BM}$, which governs the stability performance of ships, can be calculated as follows, where V is the volume of underwater portion and I_{CL} is the quadratic moment about the centerline of the water plane.

$$\overline{BM} = \frac{I_{CL}}{V} \quad \cdots\cdots (2.1)$$

Here, the above equation is a well-known basic formula in naval architecture.

This formula (2.1) for $\overline{BM}$ was firstly derived by Bouguer[6], and Nowacki[14] & Ferreiro[11-b] have introduced the historical background. It is also described by Goldberg[7-c] in the US *"Principles of Naval Architecture"*, the bible of naval architecture. More recently, it has been considered by Mégel & Kliava[22]. In Japan and other countries, it has been described by Nishikawa[8-b], Ohgushi[9-b], Akedo[12-b], Takagi[41], Sugihara[42-a] and Ohta & Kuwahara *et al.*[43] in the past, and recently by Nohara & Shoji[44], Barrass & Derrett[45], Ikeda & Furukawa *et al.*[46] and Shin[47] in many textbooks of naval architecture and nautical mechanics.

Although the result itself does not change with respect to such a basic formula for $\overline{BM}$ in Eq. (2.1), as a new development in its derivation process, it was shown that the direction of movement of the center of buoyancy due to the lateral inclination of ship is the direction of the half angle $\frac{\theta}{2}$ of the heel angle θ. By finding it, we were able to derive a metacentric radius $\overline{BM}$ suitable for its name by showing that the metacentric radius correctly represents the radius centered on the metacenter M, which is the center of inclination. The process of new derivation[48] was published in the Journal " *NAVIGATION* " of Japan Institute of Navigation in 2017, with the preparedness of receiving criticism from distinguished scholars.

We subsequently summarized the new derivation process[48),(49)] for metacentric radius $\overline{BM}$ in English, and published it on this viXra.org[50] and in the bulletin of our university, Nagasaki Institute of Applied Science[51].

In this Chapter 2, we will describe the new theory consistently.

2. 2 New Derivation of Metacentric Radius $\overline{BM}$

Fig. 2. 1 shows a three-dimensional view of the ship when it is inclined laterally by heel angle θ to the starboard side from upright position. The water line is WL and the center of buoyancy is B in the upright state, and the water line is $W'L'$ and the center of buoyancy is B' after inclination, as shown in Chapter 1. The intersection point of the center line perpendicular to WL extending from B in the upright state and the action line of the buoyancy vertically upward from B' in the inclined state is the so-called "transverse metacenter", M.

Since both hull sides of the ship can generally be assumed to be perpendicular to the water surface near the water line, the exposed part $\triangle WoW'$ and the submerged part $\triangle LoL'$ are right triangles similar in all cross-sections from the stern AP (abbreviation of *After Perpendicular*) to the bow FP (abbreviation of *Fore Perpendicular*), although the waterline breadth $2y$ differs in the longitudinal direction x. Therefore, AP-WoW'-FP and AP-LoL'-FP are three-dimensionally wedge-shaped.

Since the volume V of ship's underwater portion remains the same after inclination, the volumes of the wedge-shaped AP - WoW' - FP in the exposed portion and the wedge-shaped AP - LoL' - FP in the immersed portion are equal. If the wedge-shaped volume is v, and the centroid of the exposed volume is g and the centroid of the immersed volume is g', we can consider that a part of the underwater volume v has moved from g to g'.

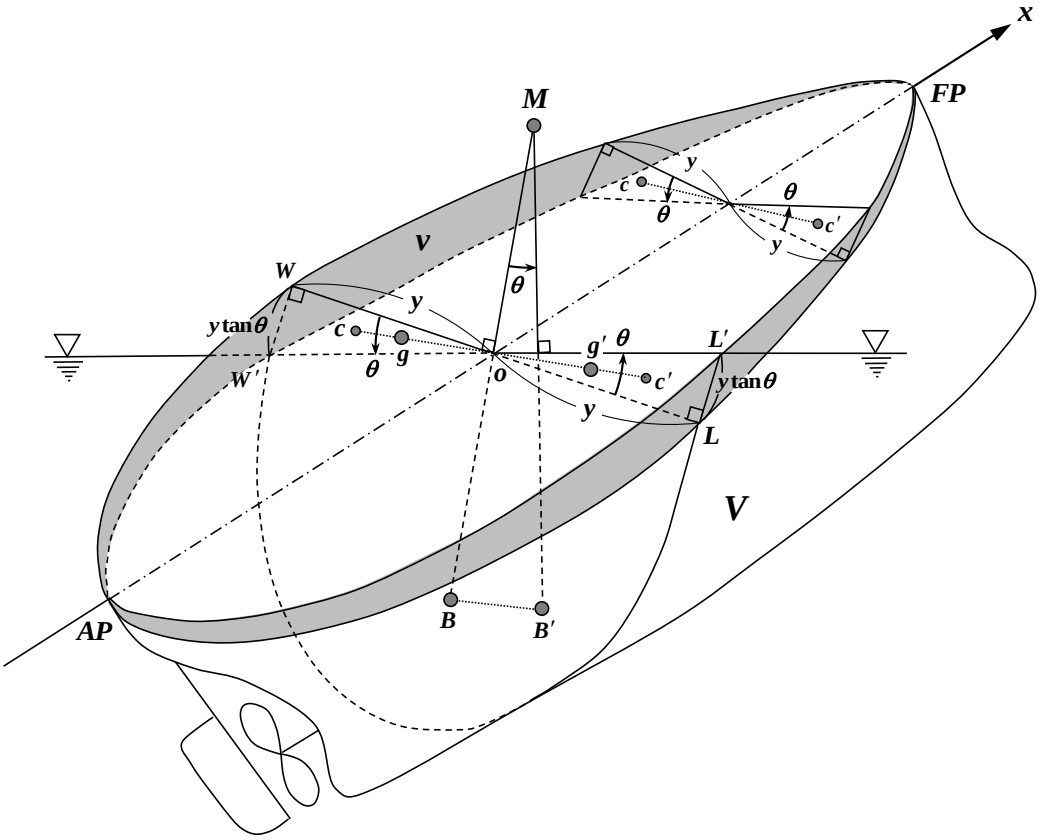

Fig. 2. 1 Three-dimensional view of the wedge-shaped exposed and immersed portions of a laterally inclined ship.

Therefore, the direction and distance $\overline{BB'}$ when the center of buoyancy, which is the centroid of the whole underwater volume V, moves from B to B' are determined as follows :

$$\left.\begin{aligned} &\overline{BB'} \;/\!/\; \overline{gg'} \\ &\overline{BB'} = \frac{v}{V}\cdot\overline{gg'} \end{aligned}\right\} \quad \cdots\cdots (2.2)$$

The result of Eq. (2.2) above is the dynamical law described in many textbooks(7-c),(8-b),(9-b),(12-b),(41),(42-a),(43)~(47) of naval architecture and nautical mechanics, as a preliminary step in deriving the formula of Eq. (2.1). In this paper, this law will be carefully explained in Appendix A.6. There, in Eq. (A.6.9) of its Appendix, A and a for area are replaced by v and V for volume.

2.2.1 Direction of movement $\overline{BB'}$ of the center of buoyancy

Fig. 2.2 depicts the cross-section of the laterally inclined ship shown in Fig. 2.1 at a certain ship's longitudinal ordinate x. Since the areas of the right triangles $\triangle WoW'$ and $\triangle LoL'$ in the exposed and immersed parts of the cross-section are equal, they are written as a, and their centroids of area are written as c and c' respectively. Since a and c, c' are functions of x, the volumes v of the wedge-shaped AP-WoW'-FP and AP - LoL'- FP, their moving moments $v\cdot\overline{gg'}$, and the direction of $\overline{gg'}$ can be obtained by integrating from AP to FP in the longitudinal direction x, respectively, as follows :

$$\left.\begin{aligned} &v = \int_{AP}^{FP} a\, dx \\ &v\cdot\overline{gg'} = \int_{AP}^{FP} a\cdot\overline{cc'}\, dx \\ &\overline{gg'} \;/\!/\; \overline{cc'} \end{aligned}\right\} \quad \cdots\cdots (2.3)$$

Here, the line segment $\overline{gg'}$ connecting g and g' coincides with the line segment $\overline{cc'}$ connecting the areal centroid of the right triangles $\triangle WoW'$ and $\triangle LoL'$ in the cross-section, though the lengths are different, as shown in Fig. 2.1 and Fig. 2.2.

Hereafter, paying attention to the right triangle $\triangle LoL'$ of the immersive part shown in Fig. 2.2, let's determine the direction of $\overline{cc'}$ according to $\overline{oc'}$ on starboard side. This is the core of the argument in this chapter. Here, the heel angle due to lateral inclination is $\angle LoL' = \theta$, the angle formed by $\overline{oc'}$ and the base $\overline{oL}$ is $\angle Loc' = \varphi$, and the length of the triangular base $\overline{oL}$ corresponding to the half breadth of the water line WL is y. Here, the centroid c' of triangle $\triangle oLL'$ is located at two-thirds of $\overline{oL} = y$ in the base direction and one-third of $\overline{LL'} = y\tan\theta$ in the height direction, so the tangent of φ is obtained as :

$$\left.\begin{aligned} &\tan\varphi = \frac{\frac{1}{3}\overline{LL'}}{\frac{2}{3}\overline{oL}} = \frac{\frac{1}{2}\overline{LL'}}{\overline{oL}} = \frac{\frac{1}{2}y\tan\theta}{y} = \frac{1}{2}\tan\theta \\ &\therefore\ \varphi = \tan^{-1}\left(\frac{1}{2}\tan\theta\right) \end{aligned}\right\} \quad \cdots\cdots (2.4)$$

This result of the former in the above equation means that if we extend $\overline{oc'}$ through the centroid c' of the triangle $\triangle oLL'$, it will pass through the midpoint of the opposite side $\overline{LL'} = y\tan\theta$, which confirms what geometry teaches.

Now, if we assume that $|\varphi| \ll 1$ and $|\theta| \ll 1$ in the 2nd line of Eq. (2.4), the angle φ can be Taylor-expanded with respect to θ as follows :

$$\begin{aligned}\varphi &= \tan^{-1}\left(\frac{1}{2}\tan\theta\right) \\ &= \frac{1}{2}\tan\theta - \frac{1}{3}\left(\frac{1}{2}\tan\theta\right)^3 + \cdots \\ &= \frac{1}{2}\left(\theta + \frac{\theta^3}{3} + \cdots\right) - \frac{1}{24}\left(\theta + \frac{\theta^3}{3} + \cdots\right)^3 + \cdots \\ &= \frac{\theta}{2} + \frac{\theta^3}{8} + \cdots \end{aligned} \quad \cdots\cdots(2.5)$$

Strictly speaking, φ is slightly larger than $\frac{\theta}{2}$ according to the above equation, but the following relational expression is obtained when the heel angle θ is small to some extent, actually up to about 20°, in the range where W and L' in Fig. 2.2 are on both hull sides. Therefore, we find that φ is a half angle of θ as follows :

$$\varphi = \angle Loc' = \frac{\theta}{2} \quad \cdots\cdots(2.6)$$

By doing so, the direction of movement of $\overline{oc'}$, *i.e.* $\overline{cc'}$, could be correctly determined within the range of linear theory regarding the heel angle θ in the cross-section at longitudinal ordinate x.

Therefore, it is found from the former part of Eq. (2.2), the latter part of Eq. (2.3) and Eq. (2.6) that $\overline{BB'}$ in underwater volume moves in the same direction as $\overline{gg'}$ in wedge shape and $\overline{cc'}$ in cross-section, as follows :

$$\angle L''BB' \left(= \angle Log' = \angle Loc'\right) = \varphi = \frac{\theta}{2} \quad \cdots\cdots(2.7)$$

The conclusion of this section is that the direction $\angle L''BB'$ of movement $\overline{BB'}$ from the upright center of buoyancy B to the inclined center of buoyancy B' is the direction of the half angle of the heel angle θ.

2.2.2 Metacentric radius $\overline{BM}$ in the true physical sense

Let's apply Eq. (2.7), which is a consequence of the previous section, to $\triangle MBB'$ in the cross-section of the inclined ship shown in Fig. 2.2. Since $\angle L''BM$ is a right angle, the angle $\angle MBB'$ can be obtained as :

$$\angle MBB' = \angle L''BM - \angle L''BB' = \frac{\pi}{2} - \varphi = \frac{\pi}{2} - \frac{\theta}{2} \quad \cdots\cdots(2.8)$$

On the other hand, since the sum of the interior angles of a triangle is π, it can be written as follows :

$$\angle MBB' + \theta + \angle MB'B = \pi \quad \cdots\cdots(2.9)$$

Now, by using Eq. (2.8) in Eq. (2.9), the angle $\angle MB'B$ can be calculated as :

$$\angle MB'B = \pi - \theta - \angle MBB' = \pi - \theta - \left(\frac{\pi}{2} - \frac{\theta}{2}\right) = \frac{\pi}{2} - \frac{\theta}{2} \quad \cdots\cdots\cdots\cdots\cdots\cdots (2.10)$$

Therefore, since the right-hand sides of Eqs. (2.8) and (2.10) are equal, the following equality relation is obtained.

$$\angle MBB' = \angle MB'B \left(= \frac{\pi}{2} - \frac{\theta}{2}\right) \quad \cdots\cdots\cdots\cdots\cdots\cdots\cdots\cdots\cdots\cdots\cdots\cdots\cdots\cdots\cdots\cdots (2.11)$$

From this relationship, we can find that $\triangle MBB'$ is an isosceles triangle with transverse metacenter M as its vertex. As a result, we were able to show the following relation.

$$\overline{BM} = \overline{B'M} \quad \cdots\cdots\cdots\cdots\cdots\cdots\cdots\cdots\cdots\cdots\cdots\cdots\cdots\cdots\cdots\cdots\cdots\cdots\cdots\cdots\cdots\cdots\cdots\cdots\cdots\cdots (2.12)$$

From this equality relation, it can be seen that both $\overline{BM}$ and $\overline{B'M}$ are geometrically the radii of the circle centered on the M, and the metacenter M correctly means *the Center of Inclination*. In this way, we have been able to derive a metacentric radius $\overline{BM}$ worthy of the name. We wouldn't like to think that it is self-righteousness of the authors to claim so.

2.2.3 Relationship between $\overline{BM}$ and $\overline{BB'}$

Let's find the moving distance $\overline{BB'}$ of the center of buoyancy according to the explanation in the

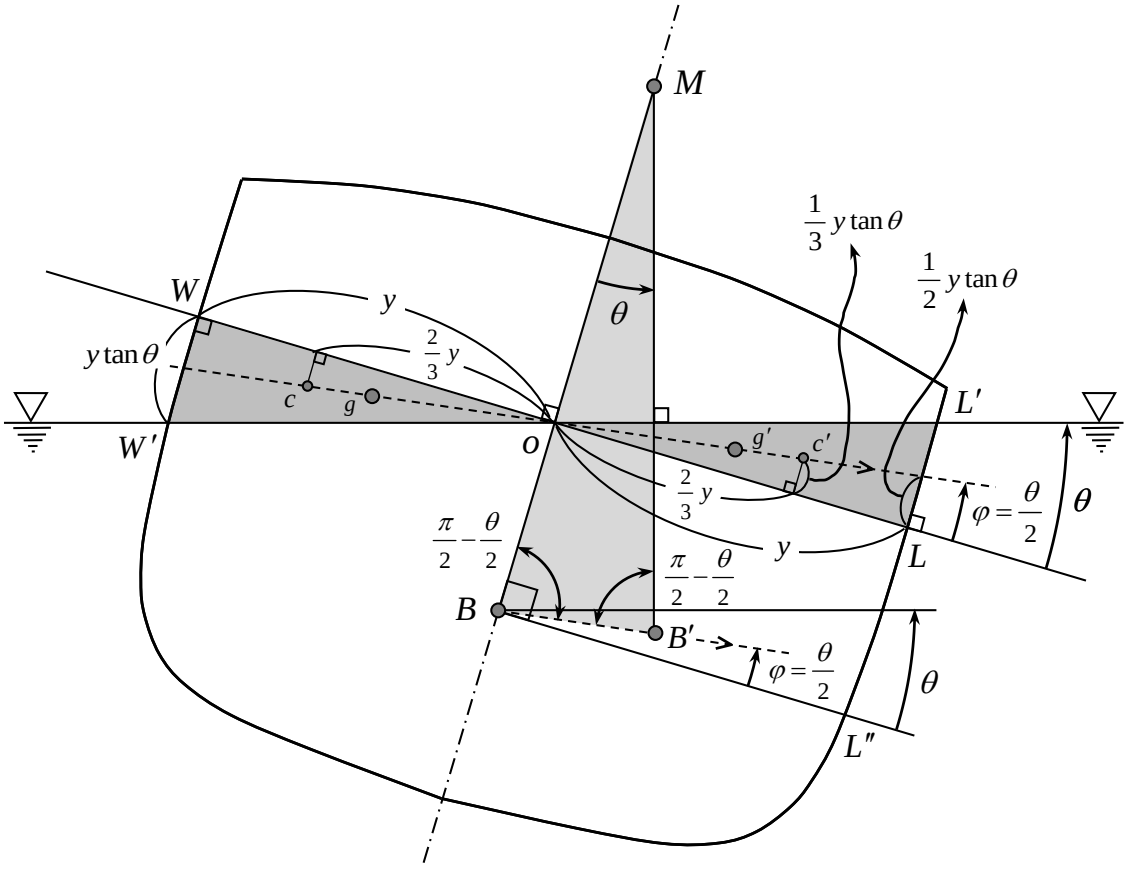

Fig. 2.2 Metacenter and movement of the center of buoyancy in the cross-section of a laterally inclined ship.

previous section. Applying the cosine theorem to the triangle $\triangle MBB'$ shown in Fig. 2.2, the square of $\overline{BB'}$ can be obtained by using Eq. (2.12), as follows :

$$\begin{aligned}\overline{BB'}^{\,2} &= \overline{BM}^{\,2} + \overline{B'M}^{\,2} - 2\,\overline{BM}\cdot\overline{B'M}\,\cos\theta \\ &= 2\,\overline{BM}^{\,2}(1-\cos\theta) = 4\,\overline{BM}^{\,2}\sin^2\frac{\theta}{2} \\ &= \overline{BM}^{\,2}\left(\theta^2 - \frac{\theta^4}{12} + \cdots\right) \end{aligned} \quad \cdots\cdots(2.13)$$

Then, by taking the square root of the above equation, $\overline{BB'}$ can be calculated as twice the sine component of the half vertex angle $\frac{\theta}{2}$ for the side length $\overline{BM}$ of isosceles triangle $\triangle MBB'$, as follows :

$$\begin{aligned}\overline{BB'} &= \overline{BM}\sqrt{2(1-\cos\theta)} = 2\,\overline{BM}\sin\frac{\theta}{2} \\ &= \overline{BM}\left(\theta - \frac{\theta^3}{24} + \cdots\right) \end{aligned} \quad \cdots\cdots(2.14)$$

Here, the bottom line of both Eqs. (2.13) and (2.14) above are the results by means of the Taylor expansion of $\cos\theta$ or $\sin\frac{\theta}{2}$ with respect to θ, assuming $|\theta| \ll 1$.

Therefore, when the heel angle θ is somewhat small, the moving distance $\overline{BB'}$ of the center of buoyancy can be obtained in a simple form by using only the 1st term in the 2nd line of Eq. (2.14), as follows :

$$\overline{BB'} = \overline{BM}\,\theta \quad \left(=\overset{\frown}{BB'}\right) \quad \cdots\cdots(2.15)$$

Hence, the result of the above Eq. (2.15) shows that the line segment $\overline{BB'}$ is equal to the arc length $\overset{\frown}{BB'}$ with $\overline{BM}$ as its radius, when θ is small to some extent.

Therefore, the metacentric radius $\overline{BM}$ can be calculated by solving Eq. (2.15) as follows :

$$\overline{BM} = \frac{\overline{BB'}}{\theta} \quad \cdots\cdots(2.16)$$

The above Eq. (2.16) shows that $\overline{BM}$ can be determined by dividing the moving distance $\overline{BB'}$ of the center of buoyancy by heel angle θ.

2.2.4 Moving distance $\overline{BB'}$ of the center of buoyancy

In this section, let us determine the moving distance $\overline{BB'}$ by using the dynamical law of Eq. (2.2). The area a of each of the right triangles $\triangle WoW'$ and $\triangle LoL'$ in the cross-section shown in Fig. 2.2 and the line segment $\overline{cc'}$ connecting their centroid can be written as follows, using the important Eq. (2.6), where $\varphi = \frac{\theta}{2}$.

$$\left.\begin{aligned} a &= \frac{1}{2}y^2\tan\theta = \frac{1}{2}y^2\left(\theta + \frac{\theta^3}{3} + \cdots\right) \\ \overline{cc'} &= 2\,\overline{oc'} = \frac{4}{3}y\sec\frac{\theta}{2} = \frac{4}{3}y\left(1 + \frac{\theta^2}{8} + \cdots\right) \end{aligned}\right\} \quad \cdots\cdots(2.17)$$

Here, in the above equation, the Taylor-expanded form for θ is also given. The moving moment $a \cdot \overline{cc'}$ is then the product of the two in Eq. (2.17), and is calculated as follows :

$$a \cdot \overline{cc'} = \frac{2}{3} y^3 \tan\theta \sec\frac{\theta}{2}$$
$$= \frac{2}{3} y^3 \left(\theta + \frac{\theta^3}{3} + \cdots \right) \cdot \left(1 + \frac{\theta^2}{8} + \cdots \right) = \frac{2}{3} y^3 \left(\theta + \frac{11}{24} \theta^3 + \cdots \right) \quad \cdots\cdots\cdots\cdots (2.18)$$

Hence, when the heel angle θ is somewhat small, the moving moment $a \cdot \overline{cc'}$ can be obtained by using the 1st order term with respect to θ in the above Eq. (2.18), as follows :

$$a \cdot \overline{cc'} = \frac{2}{3} y^3 \theta \quad \cdots\cdots\cdots\cdots\cdots\cdots\cdots\cdots\cdots\cdots\cdots\cdots\cdots\cdots\cdots\cdots\cdots\cdots\cdots\cdots (2.19)$$

Now, by integrating the above Eq. (2.19) from the stern *AP* to the bow *FP* in the longitudinal direction *x*, as shown in the middle part of Eq. (2.3), the moving moment $v \cdot \overline{gg'}$ of the wedge-shaped volume *v* can be calculated as follows :

$$v \cdot \overline{gg'} = \int_{AP}^{FP} a \cdot \overline{cc'} \, dx = \frac{2}{3} \theta \int_{AP}^{FP} y^3 dx$$
$$= \theta \int_{AP}^{FP} \frac{(2y)^3}{12} dx = I_{CL} \cdot \theta \quad \cdots\cdots\cdots\cdots\cdots\cdots\cdots\cdots\cdots\cdots\cdots (2.20)$$

Here, since the integral in the above Eq. (2.20) corresponds to the quadratic moment of the rectangle of height $2y$ and width dx, it represents the quadratic moment I_{CL} with respect to *the Center Line* of the water plane, as shown by the single-dotted line in Fig. 2.1. Therefore, the moving distance $\overline{BB'}$ of the center of buoyancy can be determined by the latter part of the dynamical law in Eq. (2.2), as follows :

$$\overline{BB'} = \frac{v \cdot \overline{gg'}}{V} = \frac{I_{CL} \cdot \theta}{V} \quad \cdots\cdots\cdots\cdots\cdots\cdots\cdots\cdots\cdots\cdots\cdots\cdots\cdots\cdots\cdots\cdots\cdots\cdots\cdots\cdots (2.21)$$

The above Eq. (2.21) shows that the moving distance $\overline{BB'}$ can be calculated by dividing the product of the quadratic moment I_{CL} and the heel angle θ shown in Eq. (2.20) by the underwater volume *V* of a ship.

2.2.5 Calculation formula for the metacentric radius $\overline{BM}$

According to the results of Sections 2.2.3 and 2.2.4, the transverse metacentric radius $\overline{BM}$ can be determined by substituting the moving distance $\overline{BB'}$ obtained in Eq. (2.21) for the numerator of the right-hand side in Eq. (2.16), as follows :

$$\overline{BM} = \frac{\overline{BB'}}{\theta} = \frac{\dfrac{I_{CL} \cdot \theta}{V}}{\theta} = \frac{I_{CL}}{V} \quad \cdots\cdots\cdots\cdots\cdots\cdots\cdots\cdots\cdots\cdots\cdots\cdots\cdots\cdots\cdots\cdots\cdots\cdots\cdots\cdots (2.22)$$

The metacentric radius $\overline{BM}$ of the above Eq. (2.22) can be calculated only by the geometric shape of the ship under the water plane, regardless of the heel angle θ which cancels out the numerator and denominator. Therefore, $\overline{BM}$ has a meaning as a parameter which governs the stability performance of a ship. The result itself is a well-known formula that can be found in any textbook [7-c),(8-b),(9-b),(12-b),(41),(42-a),(43)~(47)] of naval architecture and nautical mechanics.

2.3 Some Considerations

In this chapter, we will consider the explanations given in the textbooks so far.

In most textbooks[7-c),(8-b),(9-b)(12-b),(41),(43)], the moving direction of the center of buoyancy due to lateral inclination is approximated as follows, by assuming that heel angle θ in Fig. 2.2 is tends to zero.

$$\left.\begin{array}{l} \overline{BB'} \,/\!/\, \overline{WL} \\ \angle MBB' = \dfrac{\pi}{2} \end{array}\right\} \quad \cdots\cdots (2.23)$$

As a result, the moving distance $\overline{BB'}$ of the center of buoyancy is often described as :

$$\overline{BB'} = \overline{BM}\ \tan\theta \quad \cdots\cdots (2.24)$$

Here, Goldberg[7-c], Nishikawa[8-b], Ohgushi[9-b] and Akedo[12-b] specify the Eq. (2.23).

In addition, Sugihara[42-a], Nohara & Shoji[44], Barrass & Derrett[45], and Shin[47] do not specify the direction of movement $\overline{BB'}$, but they write its moving distance as well as Eq. (2.15) in Section 2.2.3, as follows :

$$\overline{BB'} = \overline{BM}\ \theta \quad \cdots\cdots (2.25)$$

On the other hand, recent work by Ikeda & Furukawa *et al.*[46] accurately calculated the moving component parallel to $\overline{WL}$, not the moving distance $\overline{BB'}$. If we use the results of Eqs. (2.11) and (2.12) and write it in the notation of this chapter, then it coincides with Eq. (2.14) in Section 2.2.3, as follows :

$$\left.\begin{array}{l} \overline{BB'} \cos\dfrac{\theta}{2} = \overline{B'M}\ \sin\theta \\ \therefore\ \overline{BB'} = 2\,\overline{B'M}\ \sin\dfrac{\theta}{2} = 2\,\overline{BM}\ \sin\dfrac{\theta}{2} \end{array}\right\} \quad \cdots\cdots (2.26)$$

After all, the correct direction of movement of $\overline{BB'}$ is still not mentioned, and the above researchers, other than the authors, derive the result by avoiding it.

2.4 Summary of the Obtained Results

It is claimed in this chapter that the direction $\angle L''BB'$ of movement $\overline{BB'}$ from the upright center of buoyancy B to the inclined center of buoyancy B' is the direction of the half angle of the heel angle θ due to lateral inclination, as follows :

$$\angle L''BB' \left(= \angle Log' = \angle Loc' \right) = \varphi = \frac{\theta}{2} \quad \cdots\cdots \text{previously written (2.7)}$$

Here, the above equation is obtained by the moving direction $\angle Loc'$ of a partial area from the exposed to the immersed portion, as given in Eq. (2.6).

As a result, we obtained the following relationship using by Eq. (2.7) of Section 2.2.2.

$$\angle MBB' = \angle MB'B \left(= \frac{\pi}{2} - \frac{\theta}{2} \right) \quad \cdots\cdots\cdots\cdots\cdots\cdots \text{ previously written (2.11)}$$

By doing so, since we were able to show that $\triangle MBB'$ shown in Fig. 2. 2 is an isosceles triangle with metacenter M as its vertex, the following Eq. (2.12) was found as the radii centered on the metacenter M .

$$\overline{BM} = \overline{B'M} \quad \cdots\cdots\cdots\cdots\cdots\cdots\cdots\cdots\cdots\cdots \text{ previously written (2.12)}$$

In this way, it is considered that the metacentric radius $\overline{BM}$ suitable for the name could be derived geometrically, and the metacenter *M* correctly means *the Center of Inclination*.

As mentioned above, the conclusions of this chapter can be summarized in the above Eqs. (2.7), (2.11) and (2.12), derived in Sectios 2.2.1 and 2.2.2.

Subsequently, the relationship between the metacentric radius $\overline{BM}$ and the moving distance $\overline{BB'}$ of the center of buoyancy was examined detailedly in Section 2.2.3, and the well-known formula in Eq. (2.22) for the $\overline{BM}$ was described within the framework of the linear theory for the heel angle θ , according to the usual method in Sections 2.2.4 and 2.2.5,.

2. 5 Concluding Remarks

One of the authors[52] has been teaching "*Hydrostatics of Floating Bodies*" as a compulsory subject in the Department of Naval Architecture (currently the Naval Architecture Course[53),(54)]) at *the Nagasaki Institute of Applied Science* for more than ten years. Every year, especially in the last few years, I have been guilty of somewhat misrepresenting the moving direction of the center of buoyancy $\overline{BB'}$ due to lateral inclination when explaining the theory of metacenter, which is the title of this chapter. I have been lecturing on it, telling myself that it is an approximation by a minimal angle of inclination. I was always going to the lecture with reluctant heart because I was afraid of being questioned by the excellent students.

By summarizing this chapter, we felt relieved from this worry. But we thought that it should not be self-righteous, so we submitted it. We are prepared to receive criticism from the great scholars who already know the theory developed in this chapter and are lecturing as such. In addition, if the contents of this chapter have already been published in textbooks or papers, please forgive it as a lack of searching the related literature by illiterate authors.

Chapter 3
Stable Conditions in the Upright State on the Hydrostatic Stability of Ships

In this Chapter 3, a theoretical treatment on the hydrostatic stability of ships is presented. As the simplest hull form, a columnar ship with rectangular cross-section, which is made of homogeneous squared timber with arbitrary breadth and arbitrary material, is chosen.

In this chapter, the conditions under which the ship is stable in the upright state with horizontal deck are analyzed by means of ship's hydrostatics. By doing so, the dependence of the stable conditions on the breadth and material of the ship will be clarified.

3. 1 Introduction

One of the authors [52] lectures on the hydrostatic stability of ships to 2nd year students of the naval architectural engineering course [53),(54] in the faculty of engineering at the university where the author works. In the 1st semester, the basics of the hydrostatic of floating bodies, such as buoyant force and center of buoyancy as shown in Chapter 1, are taught in the course "*Hydrostatics of Floating Bodies*" as a compulsory subject. In the 2nd semester, the theory of derivation of metacentric radius which is the main theme of the lecture on "*Theory of Ship Stability*", is explained as shown in Chapter 2, and then some simple examples are given to deepen the understanding of the theory. Probably, universities and colleges of technology in naval architecture, marine engineering and nautical mechanics all over the country also teach the above-mentioned flow of lectures, although the subject titles may differ.

As a typical example, many textbooks on naval architecture [9-c] and nautical mechanics [12-c),(42-b] describe that a columnar ship with a square cross-section, which is made of timber with half the specific weight of water, cannot float stably when one side of the square is horizontal, but the ship is stable when it is inclined laterally and the diagonal of the square is parallel to the water line. This consequence is explained by the positional relationship between the metacenter and the center of gravity.

Taking the above typical example one step further, how wide of breadth will can a columnar ship of rectangular cross-section, made of timber with half the specific weight of water, float stably with its long side horizontal ? Or, what specific weight of material (*i.e.,* lighter or heavier than timber) will can a square cross-sectional columnar ship float stably with one side horizontal ? By setting such examples, the 1st author [52] has been lecturing on this problem for several years in the subject of "*Theory of Ship Stability*" at the author's university [53),(54].

As a result, the degree of understanding of students for the hydrostatic stability of ships has improved significantly compared to before the lecture, so we think that this information should be provided to teachers and students who will teach and learn this field in the future, and we will give some examples. One of the authors gave an explanation of effective examples and published it in the journal [55] "*NAVIGATION*" of Japan Institute of Navigation at 2021.

We subsequently summarized the theoretical treatment of these examples in English, and published it on this viXra.org[56] and in the bulletin of our university, Nagasaki Institute of Applied Science[57].

In this Chapter 3, we will describe them consistently.

3. 2 Stable Conditions for a Columnar Ship of Rectangular Cross-Section with Arbitrary Material α and Arbitrary Breadth β

Fig. 3.1 shows a columnar ship of length L with a rectangular cross-section of depth h and breadth βh, which is a squared timber of specific weight γ_t made of homogeneous material. Let's consider determining the conditions under which the columnar ship can float stably with its long side βh parallel to the water line (*i.e.* upright state) in water of specific weight γ_w. The left side of Fig. 3.1 shows the upright state, and the right side shows the forces and moment acting on the cross-section inclined by heel angle θ.

As a setting variable, the ratio of the specific weight of the columnar ship, γ_t (where t is the initial letter of *timber*), to the specific weight of water, γ_w (where w is the initial letter of *water*), is defined as $\boldsymbol{\alpha}$ (hereafter referred to as ***material***), and the ratio of the breadth, βh, to the depth, h, of the cross-section (*i.e.* aspect ratio) is defined as $\boldsymbol{\beta}$ (hereafter referred to as ***breadth***), as follows :

$$\left.\begin{aligned} \alpha &\equiv \frac{\gamma_t}{\gamma_w} \quad (where,\ 0<\alpha\le 1) \\ \beta &\equiv \frac{breadth}{depth} = \frac{\beta h}{h} \quad (where,\ \beta > 0) \end{aligned}\right\} \cdots\cdots (3.1)$$

Here, when γ_w is fresh water, α represents the specific gravity of the columnar ship.

First, let us consider the determination of the draft d. *The Weight* W and *the Buoyant Force* F_B (to be described separately from the center of buoyancy B) of this columnar ship can be obtained as follows, respectively :

$$\left.\begin{aligned} W &= \gamma_t V_t = \gamma_t \cdot \beta h \cdot h \cdot L \\ F_B &= \gamma_w V_w = \gamma_w \cdot \beta h \cdot d \cdot L \end{aligned}\right\} \cdots\cdots (3.2)$$

Here, the weight W of the former is obtained as the product of the specific weight γ_t and the total volume V_t of the columnar ship. And *the buoyant force* F_B of the latter, which is hereafter denoted as *the buoyancy*, is obtained as the product of the specific weight γ_w of water and the displacement volume V_w of underwater portion, according to Archimedes' principle[1] as shown in Eq. (1.6) of Chapter 1.

The floating body is stable under the following conditions where the weight W and buoyancy F_B are in equilibrium.

$$W = F_B \cdots\cdots (3.3)$$

Substituting W and F_B in Eq. (3.2) into both sides of the above, we obtain as :

$$\gamma_t \cdot \beta h \cdot h \cdot L = \gamma_w \cdot \beta h \cdot d \cdot L \quad \cdots\cdots (3.4)$$

By solving the above equation, the undetermined draft d can be determined as α times the depth h, as follows :

$$d = \frac{\gamma_t}{\gamma_w} h = \alpha h \quad \cdots\cdots (3.5)$$

Next, let's determine the location of *the Metacenter M,* meaning *the Center of Inclination*.

The metacentric radius $\overline{BM}$ (distance between the center of buoyancy B and the metacenter M) can be calculated by using the basic formula of naval architecture, Eq. (2.22) derived in Chapter 2 :

$$\overline{BM} = \frac{I_{CL}}{V_w} \quad \cdots\cdots (3.6)$$

Here, the numerator, I_{CL}, is the quadratic moment about the center line of water plane (the single-dotted chain line in the left side of Fig. 1, where the subscript CL is the abbreviation of *Center Line*), and the denominator, V_w, is the underwater volume of a ship.

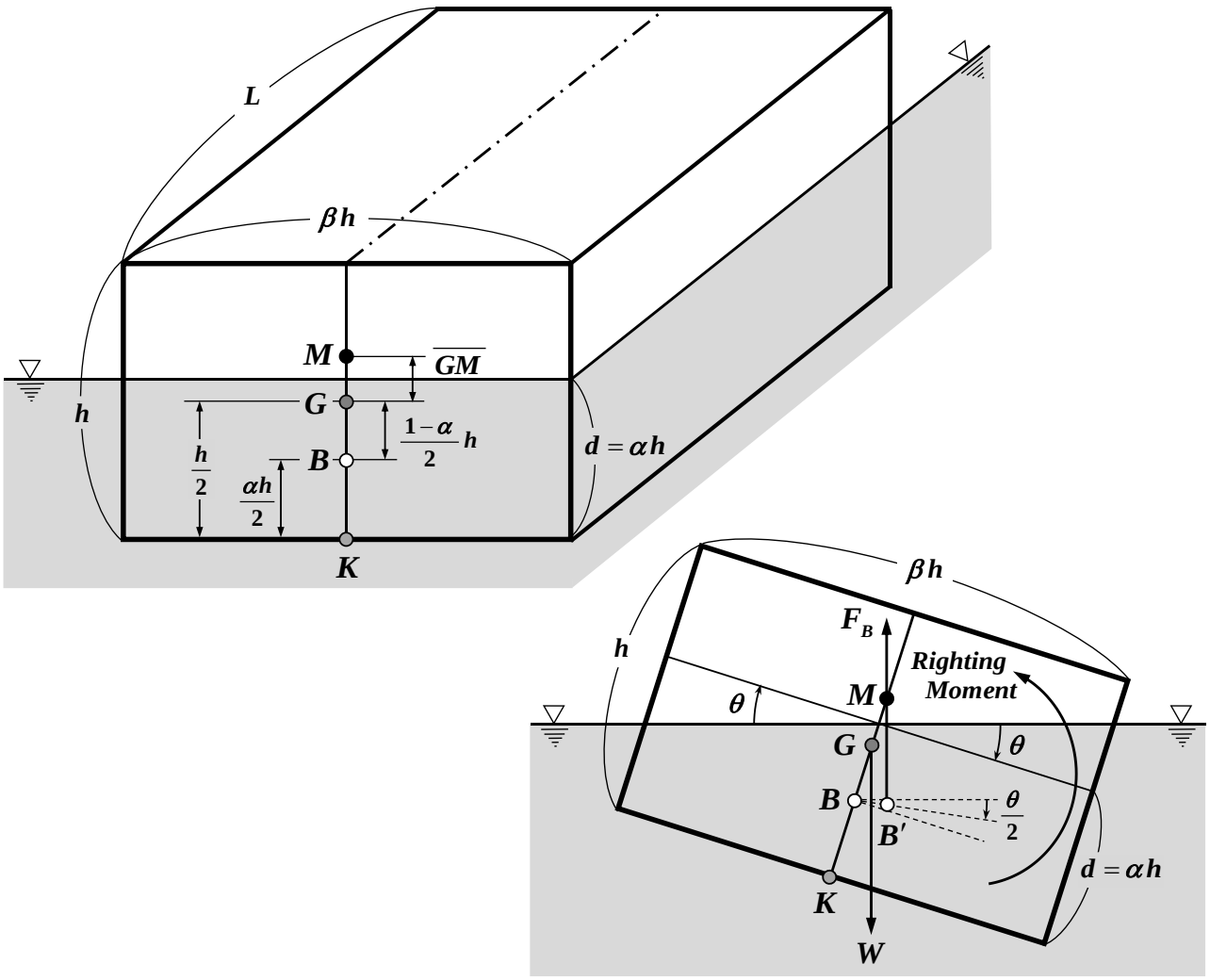

Fig. 3.1 Upright (left) and laterally Inclined (right) states of a columnar ship with rectangular cross-section.

In this case, the numerator and denominator of Eq. (3.6) can be calculated as follows :

$$\left.\begin{aligned} I_{CL} &= \frac{1}{12}(\beta h)^3 L \\ V_w &= \beta h \cdot d \cdot L = \beta h \cdot \alpha h \cdot L = \alpha \beta h^2 L \end{aligned}\right\} \quad \cdots\cdots (3.7)$$

In the above equation, the former, I_{CL}, refers to the fact that the water plane is a rectangle of length L and breadth βh, as shown in Fig. 3.1 (left), and the denominator, V_w, refers to the fact that the draft is $d = \alpha h$, as determined by Eq. (3.5).

By using the result of Eq. (3.7) into Eq. (3.6), $\overline{BM}$ can be calculated independently of the ship's length L as follows :

$$\overline{BM} = \frac{\frac{1}{12}(\beta h)^3 L}{\alpha \beta h^2 L} = \frac{\beta^2}{12\alpha} h \quad \cdots\cdots (3.8)$$

Furthermore, let's find $\overline{BG}$ (distance between the center of buoyancy B and the center of gravity G).

As shown in Fig. 3.1 (left), *the center of Gravity*, G is located at the centroid of the rectangular cross-section and *the center of Buoyancy*, B is located at the centroid of the rectangle below the water surface, as shown in Section 1.2 of Chapter 1. And the point on the centerline of the bottom of the ship is designated as K (abbreviation of *Keel*). Then, the distances from K to G and B are determined respectively as follows :

$$\left.\begin{aligned} \overline{KG} &= \frac{h}{2} \\ \overline{KB} &= \frac{d}{2} = \frac{\alpha h}{2} \end{aligned}\right\} \quad \cdots\cdots (3.9)$$

Therefore, the distance $\overline{BG}$ between B and G can be obtained as follows :

$$\begin{aligned} \overline{BG} &= \overline{KG} - \overline{KB} \\ &= \frac{h}{2} - \frac{\alpha h}{2} = \frac{1-\alpha}{2} h \end{aligned} \quad \cdots\cdots (3.10)$$

From the above preparatory calculations, *the metacentric height* $\overline{GM}$ (the distance between the center of gravity G and the metacenter M) can be determined by subtracting Eq. (3.10) from Eq. (3.8), as follows :

$$\begin{aligned} \overline{GM} &= \overline{BM} - \overline{BG} \\ &= \frac{\beta^2}{12\alpha} h - \frac{1-\alpha}{2} h = \frac{\beta^2 - 6\alpha + 6\alpha^2}{12\alpha} h \end{aligned} \quad \cdots\cdots (3.11)$$

In order to float stably in the upright state as shown in Fig. 3.1 (left), where the long side of the columnar ship is parallel to the water line, it is required that the stability force (mechanically, the righting moment) acts to return the ship from the inclined state to the upright state, as shown in Fig. 3.1

(right). For this purpose, the metacenter M must be located above the center of gravity G. In other words, the metacentric height should be a positive value, and the stable condition can be described as follows :

$$\overline{GM} > 0 \quad \cdots\cdots (3.12)$$

If we use the result obtained in Eq. (3.11) for the left-hand side of the above inequality, it can be written as follows :

$$\overline{GM} = \frac{\beta^2 - 6\alpha + 6\alpha^2}{12\alpha} h > 0 \quad \cdots\cdots (3.13)$$

Both h in the above equation and α in the denominator are a positive value. Mathematically, it is only necessary that the numerator be positive. As a result, the stable condition of this example shown in Fig. 3.1 is obtained as follows :

$$\beta^2 - 6\alpha + 6\alpha^2 > 0 \quad \cdots\cdots (3.14)$$

3.2.1 Stable conditions of a columnar ship for breadth β with fixed material α

First, in Section 3.2.1, we will fix the material α of the columnar ship and consider what breadth β will make it float stably with its long side horizontal, as shown in Fig. 3.1 (left).

By solving the stable condition in Eq. (3.14) for β, we obtain as :

$$\begin{aligned} \beta^2 &> 6\alpha - 6\alpha^2 = 6\alpha(1-\alpha) \\ &= \frac{3}{2} - 6\left(\alpha - \frac{1}{2}\right)^2 \equiv \Omega \end{aligned} \quad \cdots\cdots (3.15)$$

If the right-hand side of the above equation is written as Ω, it can be seen that it is stable when the following Eq. (3.16) is satisfied :

$$\beta > \sqrt{\Omega} = \sqrt{6\alpha(1-\alpha)} \quad \cdots\cdots (3.16)$$

As a result, it shows that $\sqrt{\Omega}$ is the limiting value of breadth for stable floating.

For example, in the case of a timber with $\alpha = \frac{1}{2}$, the stable β is calculated as follows. Thus, it indicates that the timber is stable, if the breadth is at least about 1.3 times wider than the depth.

$$\beta\Big]_{\alpha=\frac{1}{2}} > \sqrt{6 \cdot \frac{1}{2} \cdot \frac{1}{2}} = \frac{\sqrt{6}}{2} \fallingdotseq 1.225 \quad \cdots\cdots (3.17)$$

As a result, a square with $\beta = 1$ cannot float stably with one side horizontal. And it encompasses what is written in many textbooks as typical examples [12-c), 42-b)] and problems [9-c)].

Let us examine the dependence of the stable breadth limit $\sqrt{\Omega}$ on the material α.

The relationship between α and $\sqrt{\Omega}$ represents an ellips, since Eq. (3.15) can be rewritten as :

$$\frac{\sqrt{\Omega}^2}{\left(\frac{\sqrt{6}}{2}\right)^2}+\frac{\left(\alpha-\frac{1}{2}\right)^2}{\left(\frac{1}{2}\right)^2}=1 \quad \cdots\cdots\cdots (3.18)$$

As shown in Fig. 3.2, $\sqrt{\Omega}$ has a maximum value of $\frac{\sqrt{6}}{2}$ at $\alpha=\frac{1}{2}$, and becomes zero at $\alpha=0,1$ of both ends.

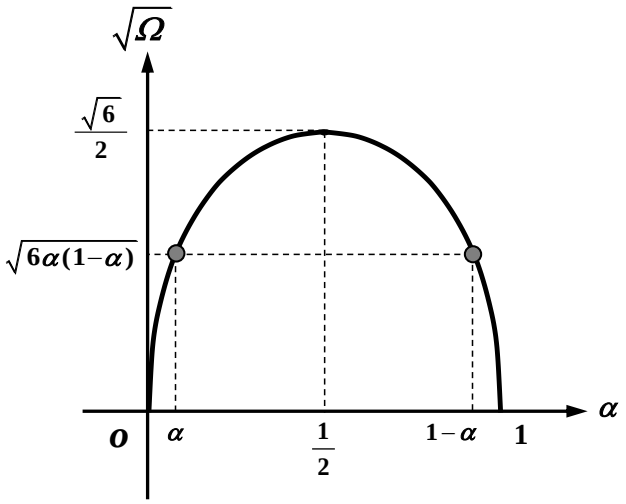

Fig. 3.2 Relationship between limiting value $\sqrt{\Omega}$ of stable breadth and material α.

Therefore, Eq. (3.17) for $\alpha=\frac{1}{2}$ above is the most stringent condition of breadth. When the material α is lighter or heavier than the above, the limiting value $\sqrt{\Omega}$ of β will be smaller, and it is stable even if the breadth is narrower than 1.3 times the depth.

As shown in the following example of calculation, the limiting value $\sqrt{\Omega}$ of β becomes smaller than 1.225 as it moves away from the center of $\alpha=\frac{1}{2}$ to both sides (the light and heavy sides). In particular, when α is $\frac{1}{5}$ or $\frac{4}{5}$, the limit value of β is 0.98, and it can be seen that the timber is stable, even if the breadth is narrower than the square ($\beta=1$).

$$\left.\begin{aligned}
&\alpha=\frac{1}{3},\frac{2}{3} \rightarrow \beta>\sqrt{6\cdot\frac{1}{3}\cdot\frac{2}{3}}=\frac{2\sqrt{3}}{3}\fallingdotseq 1.155\\
&\alpha=\frac{1}{4},\frac{3}{4} \rightarrow \beta>\sqrt{6\cdot\frac{1}{4}\cdot\frac{3}{4}}=\frac{3\sqrt{2}}{4}\fallingdotseq 1.061\\
&\alpha=\frac{1}{5},\frac{4}{5} \rightarrow \beta>\sqrt{6\cdot\frac{1}{5}\cdot\frac{4}{5}}=\frac{2\sqrt{6}}{5}\fallingdotseq 0.980
\end{aligned}\right\} \cdots\cdots\cdots\cdots\cdots\cdots (3.19)$$

It is also physically interesting to note, as we can see from the factors in Eq. (3.16) and the results in Eq. (3.19), that the limiting value $\sqrt{\Omega}$ of stable β is the same for materials α and $1-\alpha$, as shown by the symbols of ● in Fig. 3.2.

3.2.2 Stable conditions of a columnar ship for material α with fixed breadth β

Next, in section 3.2.2, we will fix the breadth β of the columnar ship and consider what kind of material α will make it float stably with its long side parallel to the water line, as shown in Fig. 3.1 (left). Let's consider about this.

In order to solve the stable condition in Eq. (3.14) for α, we put Γ on the left-hand side and complete the square as follows :

$$\begin{aligned}\Gamma &= 6\alpha^2 - 6\alpha + \beta^2 \\ &= 6\left(\alpha - \frac{1}{2}\right)^2 + \frac{2\beta^2 - 3}{2} \end{aligned} \quad \cdots\cdots\cdots (3.20)$$

Then, the stable condition in Eq. (3.14) can be written as :

$$\Gamma > 0 \quad \cdots\cdots\cdots\cdots\cdots\cdots\cdots\cdots (3.21)$$

Since the situation of the above quadratic equation Γ with respect to α differs depending on whether the constant term $2\beta^2 - 3$ is positive or negative value, the following cases (i) and (ii) are examined separately.

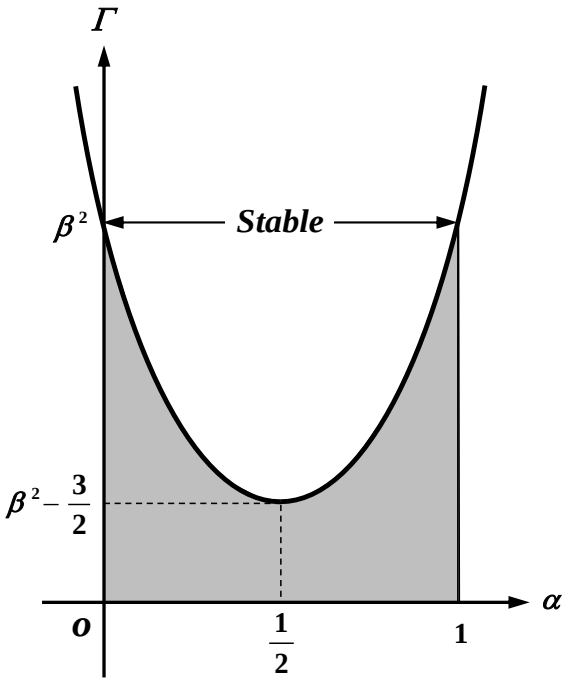

Fig. 3.3 Case of $2\beta^2 > 3$ for wide breadth.

3.2.2 (i) Case of $2\beta^2 > 3$ $\left(i.e.\ \beta > \frac{\sqrt{6}}{2}\right)$ for wide breadth

In this case, Γ in Eq. (3.20) is a downwardly convex shape and it is always positive in the range painted in gray, as shown in Fig. 3.3. Therefore, since the stable condition of Eq. (3.21) is satisfied regardless of α, the floating body is always stable in the upright state.

This case (i) coincides with the stable condition of β for $\alpha = \frac{1}{2}$ in Eq. (3.17) of Section 3.2.1.

3.2.2 (ii) Case of $2\beta^2 < 3$ $\left(i.e.\ \beta < \frac{\sqrt{6}}{2}\right)$ for narrow breadth

In this case, there are two solutions for $\Gamma = 0$ in Eq. (3.20), as follows :

$$\left.\begin{aligned}\alpha &= \frac{1}{2} \pm \frac{\sqrt{3(3-2\beta^2)}}{6} \equiv \frac{1}{2} \pm \kappa \\ &\left(where,\ \kappa \equiv \frac{\sqrt{3(3-2\beta^2)}}{6}\right)\end{aligned}\right\} \cdots\cdots\cdots\cdots\cdots\cdots\cdots\cdots (3.22)$$

These are the points of intersection with the α-axis, as indicated by the mark of ○ in Fig. 3.4. Since the quadratic equation Γ is a downwardly convex shape, the range painted in gray, which satisfies the stable condition $\Gamma > 0$ in Eq. (3.21), can be written as follows :

$$\left.\begin{array}{l} 0 < \alpha < \dfrac{1}{2} - \kappa \quad (\textit{Light Material}) \\ \dfrac{1}{2} + \kappa < \alpha \le 1 \quad (\textit{Heavy Material}) \end{array}\right\} \quad \cdots\cdots(3.23)$$

From the above, it can be seen that the light and heavy materials on both sides around $\alpha = \dfrac{1}{2}$ are stable.

Furthermore, the unstable region 2κ, where $\Gamma < 0$, is obtained centering on $\alpha = \dfrac{1}{2}$ as follows :

$$2\kappa = \frac{\sqrt{3(3-2\beta^2)}}{3} \quad \cdots\cdots(3.24)$$

Here, the above equation can be rewritten as follows, representing an ellipse with major axis β and minor axis 2κ.

$$(2\kappa)^2 + \frac{\beta^2}{\left(\dfrac{\sqrt{6}}{2}\right)^2} = 1 \quad \cdots\cdots(3.25)$$

As shown in Fig. 3.5, 2κ is given by a point on the ellipse for β, $2\kappa = 0$ at $\beta = \dfrac{\sqrt{6}}{2}$ and $2\kappa = 1$ at $\beta = 0$. Thus, it can be seen that the unstable region 2κ expands as the breadth β becomes narrower.

Below, for three specific examples of β, the value of α which satisfies $\Gamma = 0$ is calculated by using κ in Eq. (3.22) as follows :

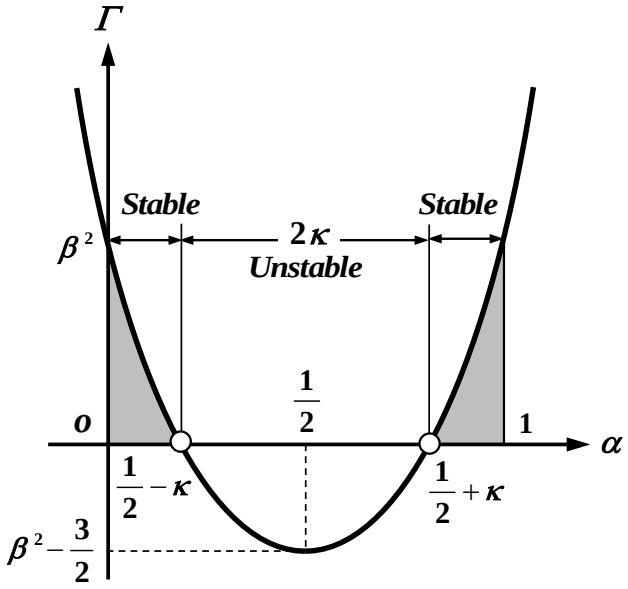

Fig. 3.4 Case of $2\beta^2 < 3$ for narrow breadth.

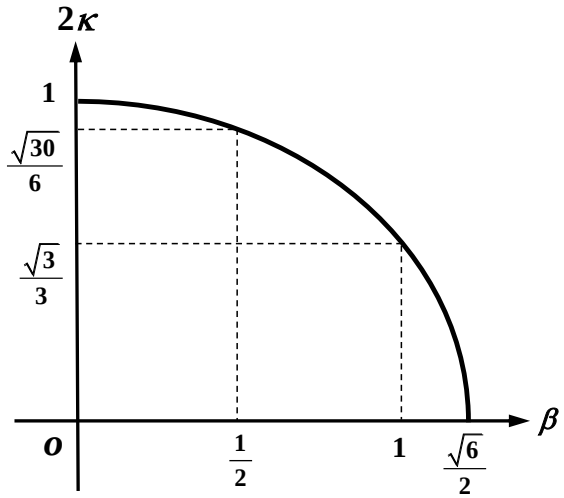

Fig. 3.5 Relationship between unstable region 2κ and breadth β.

$$\left.\begin{aligned}
&\beta = 1 \rightarrow \kappa = \frac{\sqrt{3(3-2\cdot 1)}}{6} = \frac{\sqrt{3}}{6} \fallingdotseq 0.289 \\
&\qquad \therefore \alpha = 0.5 \pm \kappa = 0.211,\ 0.789 \\
&\beta = \frac{1}{\sqrt{2}} \rightarrow \kappa = \frac{\sqrt{3\left(3-2\cdot\frac{1}{2}\right)}}{6} = \frac{\sqrt{6}}{6} \fallingdotseq 0.408 \\
&\fallingdotseq 0707 \qquad \therefore \alpha = 0.5 \pm \kappa = 0.092,\ 0.908 \\
&\beta = \frac{1}{2} \rightarrow \kappa = \frac{\sqrt{3\left(3-2\cdot\frac{1}{4}\right)}}{6} = \frac{\sqrt{30}}{12} \fallingdotseq 0.456 \\
&\qquad \therefore \alpha = 0.5 \pm \kappa = 0.044,\ 0.956
\end{aligned}\right\} \quad \cdots\cdots\cdots\cdots\cdots\cdots\cdots\cdots (3.26)$$

From the above results, it can be seen that as the breadth β becomes narrower, the stable regions outside the two α in Eq. (3.22), which satisfy $\Gamma = 0$, decrease.

3.2.3 $\alpha, \beta, \overline{GM}$ in the rectangular cross-section of Fig. 3.1

The material α and breadth β of the rectangular cross-section in Fig. 3.1 are as follows :

$$\left.\begin{aligned}
\alpha &= 0.58 \\
\beta &= 1.62
\end{aligned}\right\} \quad \cdots\cdots\cdots\cdots\cdots\cdots\cdots\cdots\cdots\cdots\cdots\cdots\cdots\cdots\cdots\cdots\cdots\cdots\cdots\cdots (3.27)$$

Then $\overline{GM}$ is calculated by using Eq. (3.13) as follows :

$$\overline{GM} = 0.167\, h > 0 \quad \cdots\cdots\cdots\cdots\cdots\cdots\cdots\cdots\cdots\cdots\cdots\cdots\cdots\cdots\cdots\cdots\cdots\cdots\cdots\cdots (3.28)$$

In fact, *B*, *G*, and *M* in Fig. 3.1 (left) show the positional relationship drawn correctly. Then as shown in Fig. 3.1 (right), the floating body is stable due to the righting moment which brings it back to the upright state from the laterally inclined state.

Further, in Fig. 3.1 (right), the center of buoyancy *B* in the upright state moves to the direction of half angle $\frac{\theta}{2}$ when it is inclined laterally by θ, as shown in Eq. (2.7) of previous Chapter 2. Then, the position of the center of buoyancy *B*′ after the inclination can be determined as the intersection of the above-mentioned half-angle directional line and the vertical line lowered from the metacenter *M*. Therefore, the position of *B*′ shown in Fig. 3.1 (right) is also the correct position under the setting variables of Eq. (3.27).

3.3 Stable Conditions for a Columnar Ship of Rectangular Cross-Section with Specified Material α and Breadth β

In Section 3.2, we have set up a problem in which both the material α and the breadth β take arbitrary values, and have shown how to solve it and determine the stable conditions.

When lecturing to students, it would be easier for them to understand, if we specify a representative value for either α or β. Section 3.3 is described from such a perspective.

3.3.1 Stable condition for breadth β of a columnar ship with material $\alpha = \frac{1}{2}$ (timber)

First, let's try to solve the example problem in Section 3.2.1 by using timber with $\alpha = \frac{1}{2}$ as the material from the beginning.

In this case, the stable condition of Eq.(3.15) becomes a very simple inequality, since the right-hand side is $\Omega = \frac{3}{2}$, as follows :

$$\beta^2 - \frac{3}{2} > 0 \quad \cdots\cdots (3.29)$$

The positive value of β satisfying the above equation can be obtained by mental calculation as follows. Then it coincides with the result of Eq.(3.17) in Section 3.2.1.

$$\beta > \sqrt{\frac{3}{2}} = \frac{\sqrt{6}}{2} \fallingdotseq 1.225 \quad \cdots\cdots (3.30)$$

This makes it easy to conclude that a rectangular columnar ship made of timber will float stably in the upright state, if its breadth is at least 1.3 times wider than its depth.

3.3.1 (i) Case of breadth $\beta = \frac{\sqrt{6}}{2}, \sqrt{3}$ with material $\alpha = \frac{1}{2}$

Here, for the stable condition related to the breadth β shown in Eq.(3.30) of Section 3.3.1, we will take two specific examples, $\beta = \frac{\sqrt{6}}{2}$, which is its limit value implying the neutral state, and $\beta = \sqrt{3}$, which satisfies its condition. And we will show the two states as follows :

By setting $\alpha = \frac{1}{2}$ in Eq.(3.13) of Section 3.2, $\overline{GM}$ in this case can be obtained as :

$$\overline{GM}\,\Big]_{\alpha=\frac{1}{2}} = \frac{2\beta^2 - 3}{12} h \quad \cdots\cdots (3.31)$$

Then, $\overline{GM}$ for the above two cases can be calculated respectively, as follows :

$$\left.\begin{aligned} &\beta = \frac{\sqrt{6}}{2}\ (\fallingdotseq 1.225) \\ &\quad \rightarrow \ \overline{GM} = \frac{2\cdot\frac{3}{2}-3}{12}h = 0 \quad (Neutral) \\ &\alpha = \sqrt{3}\ (\fallingdotseq 1.732) \\ &\quad \rightarrow \ \overline{GM} = \frac{2\cdot 3-3}{12}h = \frac{h}{4} \quad (Stable) \end{aligned}\right\} \cdots\cdots\cdots\cdots\cdots\cdots\cdots\cdots\cdots\cdots (3.32)$$

The shapes of the rectangular cross-sections and the positional relationship between *B*, *G*, and *M* for the above two states are shown in Fig. 3.6. The left figure shows the neutral state where *M* and *G* coincide. And if the breadth is even a little wider than the left, the timber can float stably with upright state as shown in the right figure. Here, in the right state of $\beta = \sqrt{3}$, *G* is located exactly midway between *B* and *M*.

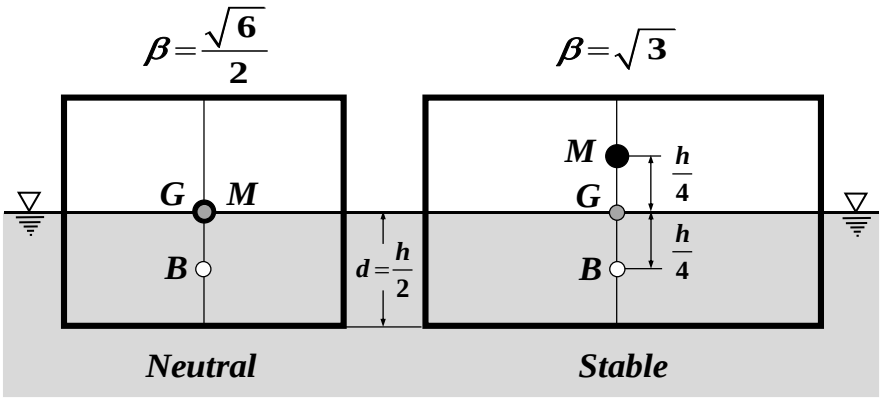

Fig. 3.6 Case of material $\alpha = \frac{1}{2}$, breadth $\beta = \frac{\sqrt{6}}{2}, \sqrt{3}$.

3.3.2 Stable condition for material α of a columnar ship with breadth $\beta = 1$ (square)

Next, let's solve the example in Section 3.2.2 by setting a square cross-section with breadth $\beta = 1$.

In this case, the stable conditions in Eqs. (3.20) and (3.21) become quadratic inequality about α, as follows :

$$\begin{aligned} \Gamma &= 6\alpha^2 - 6\alpha + 1 \\ &= 6\left(\alpha - \frac{1}{2}\right)^2 - \frac{1}{2} > 0 \end{aligned} \quad \cdots\cdots\cdots\cdots\cdots\cdots\cdots\cdots\cdots\cdots\cdots\cdots\cdots\cdots\cdots\cdots (3.33)$$

α satisfying $\Gamma = 0$ can be easily solved by the above equation for the latter completing the square, as follows :

$$\alpha = \frac{1}{2} \pm \frac{\sqrt{3}}{6} \fallingdotseq 0.211, 0.789 \quad \cdots\cdots (3.34)$$

This coincides with the result of the 1st case of Eq. (3.26) for the narrower breadth of Section 3.2.2 (ii).

Since Γ is a quadratic equation with downward convexity, as shown in Fig. 3.4, the range of α which satisfies the stable condition $\Gamma > 0$ in Eq. (3.33) is can be obtained as follows [12-c] :

$$\left.\begin{array}{l} 0 < \alpha < 0.211 \quad (\textit{Light Material : cork and Styrofoam etc.}) \\ 0.789 < \alpha \leq 1 \quad (\textit{Heavy Materials : rubber and leather etc.}) \end{array}\right\} \quad \cdots\cdots (3.35)$$

Here, in the above states, the draft of floating body for each α is $d = \alpha h$, as shown in Eq. (3.5).

On the other hand, the range of unstable α is as follows :

$$0.211 < \alpha < 0.789 \quad (\textit{Woods : Japanese cypress and larch etc.}) \quad \cdots\cdots (3.36)$$

The results show that a columnar ship of square cross-section floats stably with one side parallel to the water line for light materials such as cork and Styrofoam, and for heavy materials such as rubber and leather, as shown in Eq. (3.35). On the contrary, for woods such as Japanese cypress and larch, as shown in Eq. (3.36), the timber cannot float when one side is horizontal.

3.3.2 (i) Case of material $\alpha = \frac{1}{6}, \frac{5}{6}$ with breadth $\beta = 1$

Here, let us specifically take up light $\frac{1}{6}$ and heavy $\frac{5}{6}$ as the stable material α shown in Eq. (3.35) of Section 3.3.2, and show their stats.

The $\overline{GM}$ in this case can be calculated by setting $\beta = 1$ in Eq. (3.13) as follows :

$$\overline{GM}\,\Big]_{\beta=1} = \frac{1 - 6\alpha + 6\alpha^2}{12\alpha} h = \frac{1 - 6\alpha(1-\alpha)}{12\alpha} h \quad \cdots\cdots (3.37)$$

Therefore, using the above equation, $\overline{GM}$ for each light and heavy case can be obtained as follows:

$$\left.\begin{array}{l} \alpha = \dfrac{1}{6} \left(\fallingdotseq 0.167\right) \\ \quad \rightarrow \overline{GM} = \dfrac{1 - 6 \cdot \frac{1}{6} \cdot \frac{5}{6}}{12 \cdot \frac{1}{6}} h = \dfrac{\frac{h}{6}}{2} = \dfrac{h}{12} \\ \alpha = \dfrac{5}{6} \left(\fallingdotseq 0.833\right) \\ \quad \rightarrow \overline{GM} = \dfrac{1 - 6 \cdot \frac{5}{6} \cdot \frac{1}{6}}{12 \cdot \frac{5}{6}} h = \dfrac{\frac{h}{6}}{10} = \dfrac{h}{60} \end{array}\right\} \quad \cdots\cdots (3.38)$$

The floating states of these light and heavy materials are shown in Fig. 3.7, including the positional relationships of *B*, *G*, and *M*.

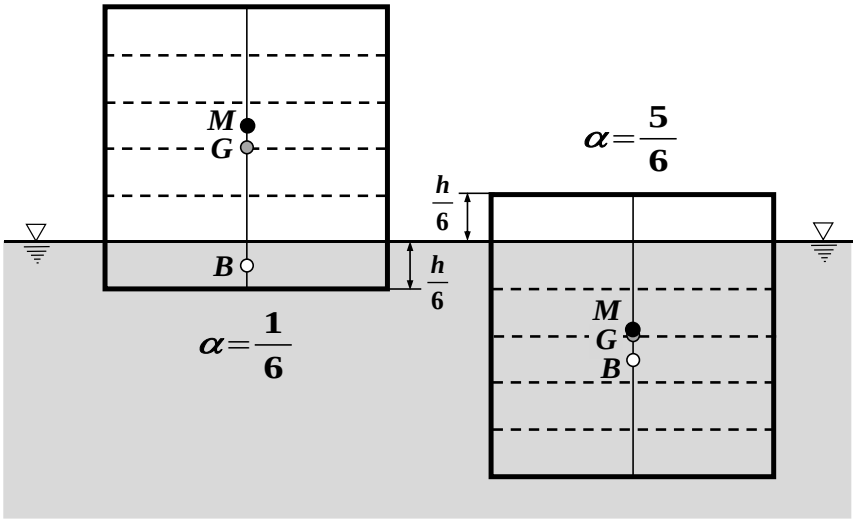

Fig. 3.7 Case of breadth $\beta = 1$, material $\alpha = \frac{1}{6}, \frac{5}{6}$.

3.4 Afterword

In this chapter, we have presented some examples which are effective in understanding the hydrostatic stability of ships from the 1st author's empirical point of view. It would be the authors' great pleasure, if this chapter could be of assistance to teachers and students who will teach and learn this field in the future.

Chapter 4
Stable Attitude in an Inclined State on the Hydrostatic Stability of Ships

In this Chapter 4, a theoretical treatment on the hydrostatic stability of ships is presented, following the previous Chapter 3. As the simplest hull form, a columnar ship with rectangular cross-section, which is made of homogeneous squared timber with arbitrary breadth and material, is chosen.

In this chapter, the stable attitude in an inclined state of the ship, which is not stable in the upright state with horizontal deck, is analyzed by means of ship's hydrostatics. By doing so, the dependence of the inclined attitude on the breadth and material of the ship will be clarified.

4. 1 Introduction

In the previous Chapter 3, as a typical example problem[55],[56],[57] related to the hydrostatic stability of ships, we solved the condition under which the ship floats stably in the upright state with horizontal deck, in terms of the positional relationship among the center of buoyancy, center of gravity and metacenter. At that time, the target hull form is a columnar ship with a rectangular cross-section, which is made of homogeneous squared timber with arbitrary breadth and material.

On the other hand, if the above conditions are not satisfied, under what inclined attitude does the ship float ? is also of interest from a mechanical point of view. Igarashi et al. of *the National Defense Academy of Japan* have elucidated this problem in detail based on geometrical considerations concerning the center of buoyancy and the center of gravity for the squared timber with square[58] and rectangular[59] cross-sections.

In this Chapter 4, as an extension of Chapter 3, we describe a theoretical treatment for solving the stable attitude of a columnar ship with a rectangular cross-section in an inclined state. The one of the authors gave an solution for the inclined attitude and published it in the journal[60] "*NAVIGATION*" of Japan Institute of Navigation at 2021.

We subsequently summarized the theoretical treatment of these examples in English, and published it on this viXra.org[61] and in the bulletin of our university, Nagasaki Institute of Applied Science[62].

In this Chapter 4, we will describe them consistently.

4. 2 Material α and Breadth β as Setting Variables

In this chapter, $\boldsymbol{\alpha}$ and $\boldsymbol{\beta}$ are defined as the setting variable, same as in the previous chapter. $\boldsymbol{\alpha}$ (hereinafter called the ***material***) is the ratio of the specific weight γ_t of the columnar ship (t in the subscript is the initial letter of *timber*) to that γ_w of water (w in the subscript is the initial letter of *water*) and $\boldsymbol{\beta}$ (hereinafter called the ***breadth***) is the aspect ratio of the breadth βh to the depth h of the cross-section, as follows :

$$\left.\begin{aligned} &\alpha \equiv \frac{\gamma_t}{\gamma_w} \quad (where,\ 0<\alpha\leq 1) \\ &\beta \equiv \frac{breadth}{depth} = \frac{\beta h}{h} \quad (where,\ \beta > 0) \end{aligned}\right\} \cdots\cdots (4.1)$$

Here, when γ_w is fresh water, α represents the specific gravity of the columnar ship.

4. 3 Stable Conditions in the Upright State for a Columnar Ship with Rectangular Cross-Section

In Eq. (3.14) of the previous chapter, the condition for stable floating in the upright state with deck horizontal can be written as the relation between α and β in Eq. (4.1), as follows :

$$\beta^2 - 6\alpha(1-\alpha) > 0 \quad \cdots\cdots (4.2)$$

Hence, summarizing the results of Figs. 3.2, 3.3 and 3.4 in Chapter 3, it was explained that the above condition can be divided into the following three cases :

● Stable conditions for breadth β with fixed material α

$$\left.\begin{aligned} &\beta > \sqrt{6\alpha(1-\alpha)} \\ &\quad e.g.\quad \alpha = \frac{1}{2} \rightarrow \beta >= \frac{\sqrt{6}}{2} \fallingdotseq 1.225 \end{aligned}\right\} \cdots\cdots (4.3)$$

● Stable conditions for material α with fixed breadth β

i) In the case of $\beta > \frac{\sqrt{6}}{2}$ for wide breadth,

the floating body is always stable regardless of material α .

ii) In the case of $\beta < \frac{\sqrt{6}}{2}$ for narrow breadth,

it is then stable in both lighter and heavier materials than wood with $\alpha = \frac{1}{2}$, as shown below :

$$\left.\begin{aligned} &0 < \alpha < \frac{1}{2} - \kappa \quad (Light\ Material) \\ &\frac{1}{2} + \kappa < \alpha \leq 1 \quad (Heavy\ Material) \\ &where,\ \left\{\begin{aligned} &\kappa \equiv \frac{\sqrt{3(3-2\beta^2)}}{6} \\ &\quad e.g.\quad \beta = 1 \rightarrow \kappa = \frac{\sqrt{3}}{6} \fallingdotseq 0.289 \end{aligned}\right. \end{aligned}\right\} \cdots\cdots (4.4)$$

4. 4 Stable Attitude for an Inclined Columnar Ship with Rectangular Cross-Section

In this section, we will try to find out what kind of inclined state is stable, when the stable condition in the upright state described in the previous chapter is not satisfied. For this purpose, let's analyze the inclined attitude, *i.e.* the heel angle, of the columnar ship.

As shown in Fig. 4.1, we shall assume that a columnar ship of length L with a rectangular cross-section of depth h and breadth βh, which is made of homogeneous material and of squared timber of specific weight γ_t, floats stably in a lateral inclined state of heel angle θ to the starboard side from an upright state. The coordinate system $o-\eta\zeta$ is fixed to an inclined ship with the origin o at the center of its bottom surface.

First, in order to determine the draft, we need to find the cross-sectional area A_w under the water surface at lateral inclination.

Since its underwater shape is a trapezoid with height βh, the lengths of its upper and lower bases can be calculated by taking into account the increase or decrease $\frac{\beta h}{2}\tan\theta$ of the port and starboard submerged lengths with respect to the draft d in the upright state. So, the underwater area A_w is obtained as follows :

$$A_w = \frac{1}{2}\left\{\left(d - \frac{\beta h}{2}\tan\theta\right) + \left(d + \frac{\beta h}{2}\tan\theta\right)\right\}\cdot \beta h$$
$$= \beta h d \qquad \cdots\cdots (4.5)$$

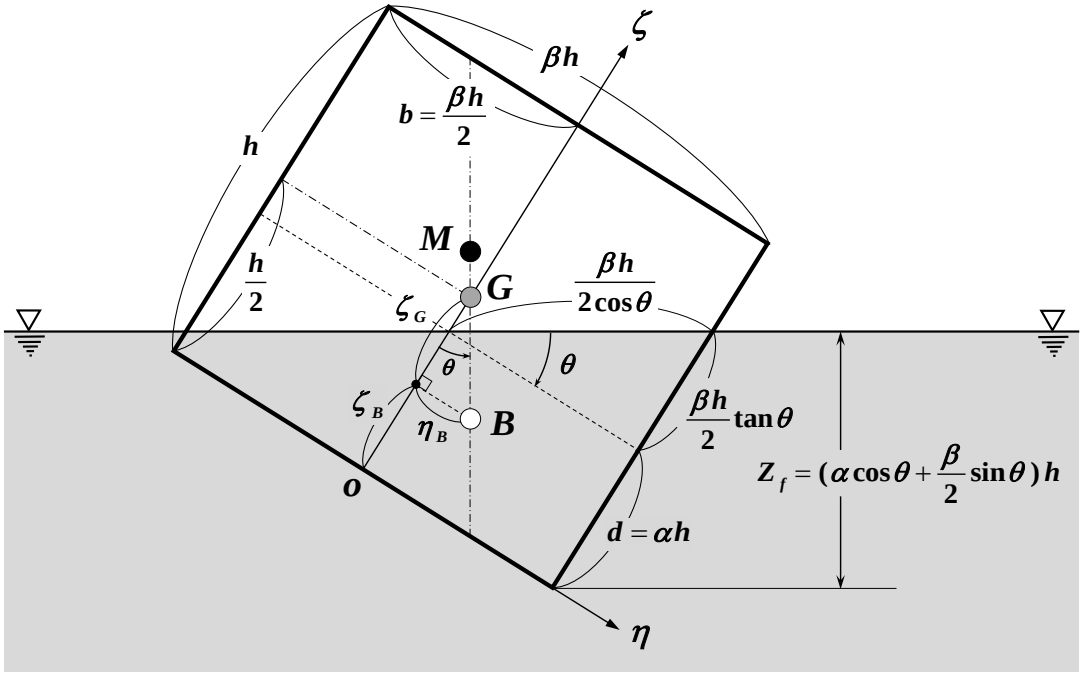

Fig. 4.1 Columnar ship, with rectangular cross-section of length L, floating stably in a lateral inclined state.

Here, the above result is equal to the area of the rectangle, which is the underwater shape in the upright state.

The weight W and the buoyant force F_B of this columnar ship can be obtained as follows, respectively :

$$\left. \begin{aligned} W &= \gamma_t V_t = \gamma_t \cdot \beta h \cdot h \cdot L \\ F_B &= \gamma_w V_w = \gamma_w A_w L = \gamma_w \cdot \beta h d \cdot L \end{aligned} \right\} \qquad (4.6)$$

Here, the weight W of the former is obtained as the product of the specific weight γ_t and the total volume V_t of the columnar ship. And the buoyant force F_B of the latter is obtained as the product of the specific weight γ_w of water and the displacement volume V_w of underwater portion, according to Archimedes' principle[1] as shown in Eq. (1.6) of Chapter 1. Then V_w is obtained by the product of the cross-sectional area A_w in Eq. (4.5) and the ship's length L.

The floating body is stable under the following conditions, where the weight W and buoyancy F_B are in equilibrium.

$$W = F_B \qquad (4.7)$$

Substituting W and F_B in Eq. (4.6) into both sides of the above, we obtain as :

$$\gamma_t \cdot \beta h \cdot h \cdot L = \gamma_w \cdot \beta h \cdot d \cdot L \qquad (4.8)$$

By solving the above equation, the undetermined draft d in the upright state can be determined as α times the depth h of the ship, as follows :

$$d = \frac{\gamma_t}{\gamma_w} h = \alpha h \qquad (4.9)$$

In this paper, to simplify the problem, it is assumed that the deck, *i.e.* upper side of a rectangular cross-section, is in the air and the bottom, *i.e.* lower side of a rectangle, is in the water over the entire breadth, even when the ship is laterally inclined, as shown in Fig. 4. 1. That is, the discussion will be limited to the case in which the cross-sectional shape under the water surface is trapezoidal, as calculated in Eq. (4.5).

The above assumptions would impose the following conditions, where the increase or decrease $\frac{\beta h}{2}\tan\theta$ of submerged length due to the lateral inclination does not exceed the freeboard $h-d$ or the draft d in the upright state, while divided into two cases with $\alpha = \frac{1}{2}$ as bifurcation.

$$\frac{\beta h}{2}\tan\theta \le \begin{cases} h-d = (1-\alpha)\,h & (\textit{for Heavy Material of } \alpha \ge \frac{1}{2}) \\ d = \alpha h & (\textit{for Light Material of } \alpha < \frac{1}{2}) \end{cases} \qquad (4.10)$$

Therefore, the heel angle θ is limited to small inclination within the following range.

$$\theta \leq \begin{cases} \tan^{-1}\left(\dfrac{2(1-\alpha)}{\beta}\right) & \left(\textit{for Heavy Material of } \alpha \geq \dfrac{1}{2}\right) \\ \tan^{-1}\left(\dfrac{2\alpha}{\beta}\right) & \left(\textit{for Light Material of } \alpha < \dfrac{1}{2}\right) \end{cases} \quad \cdots\cdots\cdots\cdots\cdots\cdots (4.11)$$

For example, it means the following setting range.

$$\left.\begin{array}{l} \beta = 1,\ \alpha = \dfrac{1}{2} \\ \quad \rightarrow \tan\theta \leq 1 \ \ \therefore \theta \leq \dfrac{\pi}{4} \end{array}\right\} \cdots\cdots\cdots\cdots\cdots\cdots\cdots\cdots\cdots\cdots\cdots\cdots\cdots\cdots\cdots\cdots\cdots\cdots (4.12)$$

The position of the center of buoyancy $B(\eta_B, \zeta_B)$ in the inclined state by heel angle θ is determined by the authors in Section 1.2 of Chapter 1, and its position is equal to the center of hydrostatic pressure $C_P(\eta_P, \zeta_P)$. As shown in Fig. 4.1, in the inclined coordinate system, which is fixed to the ship and has its origin at the center of the ship's bottom, the position (η_B, ζ_B) is obtained as shown in Eq. (1.11) of Chapter 1, when the draft and half-breadth of the ship in upright state are f and b respectively, as follows :

$$\left.\begin{array}{l} \eta_B = \dfrac{b^2}{3f}\tan\theta \\ \zeta_B = \dfrac{f}{2} + \dfrac{b^2}{6f}\tan^2\theta \end{array}\right\} \cdots\cdots\cdots\cdots\cdots\cdots\cdots\cdots\cdots\cdots\cdots\cdots\cdots\cdots\cdots\cdots\cdots\cdots (4.13)$$

Here, in order to conform to the notation of this chapter, f and b in Eq. (4.13) are replaced as follows, respectively.

$$\left.\begin{array}{l} f = d = \alpha h \\ b = \dfrac{1}{2}\beta h \end{array}\right\} \cdots\cdots\cdots\cdots\cdots\cdots\cdots\cdots\cdots\cdots\cdots\cdots\cdots\cdots\cdots\cdots\cdots\cdots (4.14)$$

Thereby, η_B and ζ_B can be written as follows :

$$\left.\begin{array}{l} \eta_B = \dfrac{\beta^2\tan\theta}{12\alpha}h \\ \zeta_B = \dfrac{\alpha h}{2} + \dfrac{\beta^2\tan^2\theta}{24\alpha}h \end{array}\right\} \cdots\cdots\cdots\cdots\cdots\cdots\cdots\cdots\cdots\cdots\cdots\cdots\cdots\cdots\cdots\cdots\cdots\cdots (4.15)$$

Next, the center of gravity of the ship is located at the centroid of the rectangular cross-section (*i.e.*, at the center of the figure), even after inclining, since homogeneous materials are assumed. Therefore, using the fact that the sum of ζ_B and ζ_G is equal to $\dfrac{h}{2}$, ζ_G in Fig. 4.1 can be obtained as follows :

$$\begin{aligned}\zeta_G &= \frac{h}{2} - \zeta_B \\ &= \frac{1-\alpha}{2}\,h - \frac{\beta^2 \tan^2\theta}{24\alpha}\,h \\ &= \frac{12\alpha(1-\alpha) - \beta^2\tan^2\theta}{24\alpha}\,h \end{aligned} \quad \cdots\cdots(4.16)$$

In order for the ship to float while maintaining the inclined state shown in Fig. 4.1, the center of buoyancy *B* and the center of gravity *G* must first be located on the same vertical line. Therefore, the following relationship is required between η_B and ζ_G.

$$\left.\begin{aligned}&\frac{\eta_B}{\zeta_G} = \tan\theta \\ &\therefore\ \eta_B = \zeta_G \tan\theta\end{aligned}\right\} \quad \cdots\cdots(4.17)$$

Here, by using the former part of Eq. (4.15) and Eq. (4.16) for η_B and ζ_G for the above equation, the following relationship is obtained.

$$\beta^2\tan^2\theta = 2\left\{6\alpha(1-\alpha) - \beta^2\right\} \quad \cdots\cdots(4.18)$$

The tangent of the inclined attitude θ for a given material α and breadth β is then obtained by the following equation.

$$\tan\theta = \frac{\sqrt{2\left\{6\alpha(1-\alpha) - \beta^2\right\}}}{\beta} \quad \cdots\cdots(4.19)$$

When the interior of the radical symbol of the right-hand side of the above equation is positive, there exists a solution for the heel angle θ. This result coincides with Eqs. (1-h) and (4-f) of Igarashi and Nakamura[59]. This requires that the interior of the braces in the numerator of the above equation take positive values, as follows :

$$6\alpha(1-\alpha) - \beta^2 > 0 \quad \cdots\cdots(4.20)$$

The inequality above is the inverse condition in which the inequality sign is opposite to the stable condition in the upright state in Eq. (4.2) of Section 4.3, and the validity of the analysis in this chapter can be confirmed.

Finally, it is necessary to examine whether the above-mentioned inclined attitude is stable or not. For this purpose, let us determine the location of *the metacenter M,* meaning *the Center of Inclination*.

The metacentric radius $\overline{BM}$ can be calculated by using the basic formula of naval architecture, Eq.(2.22) derived in Chapter 2, as follows :

$$\overline{BM} = \frac{I_{CL}}{V_w} \quad \cdots\cdots(4.21)$$

Here, I_{CL} is the quadratic moment about *the Center Line* of water plane, and V_w is the underwater volume of a ship.

I_{CL} in the numerator of the above formula can be calculated as follows, since the water plane at inclination is a rectangle of length L and breadth $\frac{\beta h}{\cos\theta}$.

$$I_{CL} = \frac{1}{12}\left(\frac{\beta h}{\cos\theta}\right)^3 L \quad \cdots\cdots (4.22)$$

And the denominator V_w can be obtained by using d in Eq. (4.9) for A_w in Eq. (4.5) and as follows :

$$V_w = A_w L = \beta h d \cdot L = \alpha \beta h^2 L \quad \cdots\cdots (4.23)$$

By substituing the obtained results I_{CL} and V_w into Eq. (4.21), $\overline{BM}$ can be determined independently of the length L of the columnar ship, as follows :

$$\overline{BM} = \frac{\frac{1}{12}\left(\frac{\beta h}{\cos\theta}\right)^3 L}{\alpha \beta h^2 L} = \frac{\beta^2}{12\alpha \cos^3\theta} h \quad \cdots\cdots (4.24)$$

$\overline{BG}$ in the inclined state is then obtained below by using the trigonometric ratio with η_B in Eq. (4.15), as shown in Fig. 4.1.

$$\overline{BG} = \frac{\eta_B}{\sin\theta} = \frac{\beta^2}{12\alpha\cos\theta} h = \overline{BM}\cos^2\theta \quad \cdots\cdots (4.25)$$

Thereby, the metacentric height $\overline{GM}$ can be determined by subtracting Eq. (4.25) from Eq. (4.24), as follows :

$$\begin{aligned} \overline{GM} &= \overline{BM} - \overline{BG} \\ &= \frac{\beta^2(1-\cos^2\theta)}{12\alpha\cos^3\theta} h = \frac{\beta^2 \sin^2\theta}{12\alpha\cos^3\theta} h \\ &= \overline{BM}\sin^2\theta \geq 0 \end{aligned} \quad \cdots\cdots (4.26)$$

From this result, the metacenter M is always located above the center of gravity G, since $\overline{GM}$ takes a positive value regardless of the heel angle θ, material α and breadth β. Therefore, it can be seen that the inclined attitude θ determined by Eq. (4.19) is constantly a stable state. However, it is necessary to check that the calculated θ is within the assumed small heel angle in Eq. (4.11).

Here, let us take few considerations on $\overline{GM}$. Eq. (4.19) shows that when $\beta^2 = 6\alpha(1-\alpha)$, which corresponds to Eq (4.30) in next section, the inside of the radical symbol is zero and $\tan\theta = 0$, so the floating body is an upright state with heel angle $\theta = 0$. At this time, since $\overline{GM} = 0$ from Eq. (4.26), M and G coincide and the floating state is neutral. On the other hand, when α and β satisfy the above condition, $\overline{GM}$ for the upright state shown in Eq. (3.13) of the previous chapter is also zero. Hence, it can be seen that its equation for the upright state and the Eq. (4.26) for the inclined state derived in this chapter are connected consistently at $\theta = 0$ in the neutral state between both formulas for the metacentric height $\overline{GM}$.

For example, in the states β and α below, the heel angle θ, $\overline{BG}$ and $\overline{GM}$ are calculated as follows by Eqs. (4.19), (4.25), and (4.26).

$$\left.\begin{aligned} &\beta = 1,\ \alpha = \frac{1}{2} \ \rightarrow\ \tan\theta = 1 \ \ \therefore\ \theta = \frac{\pi}{4} \\ &\therefore\ \overline{GM} = \overline{BG} = \frac{\sqrt{2}}{6} h \end{aligned}\right\} \quad \cdots\cdots (4.27)$$

This state corresponds to the case where the diagonal line of the square cross-section is aligned with the water line, and the heel angle θ is also within the setting range of Eq. (4.12). And $\overline{BG}$ and $\overline{GM}$ also coincide with the results described in examples of many textbooks[9-c),(12-c),(42-b)].

4.4.1 $\alpha, \beta, \theta, Z_f$ in an inclined rectangular cross-section of Fig. 4.1

Fig. 4.1 shows the following states, and the inclined attitude θ and the positions of *B*, *G* and *M* are also drawn accurately. In fact, θ falls within $36.0°$ calculated by the latter part of Eq. (4.11).

$$\left.\begin{aligned} &\alpha = 0.4,\ \beta = 1.1 \ \rightarrow\ \theta = 31.7° \ (< 36.0°) \\ &\therefore\ \overline{GM} = 0.113\,h,\ \overline{BG} = 0.296\,h,\ Z_f = 0.629\,h \end{aligned}\right\} \quad \cdots\cdots (4.28)$$

Here, Z_f in the above Eq. (4.28) is the water depth at the starboard side of the ship's bottom, and is calculated by the following equation.

$$\begin{aligned} Z_f &= \left(d + \frac{\beta h}{2}\tan\theta\right)\cos\theta \\ &= \left(\alpha\cos\theta + \frac{\beta}{2}\sin\theta\right) h \end{aligned} \quad \cdots\cdots (4.29)$$

4.5 Calculation Results for the Stable Inclined Attitude θ

In this section, the dependence of the stable attitude θ at lateral inclined state on the breadth β and material α of the columnar ship is grasped.

Fig. 4.2 shows the dependence of the above on breadth β when α is a fixed, and Fig. 4.3 shows that on material α when β is a fixed. The results in both figures are obtained by calculating the heel angle θ in Eq. (4.19) using an Excel spreadsheet.

Since $\theta = 0$ means that the ship floats with its deck horizontal and is the limit point at which the inequality sign in Eq. (4.2) becomes an equality sign, α and β satisfy the following relationship at that point.

$$\beta^2 - 6\alpha\,(1-\alpha) = 0 \quad \cdots\cdots (4.30)$$

Thereby the intersection with β-axis in Fig. 4.2 is obtained by Eq. (4.3), and that with α-axis in Fig. 4.3 is obtained by Eq. (4.4), replacing the inequality sign in both equations by an equality sign.

In both Figs. 4.2 and 4.3 above, the heel angles θ of materials α and $1-\alpha$ are obtained equally, as can be seen from the factors in the radical symbol of Eq. (4.19). The angle θ becomes smaller as breadth β becomes wider. And θ is largest for materials with $\alpha = 0.5$ such as wood, and is smaller as α becomes heavier or lighter than that.

The reason why the point is not plotted in the case of $\beta < 1$ for $\alpha = 0.5$, $\beta < 1.06$ for $\alpha = 0.4, 0.6$ and $\beta < 1.04$ for $\alpha = 0.3, 0.7$ in Fig. 4.2 is because the heel angle θ exceeds the range of the small inclination in Eq. (4.11).

Similarly, in Fig. 4.3, the part of the curve at $\beta = 1.05$, the narrowest of the 4 states with breadth β, is broken off and no point can be placed, because it exceeds the range of small inclination angles in Eq. (4.11) and the inclined attitude θ cannot be calculated using Eq. (4.19) in Section 4.4. In detail, in the lighter case of $0.32 < \alpha < 0.43$, the bottom of the ship partially rises into the air and the underwater shape becomes triangular, while in the heavier case of $0.57 < \alpha < 0.68$, the deck partially sinks into the water and the underwater shape becomes pentagonal, as both cases are different from the trapezoidal shape assumed in the present theory.

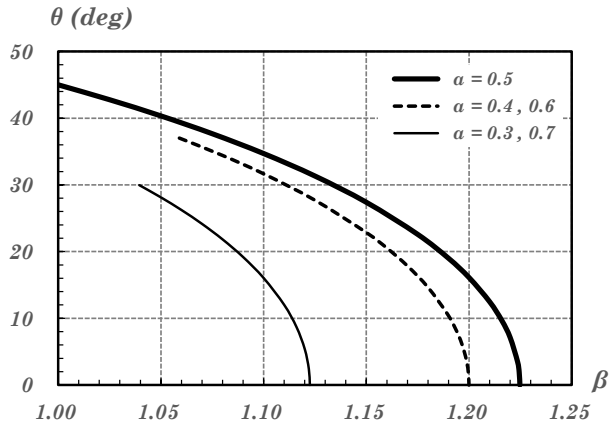

Fig. 4.2 Dependence of the stable inclined attitude θ on breadth β.

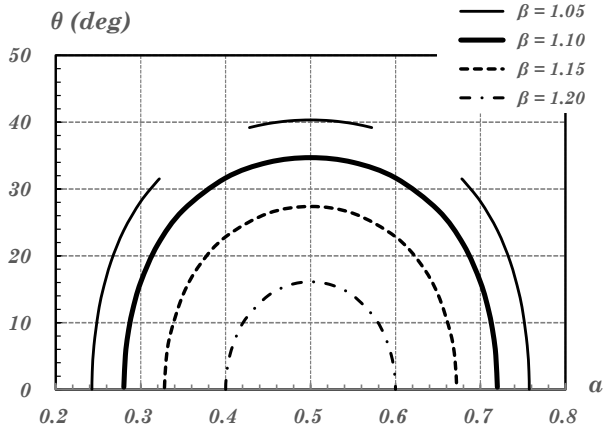

Fig. 4.3 Dependence of the stable inclined attitude θ on material α.

Igarashi *et al.*[58],[59] provide a detailed analysis of all inclined state, including cases of large heel angles (where part of the deck sinks into the water or part of the ship's bottom rises into the air), which cannot be calculated in this chapter. And they have perfectly elucidated the dependence on α and β by organizing all cases in maps and tables and verifying them experimentally, so we encourage to read their paper for anyone interested.

Fig. 4.4 illustrates the attitudes of the four states when the material is fixed at $\alpha = 0.5$ and the breadth $\beta = 1.0$, 1.1, 1.2 and 1.3, including the positions of *B*, *G* and *M*. It can be seen how the heel angle θ decreases as the breadth β increases.

Fig. 4.5 shows the five attitudes for material $\alpha = 0.25, 0.3, 0.5, 0.7$ and 0.75, with the breadth fixed at $\beta = 1.06$. It can be found that the heel angle θ decreases symmetrically around $\alpha = 0.5$, even if the draft increases or decreases as the material α becomes heavier or lighter than that.

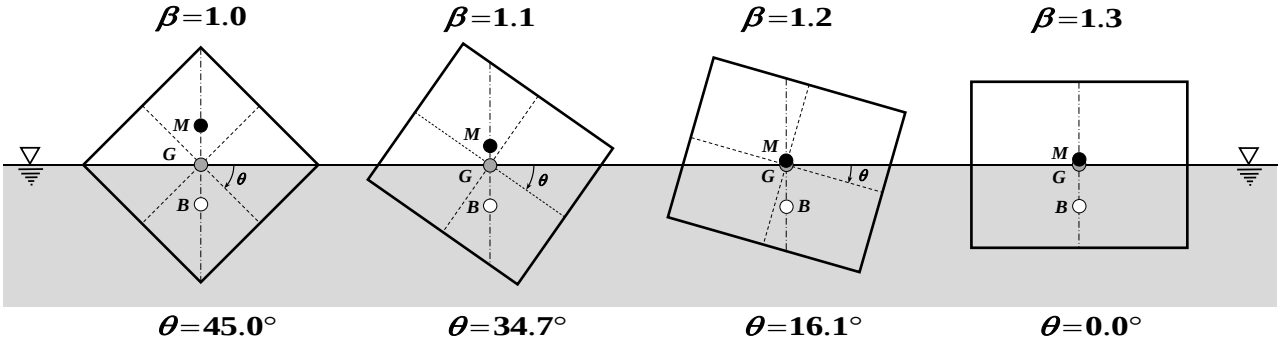

Fig. 4.4 Four attitudes for breadth $\beta = 1.0, 1.1, 1.2, 1.3$ with the material fixed at $\alpha = 0.5$.

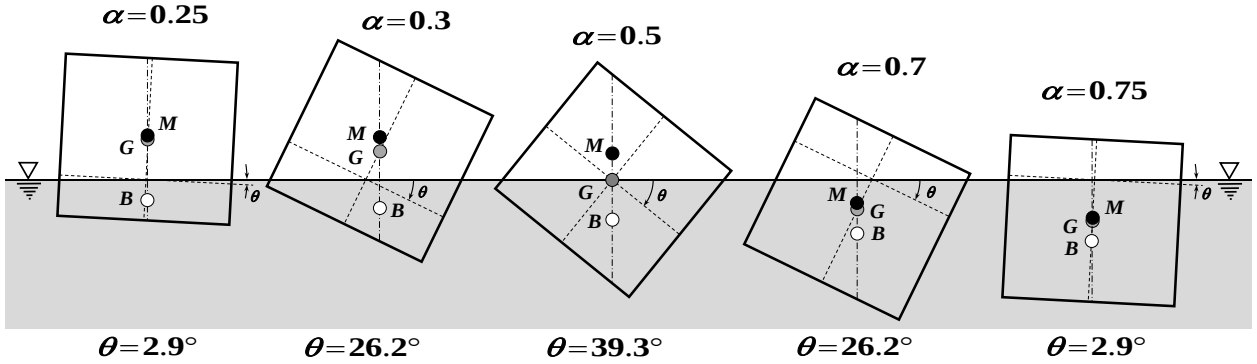

Fig. 4.5 Five attitudes for material $\alpha = 0.25, 0.3, 0.5, 0.7, 0.75$ with the breadth fixed at $\beta = 1.06$.

4. 6 Verificational Experiment

Fig. 4.6 compares the model experiment (left) and the calculation results (right) for the case of material $\alpha = 0.458$ and breadth $\beta = 1.15$.

The model of the columnar ship is length $L = 30cm$, depth $h = 10.0cm$, breadth $\beta h = 11.5cm$ and weight $W = 18.09N$. Two pieces of chemical wood were pasted together in the center at the top and bottom, and the model was manufactured by *Space Model Co., Ltd.* in Nagasaki, Japan. The verificational experiment was conducted by floating its model in a small water tank.

The inclined attitude was $\theta = 27.5°$ in the experiment and the calculated results are as follows, by Eqs. (4.11), (4.19), (4.25), (4.26) and (4.29).

$$\left.\begin{array}{l} \theta = 26.7^\circ \ (\alpha = 0.458,\ \beta = 1.15) < 38.5^\circ \\ \therefore\ \overline{GM} = 0.068\,h,\ \ \overline{BG} = 0.269\,h,\ \ Z_f = 0.668\,h \end{array}\right\} \cdots\cdots\cdots\cdots\cdots\cdots\cdots\cdots\cdots\cdots (4.31)$$

We consider that the reason why there is a difference of about 1° between the two is that the heel angle θ in the experiment was obtained by measuring $\tan\theta$ from photographs and that the center of gravity position *G* may be slightly off-center due to the manufacturing process of the model. Therefore we are able to verify that the theory in this chapter can correctly calculate the actual inclined state.

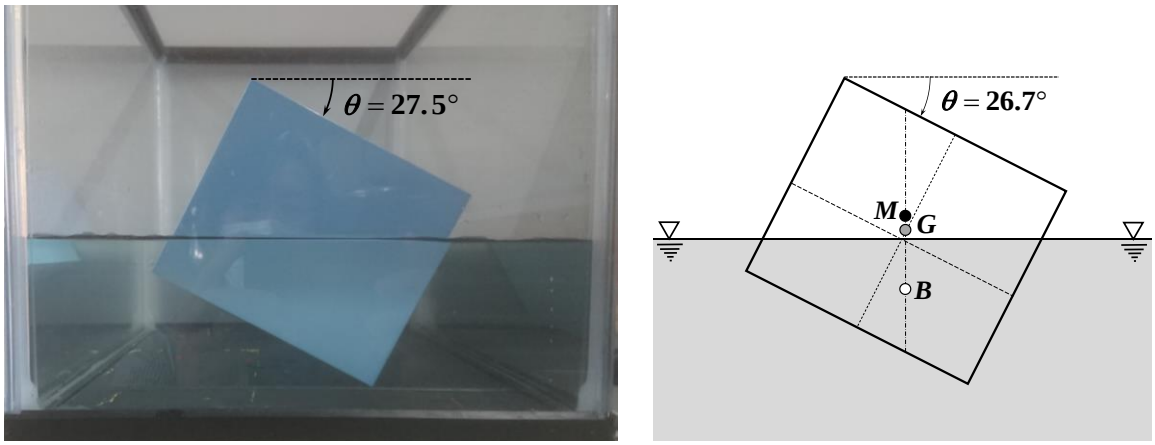

Fig. 4.6 Comparison of experimental (left) and calculated (right) results for material $\alpha = 0.458$, breadth $\beta = 1.15$.

4.7 Afterword

In this Chapter 4, as an applied example which is an extension of the previous Chapter 3, a theoretical treatment for solving the stable attitude of a columnar ship with a rectangular cross-section in a lateral inclined state is explained in an easy-to-understand manner. Therefore, the inclined states are limited to a small heel angle, in which the deck is not submerged and the ship's bottom is not floated, in order to understand essentially the stability theory of ships.

The authors would be very happy, if this chapter could be of assistance to teachers and students who will teach and learn this field in the future, going one step forward from the basic examples in the previous chapter.

In closing this chapter, we would like to pay tribute to two valuable papers[58),(59)] written by *Tamotsu IGARASHI,* Professor Emeritus of *the National Defense Academy of Japan*. The reason is that the authors were deeply impressed by both of their papers.

Acknowledgments

In closing this paper, let me express the following thanks from the 1st author[52]. I would like to communicate my deepest gratitude to my late teacher, *Pr. Masato KURIHARA*[63],[64],[65], who cordially taught me the theory of "*Hydrostatics of Ships*" with detailed figures and formulas on the blackboard when I was a 1st year undergraduate student and learned my 1st specialized subject of naval architecture at *the College of Naval Architecture of Nagasaki*. Therefore, I am following the appearance of my teacher at that time from more than 40 years ago as an exemplary example, when I currently lecture on *Hydrostatics of Floating Bodies*[66],[67],[68],[69] and *Theory of Ship Stability*[70],[71] to 2nd year students at my university[53],[54], as shown in YouTube videos of Appendix A. 7.

I then would like to express my deepest gratitude to my mentor, *Dr. Kiyoshige MATSUMURA*[72],[73] of the Department of Naval Architecture, *Osaka University*, who guided me during my doctoral course[74] at the graduate school. At that time, he said to me, "Writing a thesis is a serious endeavor for me !", and I have finally come to understand his words more than 30 years later.

Finally, we, present two authors, would like to express our heartfelt gratitude to *Dr. Yoshihiro KOBAYASHI*, former professor at *Sojo University* and current president of *Como-Techno Co., Ltd.* in Nagasaki, Japan. He always gave warm encouragement to our research and recommended that this study should be published in English. We are greatly inspired by the vigorous academic spirit with which he writes about the results of his research in books[75],[76],[77].

References ‡

(1) Archimedes : " The Works of Archimedes ", On Floating Bodies, Book I & Book II, Edited and Translated by Heath, T. L. , ***Cambridge University Press***, 1897, p.253~300.

(2) Kinbara, T. : " Fundamental Physics —Upper Volume—" (in Japanese), Chapter 7 : Fluid, Section 7.3 : Buoyancy, *Shouka-bou Publishing,* 1963 (March) 1st Printing, p.144~145.

(3) Tomochika, S. : " Fluid Dynamics " (in Japanese), Chapter 2 : Hydrostatics, *Gendai-Kougaku-sha Publishing,* 1972 (June) Reprinted Issuance, p.6~35.

(4) Newman, J. N. : " Marine Hydrodynamics ", Chapter 6 : Waves and Wave Effects, Section 6. 16 : Hydrostatics, *The MIT Press* (Cambridge, Massachusetts and London, England), 1977, p.290~295.

(5) Honma, M. : " Standard Hydraulics " (in Japanese), Chapter 2 : Hydrostatics, Section 2. 7 : Buoyancy, *Maruzen Publishing,* 1962 (September) 1st Printing, p.22~23.

(6) Bouguer, P. : " Traité du Navire, de sa Construction, et de ses Mouvemens ", (Treatise of the Ship, its Construction and its Movements), Livre II, Section II, ***Jombert, C.***, Paris, 1746, p.249~324.

(7) Lewis, E. V. (Editor) : " Principles of Naval Architecture (2nd. Revision), Volume I : Stability and Strength ", *The Society of Naval Architects and Marine Engineers*, Jersey City, NJ, 1988 (April) 1st Printing.

(a) Hamlin, N. A. : Chapter 1 : Ship Geometry, Section 2 : Displacement and Weight Relationships, Subsection 2. 1 : Archimedes' Principle, p.16.

(b) Goldberg, L. L. : Chapter 2 : Intact Stability, Section 1 : Elementary Principles, Subsection 1. 3 : Displacement and Center of Buoyancy, p.64.

(c) Goldberg, L. L. : Chapter 2 : Intact Stability, Section 3 : Metacentric Height, Subsection 3. 2 : Location of the Transverse Metacenter, p.72.

(8) Nishikawa, H. : " Primary Hydrostatics of the ship " (in Japanese), *Kaibun-dou Publishing,* 1964 (July) 1st Printing.

(a) Chapter 4 : Theory of Floating Bodies, Section 4. 2 : Buoyancy, p.83~85.

(b) Chapter 4 : Theory of Floating Bodies, Section 4. 10 : Transverse Metacenter and *BM*, p.91~94.

(9) Ohgushi, M. : "Theoretical Naval Architecture (Upper Volume) —New Revision—" (in Japanese), *Kaibun-dou Publishing,* 1971 (June) 1st Printing

(a) Chapter 1 : Water and Floating Body, Section 1.2 : Hydrostatic Pressure, p.1~3. Section 1.3 : Buoyancy, Example Problem, p.4~5.

(b) Chapter 4 : Equilibrium of Ships, Transverse and Longitudinal Metacenter, Change of Trim, Section 4.4 : Transverse Metacenter and $\overline{BM}$, p.81~83.

(c) Chapter 4 : Equilibrium of Ships, Transverse and Longitudinal Metacenter, Change of Trim, Section 4.4 : Transverse Metacenter and $\overline{BM}$, Questions 2 and 3, p. 83.

(10) Motora, S. (Supervisor) : " Kinematics of Ships and Offshore Structures " (in Japanese), Chapter 1 (written by Fujino, M.) : Hydrostatics of Floating Bodies, Section 1. 1 : Buoyancy, Section 1. 2 : Static Equilibrium of Floating bodies, *Seizan-dou Publishing,* 1982 (November) 1st Printing, p.1~5.

‡ Bold text in the list means that there is a HyperLink.

(11) Ferreiro, L. D. : "Ships and Science —The Birth of Naval Architecture in the Scientific Revolution, 1600–1800—", *The MIT Press* (Cambridge, Massachusetts and London, England), 2006 , Soft-Cover.

(a) Chapter 4 : Inventing the Metacenter,
Archimedes and the Stability of Floating Bodies, p.207 ~ 209.

(b) Chapter 4 : Inventing the Metacenter, p.210~238.

(12) Akedo, N. : "Basic Nautical Mechanics" (in Japanese), *Kaibun-dou Publishing,* 1983 (June) 1st Printing.

(a) Chapter 2 : Dynamics of Rigid Bodies, Section 2.3.7 : Center of Buoyancy, p.110~111.

(b) Chapter 2 : Dynamics of Rigid Bodies, Section 2.3.5 : Movement of Center of Gravity, p.99~100.
Chapter 3 : Stability of Ships, Section 3.1.3 : Metacentric Radius, p.121~125.

(c) Chapter 3 : Stability of Ships, Section 3.1.3 : Metacentric Radius, Examples 1 and 2, p.125~132.

(13) Hoste, P. : " Théorie de la Construction des Vaisseaux — Qui Contient Plusieurs Traitez, de Mathématique sur des Matières Nouvelles & Curieuses—", (Theoy of the Construction of Vessel), ***Chez Anisson & Posuel***, Lyon, 1697, p.1~211.

(14) Nowachi, H. and Ferriro, L. D. : "Historical Roots of the Theory of Hydrostatic Stability of Ships", 8th International Conference on the Stability of Ships and Ocean Vehicles, ***Escuela Técnica Superior de Ingenieros Navales***, 2003, pp.1~30.

(15) Komatsu, M. : "Considerations on the Center of Action of Buoyancy Acting on a Floating body" (in Japanese), *Boat Engineering*, 2007 (December), No.93, pp.21~25.

(16) Seto, H. : "Considerations of the Center of Buoyancy —Reexamination of Komatsu's Considerations on the Center of Action of Buoyancy Acting on a Floating body—" (in Japanese), *Research Committee of Propulsion and Seakeeping Performance* (Japan Society of Naval Architects and Ocean Engineers), 2010 (October), No.14, pp.1~23.

(17) Seto, H. : " Some Consideration on the Center of Action of Buoyancy " (in Japanese), *Conference Proceedings of the Japan Society of Naval Architects and Ocean Engineers*, 2011 (May), Vol.12, No.2011S-G6-22, pp.529~532.

(18) Suzuki, K. : "The Mythical Theory : the Law of the Center of Buoyancy" (in Japanese), *Private Note*, 2011 (January), pp.1~4.

(19) Yoshimura, Y. and Yasukawa, H. : "Reconsideration of the Center of Action of Buoyancy and the Stability" (in Japanese), *Research Committee of Propulsion and Seakeeping Performance* (Japan Society of Naval Architects and Ocean Engineers), 2011, No.16.

(20) Komatsu, M. : " Considerations on the Center of Action of Buoyancy by means of Coordinate Ttransformation" (in Japanese), *Research Committee of Propulsion and Seakeeping Performance* (Japan Society of Naval Architects and Ocean Engineers), 2012, No.19.

(21) Yabushita, K. and Watanabe, R. : "Relationship between the Pressure Distribution around Ship Hull and the Center of Buoyancy" (in Japanese), *Research Committee of Propulsion and Seakeeping Performance* (Japan Society of Naval Architects and Ocean Engineers), 2013, No.21.

(22) Mégel, J. and Kliava, J. : " On the Buoyancy Force and the Metacentre ", 2009 (June), ***arXiv : 0906.1112***, Classical Physics, pp.1~33.

References

(23) Kliava, J. and Mégel, J. : " Non-Uniqueness of the Point of Application of the Buoyancy Force ", ***European Journal of Physics***, 2010 (July), Vol.31, No.4, pp.741~762.

(24) Hori, T. : "A Positioning on Ship's Centre of Buoyancy Derived by Surface Integral of Hydrostatic Pressure —Proof that Centre of Buoyancy is Equal to Centre of Pressure—" (in Japanese), ***NAVIGATION*** (Journal of *Japan Institute of Navigation*), 2018 (January), ***No.203***, pp.88~92.

(25) Hori, T. : "A Positioning on Ship's Centre of Buoyancy Derived by Pressure Integral of Hydrostatic Pressure —Part 2 : In the Case of Arbitrary Sectional Form—" (in Japanese), ***NAVIGATION*** (Journal of *Japan Institute of Navigation*), 2018 (July), ***No.205***, pp.28~34.

(26) Yabushita, K. : " The Stability, Resistance and Propulsion of Ships " (in Japanese), Chapter 4 : Relationship between Center of Buoyancy and Pressure Distribution, Self-made Textbook of Department of Mechanical System Engineering, *National Defense Academy*, 2018 (May), pp.81~96.

(27) Yabushita, K. , Hibi, S. and Okahata, G. : " Identification of Center of Buoyancy Using Pressure Distribution on an Object " (in Japanese), *Research Committee of Propulsion and Seakeeping Performance* (Japan Society of Naval Architects and Ocean Engineers), 2018 (June), No.10, SPRC 10-10, pp.1~14.

(28) Hori, T. : "A Positioning on Ship's Centre of Buoyancy Derived by Surface Integral of Hydrostatic Pressure —Part 3 : The Proof for Semi-submerged Circular Cylinder—" (in Japanese), ***NAVIGATION*** (Journal of *Japan Institute of Navigation*), 2019 (April), ***No.208***, pp.60~68.

(29) Suzuki, K. : "On the Apparent Center of Buoyancy —In Connection with the Hori's Treatise[24]—" (in Japanese), *Private Note*, 2018 (April), pp.1~4.

(30) Komatsu, M. : "Considerations on the Center of Action of Buoyancy Acting on a Floating Body (Follow-up Report)" (in Japanese), *Boat Engineering*, 2018 (December), No.136, pp.12~18.

(31) Yabushita, K. , Hibi, S. and Okahata, G. : " Identification of Center of Buoyancy and Relation to Pressure Distributions " (in Japanese), *Conference Proceedings of the Japan Society of Naval Architects and Ocean Engineers*, 2020 (May), Vol.30, No.2020S-GS12-16, pp.629~636.

(32) Hori, T. : "A Positioning on Ship's Centre of Buoyancy Derived by Surface Integral of Hydrostatic Pressure —Part 5 : The Proof for Submerged Circular Cylinder—" (in Japanese), ***NAVIGATION*** (Journal of *Japan Institute of Navigation*), 2020 (October), ***No.214***, pp.62~67.

(33) Hori, T. : "A Positioning on Ship's Centre of Buoyancy Derived by Surface Integral of Hydrostatic Pressure —Part 4 : The Proof for Triangular Prism—" (in Japanese), ***NAVIGATION*** (Journal of *Japan Institute of Navigation*), 2020 (July), ***No.213***, pp.50~58.

(34) Hori, T. : "New Developments in the Fundamental Theory for Hydrostatic of Floating Bodies —Part 1 : The Proof that Centre of Buoyancy is Equal to Centre of Pressure — " (in Japanese), ***Boat Engineering***, 2018 (September), ***No.135***, pp.1~10.

(35) Hori, T. , Hori, M. : "Proof that the Center of Buoyancy is Equal to the Center of Hydrostatic Pressure (Part 2:) Semi-Submerged Circular Cylinder and Triangular Prism", ***viXra.org*** *(Pre-print Repository)*, 2023 (August), ***viXra:2308.0202*** [Ver.2], Classical Physics, pp.1~27.

(36) Hori, T., Hori, M. : "Proof that the Center of Buoyancy is Equal to the Center of Hydrostatic Pressure (Part 3:) Submerged Circular Cylinder and Arbitrary Shaped Submerged Body", ***viXra.org*** *(Pre-print Repository)*, 2023 (September), ***viXra:2309.0136*** [Ver.1], Classical Physics, pp.1~21.

(37) Hori, T. : "A Positioning on Ship's Center of Buoyancy Derived by Surface Integral of Hydrostatic Pressure —Part 6 : The Proof for Submerged and Floating Body of Arbitrary Form—" (in Japanese), ***NAVIGATION*** (Journal of *Japan Institute of Navigation*), 2021 (January), ***No.215***, pp.69~77.

(38) Hori, T. : "New Developments in the Fundamental Theory for Hydrostatic of Floating Bodies —Part 3 : The Proof that Center of Buoyancy is Equal to Center of Pressure for Submerged and Floating Body of Arbitrary Form—" (in Japanese), ***Boat Engineering***, 2021 (June), ***No.146***, pp.35~43.

(39) Hori, T. : "Proof that the Center of Buoyancy is Equal to the Center of Pressure by means of the Surface Integral of Hydrostatic Pressure Acting on the Inclined Ship", ***viXra.org*** *(Pre-print Repository)*, 2021 (September), ***viXra:2109.0008*** [Ver.5], Classical Physics, pp.1~21.

(40) Hori, T. : "Proof that the Center of Buoyancy is Equal to the Center of Pressure by means of the Surface Integral of Hydrostatic Pressure Acting on the Inclined Ship", *The Bulletin of Nagasaki Institute of Applied Science*, 2022 (January), ***Vol.61***, ***No.2***, Research Notes in Mathematical and Physical Science, pp.135~154.

(41) Takagi, Y. : "Nautical Mechanics and its Applications" (in Japanese), Chapter 6 : Stability, Section 3 : Metacenter and *BM* (metacentric radius), *Seizan-dou Publishing,* 1960 (March) 1st Printing, p.206~213.

(42) Sugihara, K. : " Nautical Theory (Ship Mechanics Division) " (in Japanese), *Kaibun-dou Publishing,* 1964 (July) 1st Printing.

(a) Chapter 3 : Transverse Stability, Section 3.3 : Calculation of $\overline{BM}$ and the Approximate Value, p.54~56.

(b) Chapter 3 : Transverse Stability, Section 3.3 : Calculation of $\overline{BM}$ and the Approximate Value, Example 2, p.58~59.

(43) Ohta, T., Kuwahara, K., Kotani, T., Tamaki, K., Nishikawa, H., Baba, K., Masui, S. and Mitamura, T. : "Naval Architectural Engineering" (in Japanese), Chapter III : Theory and Design of Ships, Section 2 : Calculation of Ships, Subsection 2.4.2 : Transverse Metacenter and the Transverse Metacentric Radius, Edited by National Naval Architectural Education Research Association, *Kaibun-dou Publishing,* 1975 (June) 1st Printing, p.164~165.

(44) Nohara, T. (Original) and Shoji, K. (Author) : "Nautical Naval Architecture (2nd Edition)" (in Japanese), Chapter 9 : Stability, Section 9.4 : Metacenter, *Kaibun-dou Publishing,* 2005 (April) 1st Printing of 2nd Edition, p.174~175, p.166~167.

(45) Barrass, C. B. and Derrett, D.R. : " Ship Stability for Masters and Mates", Part 1 : Linking Ship Stability and Ship Motions, Chapter 12 : Calculating *KB*, *BM a*nd metacentric diagrams, To find transverse *BM*, ***Elsevier Ltd.,*** 2006 (February), 6th Edition, p.106~109.

References

(46) Ikeda, Y., Furukawa, Y., Katayama, T., Fujii, T., Murai, M. and Yamaguchi, S. : "Hydrostatics of Ships and Stability —Series (i) for the Naval Architects and the Ocean Engineers—", (in Japanese), Chapter 4 : Basic of the Stability, Section 4.2.1 : Transverse Stability**,** Edited by Japan Society of Naval Architects and Ocean Engineers, Textbook Compilation Committee of the Ability Development Center, *Seizan-dou Publishing,* 2012 (April) 1st Printing, p.67~68, p.140~141.

(47) Shin, C. I. : "Capsizing and Stability of the Ships" (in Japanese), Chapter 4 : Transverse Stability of the Ships, Section 4.2 : How to Find the Metacentric Radius *BM* and the Position of the Metacenter, *Seizan-dou Publishing,* 2021 (July) 1st Printing, p.41~43.

(48) Hori, T. : " A Consideration on Derivation of Ship's Transverse Metacentric Radius $\overline{BM}$ " (in Japanese), ***NAVIGATION*** (Journal of *Japan Institute of Navigation*), 2017 (April), ***No.200*** (First 200th Anniversary Issue), pp.75~79.

(49) Hori, T. : "New Developments in the Fundamental Theory for Hydrostatics of Floating Bodies — Part 2 : A Consideration on Derivation of Ship's Transverse Metacentric Radius $\overline{BM}$ —" (in Japanese), ***Boat Engineering***, 2018 (December), ***No.136***, pp.1~5.

(50) Hori, T., Hori, M. : "A New Theory on the Derivation of Metacentric Radius Governing the Stability of Ships ", ***viXra.org*** *(Pre-print Repository)*, 2021 (November), ***viXra:2111.0023*** [Ver.4], Classical Physics, pp.1~17.

(51) Hori, T. : "A New Theory on the Derivation of Metacentric Radius Governing the Hydrostatic Stability of Ships", *The Bulletin of Nagasaki Institute of Applied Science*, 2022 (June), ***Vol.62***, ***No.1***, Research Notes in Mathematical and Physical Science, pp.51~67.

(52) Hori, T. : "Web Page on HORI's Laboratory of Ship Waves and Hydrostatic Stability " (in Japanese), Naval Architectural Engineering Course in *Nagasaki Institute of Applied Science*, ***http://www2.cncm.ne.jp/~milky-jun_0267.h/HORI-Lab/*** .

(53) Hori, T. : "Naval Architecture Course, Department of Engineering , Faculty of Engineering, Nagasaki Institute of Applied Science" (in Japanese), Introduction of Educational and Research Institutes, ***NAVIGATION*** (Journal of *Japan Institute of Navigation*), 2021 (January), ***No.215***, pp.38~45.

(54) "Naval Architecture Course's Web Site" (in Japanese), Faculty of Engineering in *Nagasaki Institute of Applied Science*, administrated by Hori, T., ***http://www.ship.nias.ac.jp/*** .

(55) Hori, T. : " A Typical Example on Ship's Stability Theorem " (Exposition in Japanese), ***NAVIGATION*** (Journal of *Japan Institute of Navigation*), 2021 (July), ***No.217***, pp.39~46.

(56) Hori, T., Hori, M. : "Theoretical Treatment on the Hydrostatic Stability of Ships (Part 1:) Stable Conditions for the Upright State", ***viXra.org*** *(Pre-print Repository)*, 2022 (March), ***viXra:2203.0180*** [Ver.4], Classical Physics, pp.1~16.

(57) Hori, T. : "Theoretical Procedure on the Hydrostatic Stability of Ships (Part 1:) Stable Conditions for the Upright State", *The Bulletin of Nagasaki Institute of Applied Science*, 2022 (December), ***Vol.62***, ***No.2***, Research Notes in Mathematical and Physical Science, pp.151~166.

(58) Igarashi, T. : "An Investigation on the Orientation of a Long Square Bar in Still Water" (in Japanese), ***NAGARE*** (Journal of *Japan Society of Fluid Mechanics*), 2000 (August), ***Vol.19***, ***No.4***, pp.253~262.

(59) Igarashi, T., Nakamura, H. : "An Investigation on the Orientation of a Long Rectangular Bar in Still Water" (in Japanese), ***NAGARE*** (Journal of *Japan Society of Fluid Mechanics*), 2007 (December), ***Vol.26***, ***No.6***, pp. 393~400.

(60) Hori, T. : "An Advanced Example on Ship's Stability Theorem —Solution for Stable Attitude of an Inclined Ship—" (Exposition in Japanese), ***NAVIGATION*** (Journal of *Japan Institute of Navigation*), 2021 (October), ***No.218***, pp. 58~65.

(61) Hori, T., Hori, M. : "Theoretical Treatment on the Hydrostatic Stability of Ships (Part 2:) Stable Attitude in an Inclined State", ***viXra.org*** *(Pre-print Repository)*, 2023 (January), ***viXra:2301.0159*** [Ver.2], Classical Physics, pp. 1~15.

(62) Hori, T. : "Theoretical Procedure on the Hydrostatic Stability of Ships (Part 2:) Stable Attitude in an Inclined State", *The Bulletin of Nagasaki Institute of Applied Science*, 2023 (June), ***Vol.63***, ***No.1***, Research Notes in Mathematical and Physical Science, pp. 55~69.

(63) Kurihara, M. : "On the Rolling Motion of a Buoy in Regular Waves" (in Japanese), *The Bulletin of the College of Naval Architecture of Nagasaki*, 1974 (June), Vol.15, No.1, pp. 1~4.

(64) Kurihara, M. : "On the Motions of a Ringed Buoy in Regular Waves" (in Japanese), *The Bulletin of Nagasaki Institute of Applied Science*, 1978 (October), Vol.19 (Commemorative issue of the name change from former the College of Naval Architecture of Nagasaki), pp. 11~15.

(65) Kurihara, M. : "On the Motions of a Floating Vertical Cylinder in Regular Waves" (in Japanese), *The Bulletin of Nagasaki Institute of Applied Science* (former the College of Naval Architecture of Nagasaki), 1979 (June), Vol.20, No.1, pp. 1~5.

(66) Hori, T. : "Lecture Video Proving that Center of Buoyancy is Equal to Center of Pressure for the Rectangular Cross-Section (80 minutes in the 1st half)" (in Japanese), 2021 (7 January), Regular Lecture No.13 of *"Hydrostatics of Floating Bodies"* (Specialized Subject of Naval Architectural Engineering Course in *Nagasaki Institute of Applied Science*), ***https://youtu.be/Wd7jKMXSqhc*** .

(67) Hori, T. : "Lecture Video Proving that Center of Buoyancy is Equal to Center of Pressure for the Rectangular Cross-Section (90 minutes in the 2nd half)" (in Japanese), 2021 (14 January), Regular Lecture No.14 of *"Hydrostatics of Floating Bodies"* (Specialized Subject of Naval Architectural Engineering Course in *Nagasaki Institute of Applied Science*), ***https://youtu.be/bniJ6-9vJPI*** .

(68) Hori, T. : "A New Derivation of Metacentric Radius (i) Positioning the metacenter (63 minutes in the 1st half)" (in Japanese), 2021 (14 October), Regular Lecture No.3 of *"Hydrostatics of Floating Bodies"* (Specialized Subject of Naval Architectural Engineering Course in *Nagasaki Institute of Applied Science*), ***https://youtu.be/lUWbQ92zJQQ*** .

(69) Hori, T. : "A New Derivation of Metacentric Radius (ii) Calculation formula for metacentric radius (82 minutes in the 2nd half)" (in Japanese), 2021 (21 October), Regular Lecture No.4 of *"Hydrostatics of Floating Bodies"* (Specialized Subject of Naval Architectural Engineering Course in *Nagasaki Institute of Applied Science*), ***https://youtu.be/qAIzLKXSY4U*** .

References

(70) Hori, T. : " Example on the Stability Theory of Ships (i) Stable condition for a columnar ship with rectangular cross-section of different breadths (85 minutes) " (in Japanese), 2020 (19 November), Regular Lecture No.8 of *" Theory of Ship Stability "* (Specialized Subject of Naval Architectural Engineering Course in *Nagasaki Institute of Applied Science*), ***https://youtu.be/PNVuRuZWYBM*** .

(71) Hori, T. : "Example on the Stability Theory of Ships (ii) Stable condition for a columnar ship with square cross-section of different materials (92 minutes) " (in Japanese), 2020 (26 November), Regular Lecture No.9 of *"Theory of Ship Stability"* (Specialized Subject of Naval Architectural Engineering Course in *Nagasaki Institute of Applied Science*), ***https://youtu.be/eeVg9ThjPd0*** .

(72) Matsumua, K. : " Perturbation Methods in Fluid Mechanics (Fundamental Version) " (Exposition in Japanese), *Journal of the Kansai Society of Naval Architects, Japan*, 1985 (June), ***No.197***, pp. 127~ 139.

(73) Matsumua, K. : "Perturbation Methods in Fluid Mechanics (Applied Version)" (Exposition in Japanese), *Journal of the Kansai Society of Naval Architects, Japan*, 1986 (June), ***No.201***, pp. 109~126.

(74) Hori, T. , Matsumua, K. and Tanaka, I. : "On the Lateral Force Caused by Wave Generation Acting on the Ship Hull with Steady Drift Angle" (in Japanese), *Journal of the Society of Naval Architects of Japan*, 1986 (June), ***Vol.159***, pp. 9~22.

(75) Kobayashi, Y. : " Tank System of LNG-LH2 —Physical Model and Thermal Flow Analysis by Using CFD —" (in Japanese), ***Seizan-dou Publishing***, 2016 (December) 1st Printing, p. 1~375.

(76) Kobayashi, Y. : " Utilization System of LNG-LH2 at Ultra-Low Temperature and Cold Heat —No Waste Energy System—" (in Japanese), *Shouwa-dou Publishing,* 2019 (April) 1st Printing, p. 1~226.

(77) Kobayashi, Y. : " Tank System of Liquefied Hydrogen : LH2 Storage & Transportation Systems — Feed-forward to LNG Systems—" (in Japanese), *Shouwa-dou Publishing,* 2023 (June) 1st Printing, p. 1~398.

(78) Hori, T. : " Proof that the Center of Buoyancy is Equal to the Center of Hydrostatic Pressure —Part 2 : Semi-Submerged Circular Cylinder and Triangular Prism —", *The Bulletin of Nagasaki Institute of Applied Science*, 2023 (December), ***Vol.63***, ***No.2***, Research Notes in Mathematical and Physical Science, pp. 117~143.

(79) Hori, T. : " Proof that the Center of Buoyancy is Equal to the Center of Hydrostatic Pressure —Part 3 : Submerged Circular Cylinder and Arbitrary Shaped Submerged Body —", *The Bulletin of Nagasaki Institute of Applied Science*, 2024 (June, *Scheduled to be Published*), *Vol.64*, *No.1*, Research Notes in Mathematical and Physical Science.

(80) Hori, T. : " Seminar on the Stability Theory of Ships (Outline explanation of the theory and model experiment in a small water tank) (15 minutes) " (in Japanese), 2020 (7 August), Inquiry learning for high school students (*Nagasaki Prefectural Seiryo High School*) conducted online, ***https://youtu.be/4T6znj1iKPI*** .

Appendices

A. 1 Centroid of the Trapezoidal Area, which is the Underwater Sectional Shape

In Appendix A. 1, the centroid of trapezoidal area, which is the cross-sectional shape under the water surface when a rectangle is inclined laterally, is geometrically obtained from the areal moment.

As shown in Fig. A. 1. 1, let's analyze in an inclined o-$\eta\zeta$ coordinate system with the origin o at the center of the bottom of the floating body and fixed to the body. This is the same coordinate system as Fig. 1. 1 in Chapter 1. Here, the draft of upright state is f , the half-breadth is b , and the heel angle is θ .

Then, we consider that the trapezoidal region under the water is divided into a rectangle (centroid g_1) and a triangle (centroid g_2) by a single dotted line.

If the area of the rectangular part is A_1 and the area of the triangular part is A_2 , each of them and their sum can be obtained as follows :

$$\left.\begin{aligned} &A_1 = 2b\,(\,f - b\tan\theta\,) \\ &A_2 = \frac{1}{2}\cdot 2b\cdot 2b\tan\theta = 2b^2\tan\theta \\ &A_1 + A_2 \,=\, 2b\,f \end{aligned}\right\} \quad \cdots\cdots\cdots (A.1.1)$$

First, we calculate the areal moment M'_η about the η - axis. Here, the superscript dash in M'_η is added to distinguish it from the moments caused by forces shown in Sections 1.2.4 and 1.3.3 in Chapter 1. Then, M'_η can be calculated as :

$$\begin{aligned} M'_\eta \,&=\, A_1 \times \frac{f - b\tan\theta}{2} \,+\, A_2 \times \left\{ (\,f - b\tan\theta\,) + \frac{2b\tan\theta}{3} \right\} \\ &=\, b\,f^{\,2} + \frac{1}{3}b^3\tan^2\theta \quad \cdots\cdots\cdots (A.1.2) \end{aligned}$$

Next, the areal moment M'_ζ about the ζ - axis can be calculated as :

$$\begin{aligned} M'_\zeta \,&=\, A_1 \times 0 \,+\, A_2 \times \left(b - \frac{2b}{3} \right) \,=\, A_2 \times \frac{b}{3} \\ &=\, \frac{2}{3}b^3\tan\theta \quad \cdots\cdots\cdots (A.1.3) \end{aligned}$$

If the coordinate of the centroid position G of the trapezoid is $(\eta_G\,,\,\zeta_G)$, the above areal moments M'_η and M'_ζ can be written as the product of the total area and the lever, respectively, as follows :

$$\left.\begin{aligned} M'_\eta \,&=\, (A_1 + A_2)\,\zeta_G \\ M'_\zeta \,&=\, (A_1 + A_2)\,\eta_G \end{aligned}\right\} \quad \cdots\cdots\cdots (A.1.4)$$

Therefore, the coordinates η_G and ζ_G of the centroid G of the area can be calculated and determined as follows :

$$\left.\begin{aligned} \eta_G &= \frac{M'_\zeta}{A_1+A_2} = \frac{b^2}{3f}\tan\theta \\ \zeta_G &= \frac{M'_\eta}{A_1+A_2} = \frac{f}{2} + \frac{b^2}{6f}\tan^2\theta \end{aligned}\right\} \quad \cdots\cdots\cdots (A.1.5)$$

Here, g_1, g_2 and G in Fig. A. 1. 1 are drawn on the correct positions in this state, and the three points are on the same straight line.

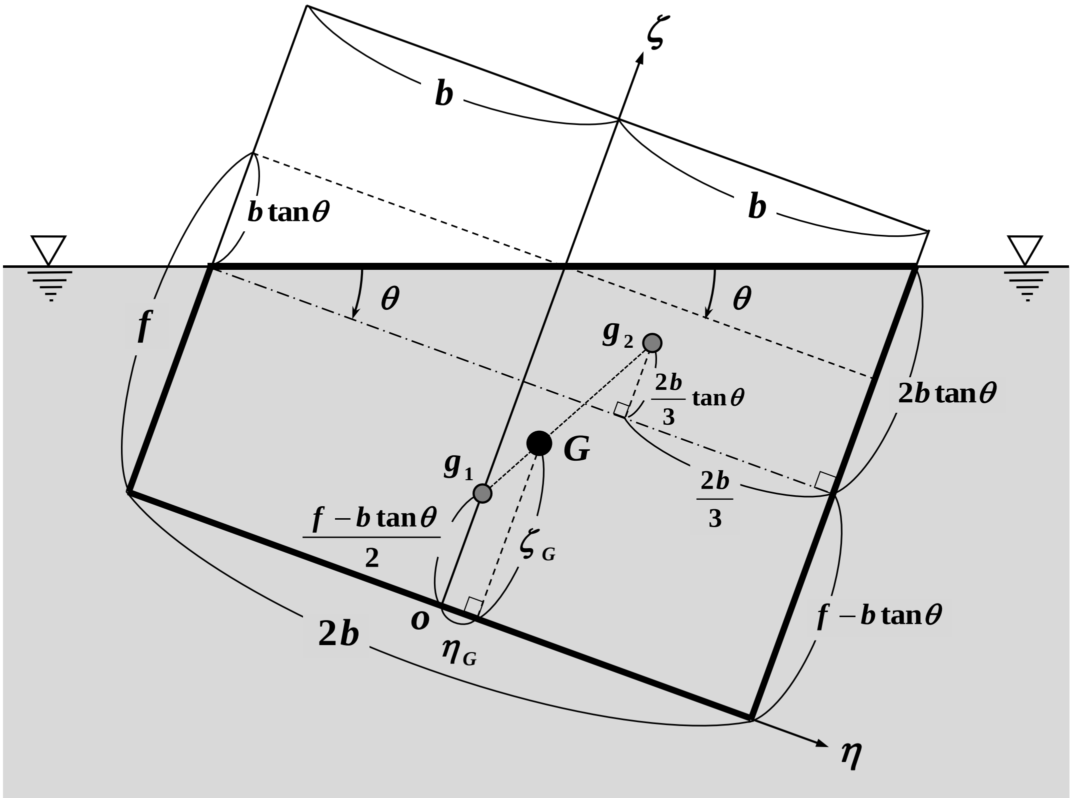

Fig. A. 1. 1 Centroid G of area of the underwater trapezoid.

A. 2 Positioning of the Center of Hydrostatic Pressure C_P Acting on the Triangular Prism

In Appendix A.2, we apply to the triangular prism[33), 2nd half of (35) and (78)] the same method developed for a rectangular cross-section in Section 1.2 of Chaper 1. It is then proved that the center of hydrostatic pressure is equal to the well-known center of buoyancy.

Fig. A.2.1 shows that a cross-section of triangular prism (breadth $2b$ draft f, freeboard h, vertex angle 2ϕ) inclines laterally with a heel angle θ to the starboard side. Here, the half breadth b of the waterline of the triangular prism in the upright state can be written, using the upright draft f and the half vertex angle ϕ, as follows :

$$b = f \tan\phi \quad \cdots\cdots (A.2.1)$$

Here, the cross-section of this triangular prism is an isosceles triangle with base (*i.e.* deck length) $2(f+h)\tan\phi$, height $f+h$, and both sides $(f+h)\sec\phi$.

A. 2. 1 Preparation calculations, including wetted lengths on both port and starboard sides

Let's consider the exposed triangle (port side, L for short) $\triangle oE_LT_L$ and the immersed triangle (starboard side, R for short) $\triangle oE_RT_R$ near the waterline in Fig. A. 2. 1. The heights $q_L = \overline{U_LT_L}$ and $q_R = \overline{U_RT_R}$ of each triangle can be expressed geometrically in two ways, using $x_L = \overline{U_LE_L}$ and $x_R = \overline{U_RE_R}$, as follows :

$$\left.\begin{aligned} q_L &= (b - x_L)\tan\theta = \frac{x_L}{\tan\phi} \\ q_R &= (b + x_R)\tan\theta = \frac{x_R}{\tan\phi} \end{aligned}\right\} \quad \cdots\cdots (A.2.2)$$

Thus, for x_L and x_R, the following relations can be obtained respectively as :

$$\left.\begin{aligned} x_L &= (b - x_L)\tan\phi\tan\theta \\ x_R &= (b + x_R)\tan\phi\tan\theta \end{aligned}\right\} \quad \cdots\cdots (A.2.3)$$

Therefore, x_L and x_R can be solved by using the relation in Eq. (A.2.1) for the half breadth b as follows :

$$\left.\begin{aligned} x_L &= \frac{\varepsilon}{1+\varepsilon} f\tan\phi \\ x_R &= \frac{\varepsilon}{1-\varepsilon} f\tan\phi \end{aligned}\right\} \quad \cdots\cdots (A.2.4)$$

Here, ε in the above equation is defined as the product of the tangent of the half vertex angle ϕ and that of the heel angle θ, as follows:

$$\varepsilon \equiv \tan\phi\tan\theta \quad \cdots\cdots (A.2.5)$$

Next, the decremental length s_L and the incremental length s_R of the wetted length on the port and starboard sides respectively, are written as :

$$\left.\begin{aligned} s_L &= \frac{x_L}{\sin\phi} = \frac{\varepsilon}{1+\varepsilon} f \sec\phi \\ s_R &= \frac{x_R}{\sin\phi} = \frac{\varepsilon}{1-\varepsilon} f \sec\phi \end{aligned}\right\} \quad \text{(A.2.6)}$$

Therefore, the wetted lengths ℓ_L and ℓ_R on the port and starboard sides are obtained as follows :

$$\left.\begin{aligned} \ell_L &= f \sec\phi - s_L = \frac{1}{1+\varepsilon} f \sec\phi \\ \ell_R &= f \sec\phi + s_R = \frac{1}{1-\varepsilon} f \sec\phi \end{aligned}\right\} \quad \text{(A.2.7)}$$

The waterline breadths b_L and b_R on both the port and starboard sides can be obtained by using x_L and x_R in Eq. (A.2.3) as follows :

$$\left.\begin{aligned} b_L &= (b - x_L) \sec\theta = \frac{1}{1+\varepsilon} f \tan\phi \sec\theta \\ b_R &= (b + x_R) \sec\theta = \frac{1}{1-\varepsilon} f \tan\phi \sec\theta \end{aligned}\right\} \quad \text{(A.2.8)}$$

Thus, the total waterline breadth is written as :

$$b_L + b_R = \frac{2}{1-\varepsilon^2} f \tan\phi \sec\theta \quad \text{(A.2.9)}$$

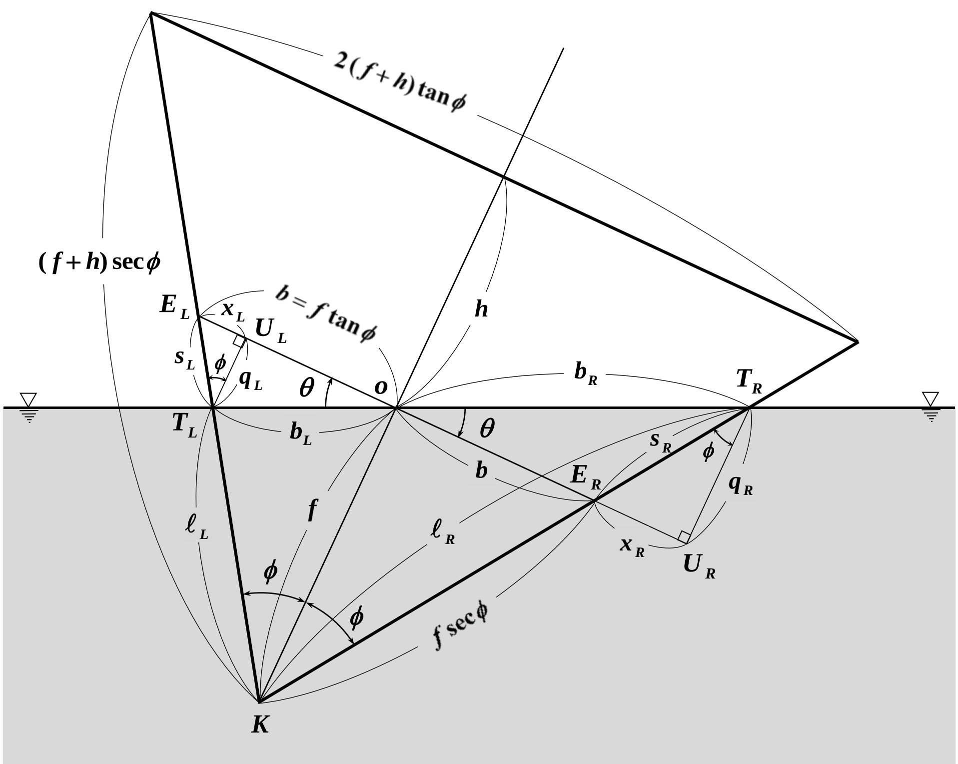

Fig. A.2.1 Cross-section of an inclined triangular prism.

Therefore, the area *A* of triangle $\triangle K T_L T_R$ below the water surface of a triangular prism, which is inclined laterally with heel angle θ, is obtained as follows :

$$A = \frac{1}{2}(b_L + b_R) \cdot f \cos\theta = \frac{1}{1-\varepsilon^2} f^2 \tan\phi \qquad \text{(A.2.10)}$$

Since the underwater area A_0 in the upright state ($\theta = 0$ *i.e.* $\varepsilon = 0$) is shown below, the underwater area *A* in the above inclined state is increased by $\frac{\varepsilon^2}{1-\varepsilon^2} A_0$ from the upright state.

$$A_0 \equiv A\Big]_{\theta=0} = f^2 \tan\phi \ \ (= bf) \qquad \text{(A.2.11)}$$

A. 2. 2 Forces due to hydrostatic pressure acting on three surfaces around a triangular prism

Fig. A. 2. 2 shows the pressure distribution and the forces generated by integrating it, acting on the cross-section of the triangular prism drawn in Fig. A. 2. 1. The coordinate systems are $o - yz$ fixed in space with the *z*-axis pointing vertically downward, and $o - \eta\zeta$ fixed on the prism and tilted, both with the origin *o* at the center of still water surface.

The atmospheric pressure is denoted by p_0 and the specific weight of water is denoted by γ. The atmospheric pressure p_0 is shown as a dashed line, and the hydrostatic pressure γz as a solid line. The respective pressures are shown as thin vectors, and the forces as thick vectors. Then, all are acting perpendicularly to the surface of the triangular prism.

The water depth Z_f at the vertex *K* of the triangle corresponding to the ship's bottom is denoted as :

$$Z_f = f \cos\theta \qquad \text{(A.2.12)}$$

The forces P_{Left} and P_{Right} acting on the port (subscripts in Left) and starboard (subscripts in Right) sides are obtained by summing the forces $P_{Left}^{(0)}$, $P_{Right}^{(0)}$ due to uniformly distributed atmospheric pressure acting on the entire port side and the forces $P_{Left}^{(0)}$, $P_{Right}^{(0)}$ due to the triangularly distributed hydrostatic pressure acting on the submerged part respectively, by using the wetted lengths ℓ_L , ℓ_R in Eq. (A.2.7), as follows :

$$\left.\begin{aligned}
P_{Left} &= P_{Left}^{(0)} + P_{Left}^{(\gamma)} \\
&= p_0(f+h)\sec\phi + \frac{1}{2}\gamma Z_f \,\ell_L \\
&= p_0(f+h)\sec\phi + \frac{1}{2}\gamma f^2 \frac{\sec\phi\cos\theta}{1+\varepsilon} \\
P_{Right} &= P_{Right}^{(0)} + P_{Right}^{(\gamma)} \\
&= p_0(f+h)\sec\phi + \frac{1}{2}\gamma Z_f \,\ell_R \\
&= p_0(f+h)\sec\phi + \frac{1}{2}\gamma f^2 \frac{\sec\phi\cos\theta}{1-\varepsilon}
\end{aligned}\right\} \qquad \text{(A.2.13)}$$

The force P_{Upper} acting on the deck (subscripts in Upper) is only $P_{Upper}^{(0)}$ due to atmospheric pressure, so it is obtained as :

$$\begin{aligned} P_{Upper} &= P_{Upper}^{(0)} \\ &= 2\,p_0(f+h)\tan\phi \qquad \cdots\cdots (A.2.14) \end{aligned}$$

A. 2. 3 Combined forces $F_{-\eta}$ and $F_{-\zeta}$ in the $-\eta$ and $-\zeta$ directions acting on the prism surface

The combined forces $F_{-\eta}$ and $F_{-\zeta}$ acting in the $-\eta$ and $-\zeta$ directions fixed to the inclined floating prism are obtained by using P_{Left} , P_{Right} and P_{Upper} in Eqs. (A.2.13) and (A.2.14), as follows :

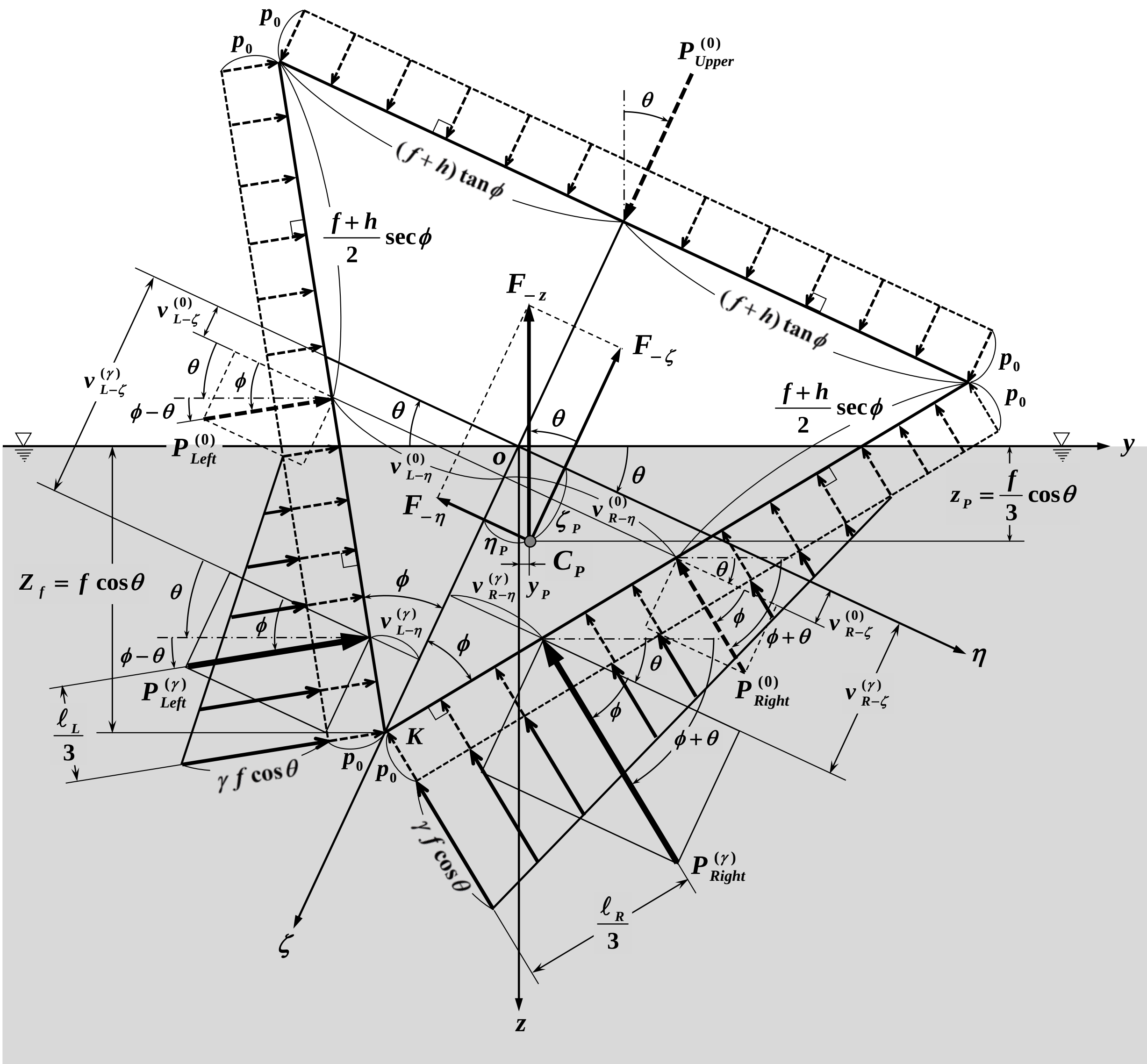

Fig. A. 2. 2 Hydrostatic pressure and the center of pressure acting on the cross-section of an inclined triangular prism.

$$\left.\begin{aligned}
F_{-\eta} &= P_{Right}\cos\phi - P_{Left}\cos\phi \\
&= \frac{1}{2}\gamma f^2\cos\theta\left(\frac{1}{1-\varepsilon}-\frac{1}{1+\varepsilon}\right) + p_0(f+h) - p_0(f+h) \\
&= \gamma f^2\frac{\varepsilon}{1-\varepsilon^2}\cos\theta = \gamma f^2\frac{\tan\phi}{1-\varepsilon^2}\sin\theta = \gamma A\sin\theta \\
F_{-\zeta} &= P_{Right}\sin\phi + P_{Left}\sin\phi - P_{Upper} \\
&= \frac{1}{2}\gamma f^2\tan\phi\cos\theta\left(\frac{1}{1-\varepsilon}+\frac{1}{1+\varepsilon}\right) + 2p_0(f+h)\tan\phi - P_{Upper}^{(0)} \\
&= \gamma f^2\frac{\tan\phi}{1-\varepsilon^2}\cos\theta = \gamma A\cos\theta
\end{aligned}\right\} \cdots\cdots\cdots\text{(A.2.15)}$$

Here, $F_{-\eta}$ and $F_{-\zeta}$ of the above are obtained as the sine and cosine components of the buoyant force γA, as shown by F_{-z} of Eq. (A.2.17) in the next section, with respect to the heel angle θ. This result indicates that the atmospheric pressure p_0 cancels out and does not contribute to the combined forces acting on the floating prism.

A.2.4 Forces F_{-y} and F_{-z} converted in the $-y$ and $-z$ directions

The horizontal component (in the $-y$ direction) F_{-y} and the vertical component (in the $-z$ direction) F_{-z} of the force acting on the triangular prism are obtained by coordinate transformation of $F_{-\eta}$ and $F_{-\zeta}$ in Eq. (A.2.15) of the previous section.

Then, the horizontal component F_{-y} is converted as :

$$\begin{aligned}
F_{-y} &= F_{-\eta}\cos\theta - F_{-\zeta}\sin\theta \\
&= \gamma A(\sin\theta\cdot\cos\theta - \cos\theta\cdot\sin\theta) \\
&= 0 \qquad \cdots\cdots\cdots\text{(A.2.16)}
\end{aligned}$$

From the above result, the horizontal component of the combined force does not generate, even in an left-right asymmetric pressure field due to lateral inclination.

And, the vertical component F_{-z} is similarly converted as :

$$\begin{aligned}
F_{-z} &= F_{-\zeta}\cos\theta + F_{-\eta}\sin\theta \\
&= \gamma A(\cos^2\theta + \sin^2\theta) \\
&= \gamma A \ (= Buoyant\ Force) \qquad \cdots\cdots\cdots\text{(A.2.17)}
\end{aligned}$$

The above result shows that the vertical component is obtained by the product of the specific weight γ of water and the cross-sectional area A under the water surface of the triangular prism shown in Eq. (A.2.10). This indicates that F_{-z} is the very buoyant force taught by Archimedes' principle[(1)].

On the other hand, the F_{-y} and F_{-z} can also be obtained directly from P_{Left}, P_{Right} and P_{Upper} in Eqs. (A.2.13) and (A.2.14), as follows :

First, the horizontal component F_{-y} is calculated as :

$$
\begin{aligned}
F_{-y} &= P_{Right}\cos(\phi+\theta) - P_{Left}\cos(\phi-\theta) + P_{Upper}\sin\theta \\
&= \frac{1}{2}\gamma f^2 \sec\phi\cos\theta \left\{ \frac{\cos(\phi+\theta)}{1-\varepsilon} - \frac{\cos(\phi-\theta)}{1+\varepsilon} \right\} \\
&\quad + p_0(f+h)\left[\sec\phi\left\{\cos(\phi+\theta)-\cos(\phi-\theta)\right\} + 2\tan\phi\sin\theta\right] \\
&= -\gamma f^2 \sec\phi\cos\theta \,\frac{\sin\phi\sin\theta - \varepsilon\cos\phi\cos\theta}{1-\varepsilon^2} - 2p_0(f+h)\sin\theta\,(\sin\phi\sec\phi - \tan\phi) \\
&= 0 \qquad \cdots\cdots (\text{A.2.18})
\end{aligned}
$$

Next, the vertical component F_{-z} is calculated as :

$$
\begin{aligned}
F_{-z} &= P_{Right}\sin(\phi+\theta) + P_{Left}\sin(\phi-\theta) - P_{Upper}\cos\theta \\
&= \frac{1}{2}\gamma f^2 \sec\phi\cos\theta \left\{ \frac{\sin(\phi+\theta)}{1-\varepsilon} + \frac{\sin(\phi-\theta)}{1+\varepsilon} \right\} \\
&\quad + p_0(f+h)\left[\sec\phi\left\{\sin(\phi+\theta)+\sin(\phi-\theta)\right\} - 2\tan\phi\cos\theta\right] \\
&= \gamma f^2 \sec\phi\cos\theta \,\frac{\sin\phi\cos\theta + \varepsilon\cos\phi\sin\theta}{1-\varepsilon^2} + 2p_0(f+h)\cos\theta\,(\sin\phi\sec\phi - \tan\phi) \\
&= \gamma f^2 \sec\phi\cos\theta \,\frac{\sin\phi\sec\theta}{1-\varepsilon^2} = \gamma f^2 \frac{1}{1-\varepsilon^2}\tan\phi \\
&= \gamma A \qquad \cdots\cdots (\text{A.2.19})
\end{aligned}
$$

Both of the above equations cancel out the atmospheric pressure p_0 and are identical to Eqs. (A.2.16) and (A.2.17) obtained by transforming the coordinates of $F_{-\eta}$ and $F_{-\eta}$. This confirms that the forces due to pressure in Section A.2.2 have been calculated correctly.

A.2.5 Moments M_η and M_ζ due to pressure in the η and ζ directions acting on the prism surface

First, let's consider the calculation of the moment M_η about the origin o, generated by the η-directional components of the forces P_{Left} and P_{Right} due to pressure acting perpendicularly on the sides of a triangular prism.

The levers $v^{(0)}_{L-\zeta}$ and $v^{(0)}_{R-\zeta}$ parallel to the ζ-axis on both the port and starboard sides by the atmospheric pressure components $^{(0)}$ of the uniform distribution are obtained as the same length on both sides, since the both side lengths including freeboard are $(f+h)\sec\phi$, as follows :

$$
v^{(0)}_{L-\zeta} = v^{(0)}_{R-\zeta} = f - \frac{(f+h)\sec\phi}{2}\cos\phi = \frac{f-h}{2} \qquad \cdots\cdots (\text{A.2.20})
$$

The levers $v^{(\gamma)}_{L-\zeta}$ and $v^{(\gamma)}_{R-\zeta}$ parallel to the ζ-axis on both port and starboard sides due to the hydrostatic components $^{(\gamma)}$ of the triangular distribution are obtained by using the wetted lengths ℓ_L and ℓ_R in Eq. (A.2.7) as follows :

$$\left.\begin{aligned} v_{L-\zeta}^{(\gamma)} &= f - \frac{\ell_L}{3}\cos\phi = f - \frac{1}{3(1+\varepsilon)} f = \frac{2+3\varepsilon}{3(1+\varepsilon)} f \\ v_{R-\zeta}^{(\gamma)} &= f - \frac{\ell_R}{3}\cos\phi = f - \frac{1}{3(1-\varepsilon)} f = \frac{2-3\varepsilon}{3(1-\varepsilon)} f \end{aligned}\right\} \quad\cdots\cdots\text{(A.2.21)}$$

By the above two equations, the clockwise moment M_η due to pressure in the η - direction about the origin o can be obtained independently of the atmospheric pressure p_0, using Eqs. (A.2.13), (A.2.20) and (A.2.21), as follows :

$$\begin{aligned} M_\eta &= P_{Right}^{(0)}\cos\phi\cdot v_{R-\zeta}^{(0)} + P_{Right}^{(\gamma)}\cos\phi\cdot v_{R-\zeta}^{(\gamma)} \\ &\quad - (P_{Left}^{(0)}\cos\phi\cdot v_{L-\zeta}^{(0)} + P_{Left}^{(\gamma)}\cos\phi\cdot v_{L-\zeta}^{(\gamma)}) \\ &= \frac{1}{6}\gamma f^3\cos\theta\left\{\frac{2-3\varepsilon}{(1-\varepsilon)^2} - \frac{2+3\varepsilon}{(1+\varepsilon)^2}\right\} + p_0(f+h)\cdot(v_{R-\zeta}^{(0)} - v_{L-\zeta}^{(0)}) \\ &= \frac{1}{3}\gamma f^3\frac{\varepsilon(1-3\varepsilon^2)}{(1-\varepsilon^2)^2}\cos\theta = \frac{1}{3}\gamma f A\frac{1-3\varepsilon^2}{1-\varepsilon^2}\sin\theta \quad\cdots\cdots\text{(A.2.22)} \end{aligned}$$

Next, let's calculate the moment M_ζ around point o , generated by P_{Upper} and the ζ - directional components of P_{Left} and P_{Right} .

The levers $v_{L-\eta}^{(0)}$ and $v_{R-\eta}^{(0)}$ parallel to the η - axis due to the atmospheric pressure components $^{(0)}$ are obtained as :

$$v_{L-\eta}^{(0)} = v_{R-\eta}^{(0)} = \frac{(f+h)\sec\phi}{2}\sin\phi = \frac{f+h}{2}\tan\phi \quad\cdots\cdots\text{(A.2.23)}$$

Here, the above equation, like Eq. (A.2.20), has the same length on both sides.

The levers $v_{L-\eta}^{(\gamma)}$ and $v_{L-\eta}^{(\gamma)}$ parallel to the η - axis on both the port and starboard sides due to the hydrostatic components $^{(\gamma)}$ can be obtained by using ℓ_L and ℓ_R in Eq. (A.2.7), as follows :

$$\left.\begin{aligned} v_{L-\eta}^{(\gamma)} &= \frac{\ell_L}{3}\sin\phi = \frac{\tan\phi}{3(1+\varepsilon)} f \\ v_{R-\eta}^{(\gamma)} &= \frac{\ell_R}{3}\sin\phi = \frac{\tan\phi}{3(1-\varepsilon)} f \end{aligned}\right\} \quad\cdots\cdots\text{(A.2.24)}$$

Therefore, the counterclockwise moment M_ζ due to pressure in the ζ - direction about the origin o can be calculated by Eqs. (A.2.13), (A.2.14), (A.2.23) and (A.2.24), as follows :

$$\begin{aligned} M_\zeta &= P_{Right}^{(0)}\sin\phi\cdot v_{R-\eta}^{(0)} + P_{Right}^{(\gamma)}\sin\phi\cdot v_{R-\eta}^{(\gamma)} \\ &\quad - (P_{Left}^{(0)}\sin\phi\cdot v_{L-\eta}^{(0)} + P_{Left}^{(\gamma)}\sin\phi\cdot v_{L-\eta}^{(\gamma)}) + P_{Upper}\times 0 \\ &= \frac{1}{6}\gamma f^3\tan^2\phi\cos\theta\left\{\frac{1}{(1-\varepsilon)^2} - \frac{1}{(1+\varepsilon)^2}\right\} + p_0(f+h)\tan\phi\cdot(v_{R-\eta}^{(0)} - v_{L-\eta}^{(0)}) \\ &= \frac{2}{3}\gamma f^3\frac{\varepsilon\tan^2\phi}{(1-\varepsilon^2)^2}\cos\theta = \frac{2}{3}\gamma f A\frac{\tan^2\phi}{1-\varepsilon^2}\sin\theta \quad\cdots\cdots\text{(A.2.25)} \end{aligned}$$

Here, M_ζ, like M_η, is obtained independently of the atmospheric pressure p_0.

A. 2. 6 Positioning of the center of hydrostatic pressure C_P for the triangular prism at lateral inclination

To locate the center of pressure C_P in $o-\eta\zeta$ coordinate system fixed to the inclined triangular prism, the hydraulic method(9-a) used in Chapter 1 for the rectangular and arbitrary shaped cross-section is applied.

Since the forces $F_{-\eta}$ and $F_{-\zeta}$ due to the hydrostatic pressure obtained in Section A. 2. 3 act on the center of pressure $C_P\ (\eta_P, \zeta_P)$, the moments M_η and M_ζ due to the same pressure obtained in Section A. 2. 5 can be expressed exactly same as Eq. (1.27) in Chapter 1, as follows :

$$\left.\begin{aligned} M_\eta &= F_{-\eta}\,\zeta_P \\ M_\zeta &= F_{-\zeta}\,\eta_P \end{aligned}\right\} \qquad \text{(A.2.26)}$$

Therefore, the unknown coordinate (η_P, ζ_P) of the center of pressure C_P can be determined by the above relation. Here, the η - coordinate, η_P, can be calculated by using the latter in Eq. (A.2.15) for $F_{-\zeta}$ and the Eq. (A.2.25) for M_ζ due to the hydrostatic pressure in the $-\zeta$ direction, as follows :

$$\begin{aligned} \eta_P = \frac{M_\zeta}{F_{-\zeta}} &= \frac{\dfrac{2}{3}\gamma f A \dfrac{\tan^2\phi}{1-\varepsilon^2}\sin\theta}{\gamma A\cos\theta} \\ &= \frac{2}{3} f \frac{\varepsilon\tan\phi}{1-\varepsilon^2} \end{aligned} \qquad \text{(A.2.27)}$$

And, the ζ - coordinate, ζ_P, can be calculated by using the former in Eq. (A.2.15) for $F_{-\eta}$ and the Eq. (A.2.22) for M_η due to the hydrostatic pressure in the $-\eta$ direction, as follows :

$$\begin{aligned} \zeta_P = \frac{M_\eta}{F_{-\eta}} &= \frac{\dfrac{1}{3}\gamma f A \dfrac{1-3\varepsilon^2}{1-\varepsilon^2}\sin\theta}{\gamma A\sin\theta} \\ &= \frac{1}{3} f \frac{1-3\varepsilon^2}{1-\varepsilon^2} \end{aligned} \qquad \text{(A.2.28)}$$

Considering the above, ζ_P of vertical component can be obtained by offsetting the zero factor $\sin\theta$ at the heel angle $\theta \to 0$ with the denominator and numerator, as shown in Eq. (A.2.28). Here, if we start the calculation from the beginning as the upright state with $\theta = 0$, both the denominator $F_{-\eta}$ and the numerator M_η are in equilibrium and become zero, so the fraction becomes indeterminate forms and ζ_P cannot be determined. This is the reason why we were able to determine the position of the center of pressure in the ζ - direction by inclining the floating body laterally.

On the other hand, in the calculation of η_P in Eq. (A.2.27), even if the heel angle is $\theta = 0$ from the beginning, the numerator M_ζ is in equilibrium and zero, but the denominator $F_{-\zeta}$ takes a finite value as the cosine component of the buoyancy. Therefore, the horizontal component η_P can be determine,

even if we start the calculation as the upright state.

Let us now transform the resulting center of pressure $C_P(\eta_P, \zeta_P)$ in the floating prism - fixed coordinates into the space - fixed coordinate system (y_P, z_P).

First, y_P in the horizontal direction becomes as :

$$y_P = \eta_P \cos\theta - \zeta_P \sin\theta$$
$$= \frac{1}{3} f \frac{2\varepsilon\tan\phi\cos\theta - (1-3\varepsilon^2)\sin\theta}{1-\varepsilon^2}$$
$$= \frac{1}{3} f \frac{2\tan^2\phi + 3\varepsilon^2 - 1}{1-\varepsilon^2} \sin\theta \qquad \cdots\cdots (A.2.29)$$

Next, z_P in the vertical direction becomes as :

$$z_P = \zeta_P \cos\theta + \eta_P \sin\theta$$
$$= \frac{1}{3} f \frac{(1-3\varepsilon^2)\cos\theta + 2\varepsilon\tan\phi\sin\theta}{1-\varepsilon^2}$$
$$= \frac{1}{3} f \frac{(1-3\varepsilon^2) + 2\varepsilon^2}{1-\varepsilon^2} \cos\theta = \frac{1}{3} f \cos\theta \qquad \cdots\cdots (A.2.30)$$

From the above results, it is clear that the latter z_P indicates the vertical position of figure centroid of a triangle of height $f\cos\theta$, with the water surface as its base. Hence, we will verify in the next section, whether the former y_P also coincides with the horizontal position of figure centroid of underwater triangle.

A. 2. 7 Verification by the position of the figure centroid of the triangle below the water surface

Fig. A. 2. 3 shows an extract of the area under the water surface for the cross - section of the triangular prism in Figs. A. 2. 1 and A. 2. 2. Let us divide the triangle $\triangle K T_L T_R$ into two parts by the z' - axis connecting the vertex K of the triangle and the origin o' taken vertically above the vertex K.

For the *__L__eft* triangle $\triangle K o' T_L$, the area is A_L and the base is y_L, and for the *__R__ight* triangle $\triangle K o' T_R$, the area is A_R and the base is y_R. And the height is the common on both left and right triangles, $\overline{o'K} = Z_f$.

In this case, the areas A_L and A_R of the left and right triangles respectively, are written as :

$$\left.\begin{aligned} A_L &= \frac{1}{2} Z_f\, y_L \\ A_R &= \frac{1}{2} Z_f\, y_R \end{aligned}\right\} \qquad \cdots\cdots (A.2.31)$$

The base of the triangle $\triangle K T_L T_R$ can be written in the following two ways, by using y_L and y_R in Fig. A. 2. 3 and b_L and b_R in Fig. A. 2. 1.

Appendices
A. 2 Positioning of the Center of Hydrostatic Pressure C_P Acting on the Triangular Prism

$$y_L + y_R = b_L + b_R \ (= base\ of\ \triangle K T_L T_R) \quad \cdots\cdots (A.2.32)$$

Therefore, the area A of $\triangle K T_L T_R$, which is the sum of A_L and A_R above, is expressed by Eq. (A.2.10) in Section A.2.1, as follows :

$$\begin{aligned} A &= A_L + A_R \\ &= \frac{1}{2} Z_f (y_L + y_R) \\ &= \frac{1}{2} f \cos\theta \, (b_L + b_R) = \frac{1}{1-\varepsilon^2} f^2 \tan\phi \end{aligned} \quad \cdots\cdots (A.2.33)$$

And, y_L and y_R, which correspond to the bases of the divided two parts of $\triangle K T_L T_R$, become respectively, using ϕ and θ, as follows :

$$\left.\begin{aligned} y_L &= Z_f \tan(\phi - \theta) = Z_f \frac{\tan\phi - \tan\theta}{1+\varepsilon} \\ y_R &= Z_f \tan(\phi + \theta) = Z_f \frac{\tan\phi + \tan\theta}{1-\varepsilon} \end{aligned}\right\} \quad \cdots\cdots (A.2.34)$$

The areal moment M_z' of triangle $\triangle K T_L T_R$ about the z'-axis can be obtained by using Eq. (A.2.31) for A_L and A_R as follows, since the two horizontal distances from the z'-axis to the figure centroids g_L and g_R of the divided left and right triangles $\triangle K o' T_L$ and $\triangle K o' T_R$ respectively are the levers of moment.

$$\begin{aligned} M_z' &= A_R \times \frac{y_R}{3} - A_L \times \frac{y_L}{3} \\ &= \frac{1}{6} Z_f (y_R^2 - y_L^2) \end{aligned} \quad \cdots\cdots (A.2.35)$$

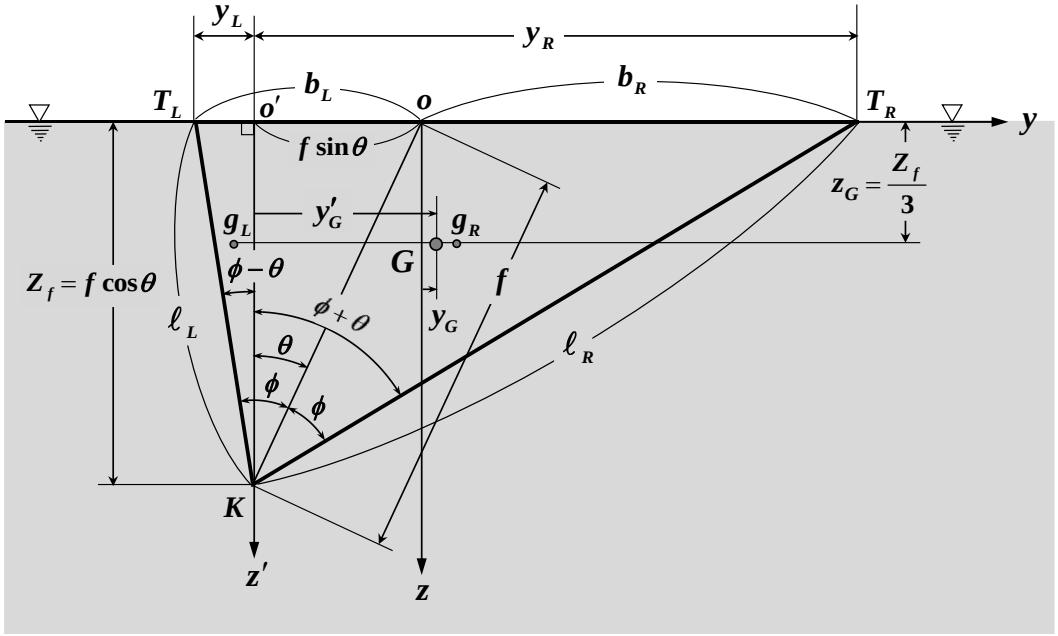

Fig. A.2.3 Figure centroid of triangular cross-section below the water surface.

Here, the superscript dash in the above M_z' is added to distinguish the areal moment from the moments due to forces shown in Section A.2.5.

Proceeding with the calculation, by using Eq. (A.2.34) for y_L and y_R, Eq. (A.2.12) for Z_f, and Eq. (A.2.5) for ε, the areal moment M_z' can be obtained in terms of A in Eq. (A.2.33), as follows :

$$\begin{aligned} M_z' &= \frac{1}{6} Z_f{}^3 \left\{ \frac{(\tan\phi + \tan\theta)^2}{(1-\varepsilon)^2} - \frac{(\tan\phi - \tan\theta)^2}{(1+\varepsilon)^2} \right\} \\ &= \frac{1}{6} Z_f{}^3 \frac{4\varepsilon \sec^2\phi \sec^2\theta}{(1-\varepsilon^2)^2} \\ &= \frac{2}{3} f^3 \frac{\tan\phi \sec^2\phi}{(1-\varepsilon^2)^2} \sin\theta = \frac{2}{3} f A \frac{\sec^2\phi}{1-\varepsilon^2} \sin\theta \end{aligned} \quad \cdots\cdots\cdots\cdots\cdots\cdots\cdots\cdots\cdots\cdots (A.2.36)$$

Therefore, the horizontal distance y_G' of the figure centroid G of triangular $\triangle K T_L T_R$ from the z'-axis is determined by dividing M_z' in Eq. (A.2.36) by the area A in Eq. (A.2.33), as follows :

$$\begin{aligned} y_G' &= \frac{M_z'}{A} \\ &= \frac{2}{3} f \frac{\sec^2\phi}{1-\varepsilon^2} \sin\theta \end{aligned} \quad \cdots\cdots\cdots\cdots\cdots\cdots\cdots\cdots\cdots\cdots\cdots\cdots\cdots\cdots\cdots\cdots\cdots\cdots\cdots\cdots\cdots\cdots (A.2.37)$$

Finally, let's consider finding the horizontal distance y_G of the figure centroid G from the original z-axis. Here, the distance $\overline{o'o}$ between the two origin points is measured as follows, by using Fig. A.2.3 or the former part of Eqs. (A.2.8) and (A.2.34).

$$\overline{o'o} = b_L - y_L = f \sin\theta \quad \cdots\cdots\cdots\cdots\cdots\cdots\cdots\cdots\cdots\cdots\cdots\cdots\cdots\cdots\cdots\cdots\cdots\cdots\cdots\cdots\cdots\cdots\cdots\cdots\cdots\cdots\cdots\cdots (A.2.38)$$

Hence, y_G is calculated by using Eqs. (A.2.37) and (A.2.38), as follows :

$$\begin{aligned} y_G &= y_G' - \overline{o'o} \\ &= y_G' - f \sin\theta \\ &= \frac{1}{3} f \frac{2\sec^2\phi - 3(1-\varepsilon^2)}{1-\varepsilon^2} \sin\theta = \frac{1}{3} f \frac{2\tan^2\phi + 3\varepsilon^2 - 1}{1-\varepsilon^2} \sin\theta \end{aligned} \quad \cdots\cdots\cdots\cdots\cdots\cdots\cdots\cdots\cdots\cdots\cdots\cdots\cdots\cdots\cdots\cdots\cdots\cdots\cdots\cdots\cdots\cdots\cdots\cdots\cdots\cdots\cdots\cdots (A.2.39)$$

On the other hand, the vertical distance z_G from the y-axis to the figure centroid G need not be calculated and is obtained by the well-known geometry as follows, since $\triangle K T_L T_R$ is a triangle of height $Z_f = f\cos\theta$ whose base is the water surface (*i.e.* y-axis).

$$z_G = \frac{1}{3} f \cos\theta \quad \cdots\cdots\cdots\cdots\cdots\cdots\cdots\cdots\cdots\cdots\cdots\cdots\cdots\cdots\cdots\cdots\cdots\cdots\cdots\cdots\cdots\cdots\cdots\cdots\cdots\cdots\cdots\cdots\cdots\cdots\cdots\cdots (A.2.40)$$

Thus, by comparing Eqs. (A.2.29) and (A.2.39) and Eqs. (A.2.30) and (A.2.40), we find as follows :

$$\left.\begin{aligned} y_P &= y_G \\ z_P &= z_G \end{aligned}\right\} \quad \cdots\cdots \text{(A.2.41)}$$

This result proves that the center of hydrostatic pressure is the well-known position of the center of buoyancy, since it indicates that the center of pressure of the asymmetrical triangular cross - section at lateral inclination coincides with the figure centroid below the water surface.

A. 2. 8 Positioning of the center of pressure C_P for the upright triangular prism

In order to clarify the consequences obtained in Eq. (A.2.41) of the previous section, we find the position of the center of pressure C_P of the triangular prism in the upright state. As a final step, let us set $\theta \to 0$ in the coordinates (η_P, ζ_P) of the center of pressure obtained for the inclined state.

Here, if the heel angle θ tends to zero, ε in Eq. (A.2.5) becomes as :

$$\varepsilon\,\big]_{\theta=0} = \tan\phi \tan\theta\,\big]_{\theta=0} = 0 \quad \cdots\cdots \text{(A.2.42)}$$

Thus, by Eqs. (A.2.27) and (A.2.28) in Section A. 2. 6, C_P is determined as follows :

$$C_P\,(\eta_P, \zeta_P)\,\big]_{\theta=0} = \left(0\,,\ \frac{f}{3}\right) \quad \cdots\cdots \text{(A.2.43)}$$

Alternatively, since the o - $\eta\zeta$ and o - yz coordinate systems coincide in the case of $\theta \to 0$, the following conclusion can be obtained by Eqs. (A.2.29) and (A.2.30) as well.

$$C_P\,(y_P, z_P)\,\big]_{\theta=0} = \left(0\,,\ \frac{f}{3}\right) \quad \cdots\cdots \text{(A.2.44)}$$

Since the both of Eqs. (A.2.43) and (A.2.44) above clearly show the position of the figure centroid of the isosceles triangle below the water surface, it is proved that the center of hydrostatic pressure is the well-known center of buoyancy for the triangular prism.

A. 3 Positioning of the Center of Hydrostatic Pressure C_P Acting on the Semi-Submerged Circular Cylinder

In Appendix A. 3, we apply to the semi-submerged circular cylinder (28), 1st half of (35) and (78) the same method developed for an arbitrary shaped cross-section in Section 1. 3 of Chaper 1. It is then proved that the center of hydrostatic pressure is equal to the well-known center of buoyancy.

Fig. A. 3. 1 shows that a cross-section of semi-submerged circular cylinder with radius R (breadth $2R$ and draft R) inclines laterally with a heel angle θ to the starboard side. The origin o is placed at the center of the still water surface, and the coordinate system fixed in space with the z-axis pointing vertically downward is o-yz, and that fixed to the inclined circular cylinder is o-$\eta\zeta$.

If the argument measured counterclockwise from the ζ-axis is ϕ as shown in Fig. A. 3. 1, then the argument of the water surface on the port side ϕ_L (subscript in *<u>L</u>eft*) on the starboard side ϕ_R (subscript in *<u>R</u>ight*) can be written respectively, as follows :

$$\left.\begin{aligned} \phi_L &= -\frac{\pi}{2}+\theta \\ \phi_R &= \frac{\pi}{2}+\theta \end{aligned}\right\} \qquad \cdots\cdots (A.3.1)$$

Here, the aerial part $c^{(0)}$ and the submerged part $c^{(\gamma)}$ can be written in terms of argument ϕ respectively, as follows :

$$\left.\begin{aligned} c^{(0)}:&\ \ \phi_R \le \phi \le \phi_L + 2\pi \ \rightarrow \ \frac{\pi}{2}+\theta \le \phi \le \frac{3\pi}{2}+\theta \\ c^{(\gamma)}:&\ \ \phi_L \le \phi \le \phi_R \qquad\ \ \rightarrow -\frac{\pi}{2}+\theta \le \phi \le \frac{\pi}{2}+\theta \end{aligned}\right\} \qquad \cdots\cdots (A.3.2)$$

The water depth $z(\phi)$ on the cylinder surface $(\eta,\zeta)=(R\sin\phi, R\cos\phi)$ is then obtained as :

$$\begin{aligned} z(\phi) &= (\zeta+\eta\tan\theta)\cos\theta \\ &= R(\cos\phi\cos\theta+\sin\phi\sin\theta) \\ &= R\cos(\phi-\theta) \qquad \cdots\cdots (A.3.3) \end{aligned}$$

Here, the notation in the 3rd line of the above equation is evident from Fig. A. 3. 1.

And in the figure, the outward unit normal vector $\boldsymbol{n}$, standing on the cylinder surface, can be written using the argument ϕ, as follows :

$$\begin{aligned} \boldsymbol{n} &= n_\eta \boldsymbol{j} + n_\zeta \boldsymbol{k} \\ &= \sin\phi\, \boldsymbol{j} + \cos\phi\, \boldsymbol{k} \qquad \cdots\cdots (A.3.4) \end{aligned}$$

Here, n_η and n_ζ are the directional cosines in the η and ζ coordinates fixed to the cylinder, and $\boldsymbol{j}$ and $\boldsymbol{k}$ are the basic vectors in the η and ζ directions, similarly.

In Fig. A. 3. 1, the atmospheric pressure p_0 is shown as a dashed vector and hydrostatic pressure γz as a solid vector, and all are acting on $-\boldsymbol{n}$ direction perpendicular to the cylinder surface. Here, γ is the specific weight of water.

The pressure $p(\phi)$ acting on the cylinder surface, for positive and negative z, can be written as :

$$p(\phi) = \begin{cases} p_0 & (\textit{for } z < 0 \ ; \ c^{(0)} \textit{ in Air}) \\ p_0 + \gamma z(\phi) & (\textit{for } z \geq 0 \ ; \ c^{(\gamma)} \textit{ in Water}) \end{cases} \quad \cdots\cdots (A.3.5)$$

A. 3. 1 Forces $F_{-\eta}$ and $F_{-\zeta}$ due to pressure in the $-\eta$ and $-\zeta$ directions acting on the cylinder surface

The total force $\boldsymbol{F}$ acting on the cylinder is calculated by pressure integration over the circumference of the cylinder surface $c^{(0)} + c^{(\gamma)}$, as follows :

$$\begin{aligned} \boldsymbol{F} &= -\oint_{c^{(0)}+c^{(\gamma)}} p(\phi)\, \boldsymbol{n}\, d\ell \\ &= F_{-\eta}(-\boldsymbol{j}) + F_{-\zeta}(-\boldsymbol{k}) \quad \cdots\cdots (A.3.6) \end{aligned}$$

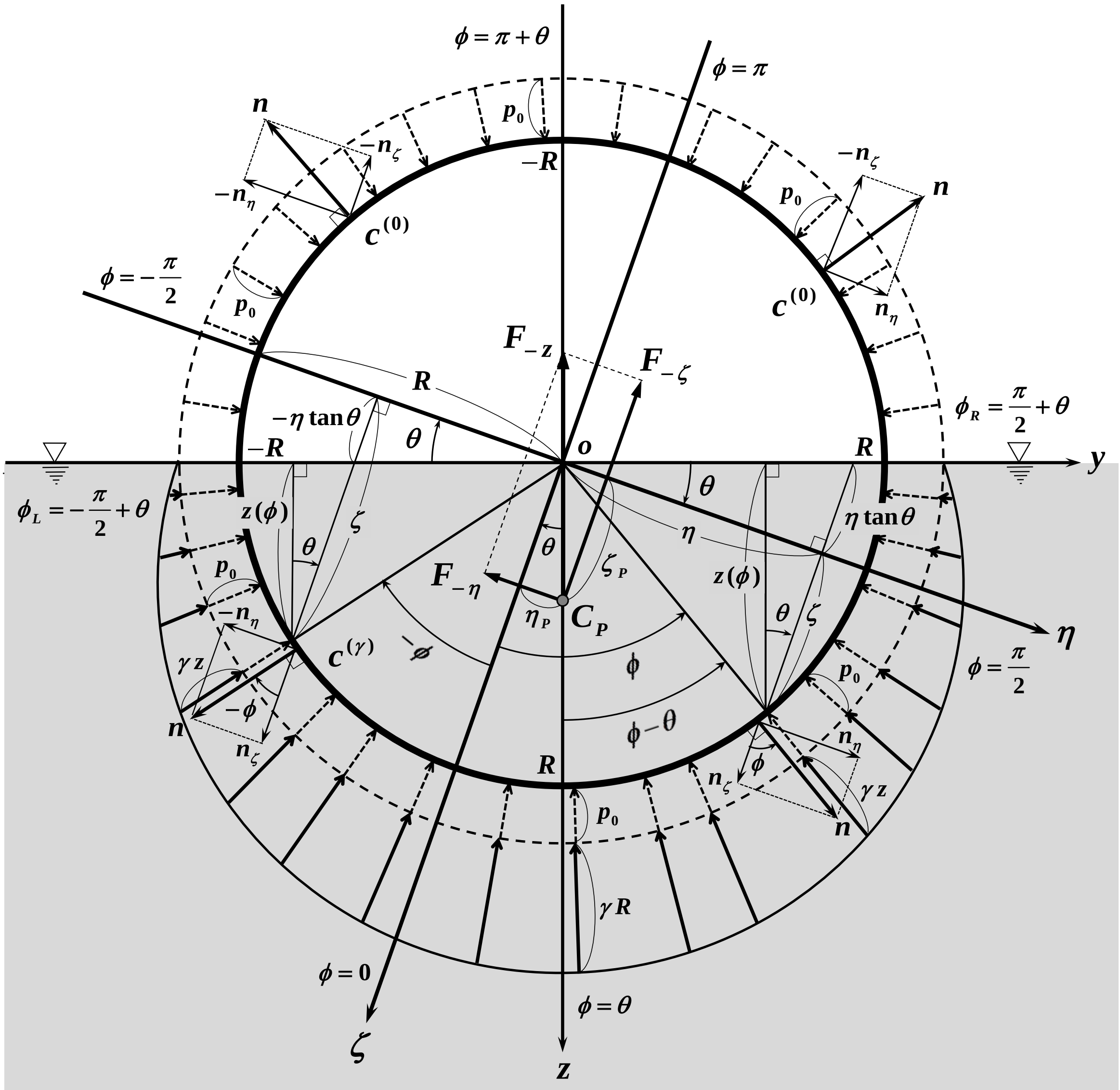

Fig. A. 3. 1 Hydrostatic pressure and the center of pressure acting on the cross-section of an inclined semi-submerged circular cylinder.

The $-\eta$ directional component $F_{-\eta}$ and the $-\zeta$ directional component $F_{-\zeta}$ of the above total force $\boldsymbol{F}$ can be obtained by integrating the $-\eta$ and $-\zeta$ components of the hydrostatic pressure $p(\phi)$ in Eq. (A.3.5). Then, $F_{-\eta}$ and $F_{-\zeta}$ are calculated by the sum of the force due to atmospheric pressure p_0 acting on the aerial part $c^{(0)}$ and the force due to hydrostatic pressure $p_0+\gamma z(\phi)$ acting on the submerged part $c^{(\gamma)}$ respectively, as follows :

$$\left.\begin{aligned} F_{-\eta} &= \oint_{c^{(0)}+c^{(\gamma)}} p(\phi) n_\eta \, d\ell \\ &= \int_{c^{(0)}} p_0 n_\eta \, d\ell + \int_{c^{(\gamma)}} \{ p_0 + \gamma z(\phi) \} \, n_\eta \, d\ell \\ F_{-\zeta} &= \oint_{c^{(0)}+c^{(\gamma)}} p(\phi) n_\zeta \, d\ell \\ &= \int_{c^{(0)}} p_0 n_\zeta \, d\ell + \int_{c^{(\gamma)}} \{ p_0 + \gamma z(\phi) \} \, n_\zeta \, d\ell \end{aligned}\right\} \quad \cdots\cdots\cdots\cdots\cdots\cdots\cdots\cdots\cdots\cdots (A.3.7)$$

Here, on the cylinder surface ($\sqrt{\eta^2+\zeta^2}=R$), the line element is $d\ell = R\,d\phi$, and the directional cosines in the η and ζ directions are $n_\eta = \sin\phi$ and $n_\zeta = \cos\phi$ according to Eq. (A.3.4), so that for each part of $c^{(0)}$ and $c^{(\gamma)}$, both $F_{-\eta}$ and $F_{-\zeta}$ can be expressed by integration with respect to the argument ϕ in the interval of Eq. (A.3.2).

Therefore, $F_{-\eta}$ acting in the $-\eta$ direction is expressed as :

$$\begin{aligned} F_{-\eta} &= \int_{\frac{\pi}{2}+\theta}^{\frac{3\pi}{2}+\theta} p_0 \sin\phi \cdot R d\phi + \int_{-\frac{\pi}{2}+\theta}^{\frac{\pi}{2}+\theta} \{ p_0 + \gamma z(\phi) \} \sin\phi \cdot R d\phi \\ &= p_0 R \int_{-\frac{\pi}{2}+\theta}^{\frac{3\pi}{2}+\theta} \sin\phi \, d\phi + \gamma R \int_{-\frac{\pi}{2}+\theta}^{\frac{\pi}{2}+\theta} z(\phi) \sin\phi \, d\phi \\ &= \gamma R \int_{-\frac{\pi}{2}+\theta}^{\frac{\pi}{2}+\theta} z(\phi) \sin\phi \, d\phi \end{aligned} \quad \cdots\cdots\cdots\cdots\cdots\cdots\cdots\cdots\cdots\cdots (A.3.8)$$

Similarly, $F_{-\zeta}$ acting in the $-\zeta$ direction is expressed as :

$$\begin{aligned} F_{-\zeta} &= \int_{\frac{\pi}{2}+\theta}^{\frac{3\pi}{2}+\theta} p_0 \cos\phi \cdot R d\phi + \int_{-\frac{\pi}{2}+\phi}^{\frac{\pi}{2}+\theta} \{ p_0 + \gamma z(\phi) \} \cos\phi \cdot R d\phi \\ &= p_0 R \int_{-\frac{\pi}{2}+\theta}^{\frac{3\pi}{2}+\theta} \cos\phi \, d\phi + \gamma R \int_{-\frac{\pi}{2}+\theta}^{\frac{\pi}{2}+\theta} z(\phi) \cos\phi \, d\phi \\ &= \gamma R \int_{-\frac{\pi}{2}+\theta}^{\frac{\pi}{2}+\theta} z(\phi) \cos\phi \, d\phi \end{aligned} \quad \cdots\cdots\cdots\cdots\cdots\cdots\cdots\cdots\cdots\cdots (A.3.9)$$

The results of the above equations for both $F_{-\eta}$ and $F_{-\zeta}$ show that the integral over the entire circumference of cylinder with respect to the atmospheric pressure p_0 in the 1st term of 2nd line is zero and does not contribute to the force. Therefore, we can calculate only the 2nd term by using Eq. (A.3.3) for the water depth $z(\phi)$, so that $F_{-\eta}$ is obtained as :

$$
\begin{aligned}
F_{-\eta} &= \gamma R^2 \int_{-\frac{\pi}{2}+\theta}^{\frac{\pi}{2}+\theta} (\cos\theta\cos\phi + \sin\theta\sin\phi)\sin\phi\, d\phi \\
&= \gamma R^2 \left\{ \cos\theta \int_{-\frac{\pi}{2}+\theta}^{\frac{\pi}{2}+\theta} \sin\phi\cos\phi\, d\phi + \sin\theta \int_{-\frac{\pi}{2}+\theta}^{\frac{\pi}{2}+\theta} \sin^2\phi\, d\phi \right\} \\
&= \frac{1}{2}\gamma R^2 \left\{ \cos\theta \int_{-\frac{\pi}{2}+\theta}^{\frac{\pi}{2}+\theta} \sin 2\phi\, d\phi + \sin\theta \left(\int_{-\frac{\pi}{2}+\theta}^{\frac{\pi}{2}+\theta} d\phi - \int_{-\frac{\pi}{2}+\theta}^{\frac{\pi}{2}+\theta} \cos 2\phi\, d\phi \right) \right\} \\
&= \gamma \frac{\pi R^2}{2} \sin\theta \qquad \cdots\cdots\cdots (\text{A.3.10})
\end{aligned}
$$

And, $F_{-\zeta}$ is obtained as :

$$
\begin{aligned}
F_{-\zeta} &= \gamma R^2 \int_{-\frac{\pi}{2}+\theta}^{\frac{\pi}{2}+\theta} (\sin\theta\sin\phi + \cos\theta\cos\phi)\cos\phi\, d\phi \\
&= \gamma R^2 \left\{ \sin\theta \int_{-\frac{\pi}{2}+\theta}^{\frac{\pi}{2}+\theta} \sin\phi\cos\phi\, d\phi + \cos\theta \int_{-\frac{\pi}{2}+\theta}^{\frac{\pi}{2}+\theta} \cos^2\phi\, d\phi \right\} \\
&= \frac{1}{2}\gamma R^2 \left\{ \sin\theta \int_{-\frac{\pi}{2}+\theta}^{\frac{\pi}{2}+\theta} \sin 2\phi\, d\phi + \cos\theta \left(\int_{-\frac{\pi}{2}+\theta}^{\frac{\pi}{2}+\theta} d\phi + \int_{-\frac{\pi}{2}+\theta}^{\frac{\pi}{2}+\theta} \cos 2\phi\, d\phi \right) \right\} \\
&= \gamma \frac{\pi R^2}{2} \cos\theta \qquad \cdots\cdots\cdots (\text{A.3.11})
\end{aligned}
$$

These are because the integrals of $\sin 2\phi$ and $\cos 2\phi$ are zero, and the integral value of 2nd term is π in the 3rd line of both equations above. Both results indicate that $F_{-\eta}$ and $F_{-\zeta}$ are obtained as $-\eta$ and $-\zeta$ directional components of the buoyancy $\gamma \frac{\pi R^2}{2}$, as shown by F_{-z} of Eq. (A.3.12) in the next section.

A. 3. 2 Forces F_{-y} and F_{-z} converted in the $-y$ and $-z$ directions

The horizontal component F_{-y} and the vertical component F_{-z} of the force acting on the semi-submerged cylinder are obtained as follows, by converting $F_{-\eta}$ and $F_{-\zeta}$ obtained in Eqs. (A.3.10) and (A.3.11) of the previous section.

$$
\left.
\begin{aligned}
F_{-y} &= F_{-\eta}\cos\theta - F_{-\zeta}\sin\theta \\
&= \gamma \frac{\pi R^2}{2} (\sin\theta\cdot\cos\theta - \cos\theta\cdot\sin\theta) = 0 \\
F_{-z} &= F_{-\zeta}\cos\theta + F_{-\eta}\sin\theta \\
&= \gamma \frac{\pi R^2}{2} (\cos^2\theta + \sin^2\theta) = \gamma \frac{\pi R^2}{2} \quad (= \mathit{Buoyant\ Force})
\end{aligned}
\right\} \cdots\cdots\cdots (\text{A.3.12})
$$

The above results show that the horizontal component F_{-y} does not act as a combined force due to pressure integration. The vertical component F_{-z} is the product of the specific weight γ of water and the area $\frac{\pi R^2}{2}$ of semicircle below the water surface, and is indeed buoyant force itself acted vertically upward, as Archimedes' principle(1) teaches.

A. 3. 3 Moments M_η and M_ζ due to pressure in the η and ζ directions acting on the cylinder surface

The clockwise moment M_η about the origin o due to the pressure p in the $-\eta$ direction acting on the cylinder surface and the counterclockwise moment M_ζ due to the pressure in the $-\zeta$ direction can be computed by multiplying the integrand in Eq. (A.3.7) by ζ or η as the lever of the moment respectively, as follows :

$$\left.\begin{aligned} M_\eta &= \oint_{c^{(0)}+c^{(\gamma)}} p(\phi)\, n_\eta \cdot \zeta\, d\ell \\ &= \int_{c^{(0)}} p_0 n_\eta \cdot \zeta\, d\ell + \int_{c^{(\gamma)}} \{ p_0 + \gamma z(\phi) \}\, n_\eta \cdot \zeta\, d\ell \\ M_\zeta &= \oint_{c^{(0)}+c^{(\gamma)}} p(\phi)\, n_\zeta \cdot \eta\, d\ell \\ &= \int_{c^{(0)}} p_0 n_\zeta \cdot \eta\, d\ell + \int_{c^{(\gamma)}} \{ p_0 + \gamma z(\phi) \}\, n_\zeta \cdot \eta\, d\ell \end{aligned}\right\} \cdots\cdots (A.3.13)$$

Here, if the above moments are expressed by termwise integration with respect to the argument ϕ as in Eqs. (A.3.8) and (A.3.9) for $F_{-\eta}$ and $F_{-\zeta}$ in the previous section, M_η becomes as :

$$\begin{aligned} M_\eta &= \int_{\frac{\pi}{2}+\theta}^{\frac{3\pi}{2}+\theta} p_0 \sin\phi \cdot R\cos\phi \cdot R d\phi + \int_{-\frac{\pi}{2}+\theta}^{\frac{\pi}{2}+\theta} \{ p_0 + \gamma z(\phi) \} \sin\phi \cdot R\cos\phi \cdot R d\phi \\ &= \frac{1}{2} p_0 R^2 \int_{-\frac{\pi}{2}+\theta}^{\frac{3\pi}{2}+\theta} \sin 2\phi\, d\phi + \gamma R^2 \int_{-\frac{\pi}{2}+\theta}^{\frac{\pi}{2}+\theta} z(\phi) \sin\phi \cos\phi\, d\phi \\ &= \gamma R^2 \int_{-\frac{\pi}{2}+\theta}^{\frac{\pi}{2}+\theta} z(\phi) \sin\phi \cos\phi\, d\phi \qquad \cdots\cdots (A.3.14) \end{aligned}$$

And, M_ζ becomes as :

$$\begin{aligned} M_\zeta &= \int_{\frac{\pi}{2}+\theta}^{\frac{3\pi}{2}+\theta} p_0 \cos\phi \cdot R\sin\phi \cdot R d\phi + \int_{-\frac{\pi}{2}+\theta}^{\frac{\pi}{2}+\theta} \{ p_0 + \gamma z(\phi) \} \cos\phi \cdot R\sin\phi \cdot R d\phi \\ &= \frac{1}{2} p_0 R^2 \int_{-\frac{\pi}{2}+\theta}^{\frac{3\pi}{2}+\theta} \sin 2\phi\, d\phi + \gamma R^2 \int_{-\frac{\pi}{2}+\theta}^{\frac{\pi}{2}+\theta} z(\phi) \cos\phi \sin\phi\, d\phi \\ &= \gamma R^2 \int_{-\frac{\pi}{2}+\theta}^{\frac{\pi}{2}+\theta} z(\phi) \sin\phi \cos\phi\, d\phi \qquad \cdots\cdots (A.3.15) \end{aligned}$$

The above results show that both equations for M_η and M_ζ are equivalent. Thus, the total counterclockwise moment M_o around the origin o due to pressure is zero, as follows :

$$M_o = M_\zeta - M_\eta = 0 \qquad \cdots\cdots (A.3.16)$$

This is confirmed by the fact that the pressure acts perpendicular to the cylinder surface, so it is all directed toward the center o of the circle.

Then, in both Eqs. (A.3.14) and (A.3.15), the integration of $\sin 2\phi$ with respect to atmospheric pressure p_0 in the 1st term of 2nd line is zero. Hence, we can calculate only the 2nd term by using Eq. (A.3.3) for the water depth $z(\phi)$, as follows :

$$
\begin{aligned}
M_\eta &= M_\zeta \\
&= \gamma R^3 \int_{-\frac{\pi}{2}+\theta}^{\frac{\pi}{2}+\theta} (\cos\theta\cos\phi + \sin\theta\sin\phi)\sin\phi\cos\phi\, d\phi \\
&= \gamma R^3 \left\{ \cos\theta \int_{-\frac{\pi}{2}+\theta}^{\frac{\pi}{2}+\theta} \sin\phi\cos^2\phi\, d\phi + \sin\theta \int_{-\frac{\pi}{2}+\theta}^{\frac{\pi}{2}+\theta} \sin^2\phi\cos\phi\, d\phi \right\} \quad \cdots\cdots\cdots\cdots (A.3.17)
\end{aligned}
$$

So, if we put $p = \cos\phi$ for the 1st term and $q = \sin\phi$ for the 2nd term and do a substitution integral for each, we obtain by folding the integral interval in half, as follows :

$$
\begin{aligned}
M_\eta &= M_\zeta \\
&= 2\gamma R^3 \left(\cos\theta \int_0^{\sin\theta} p^2\, dp + \sin\theta \int_0^{\cos\theta} q^2\, dq \right) \\
&= 2\gamma R^3 \left(\cos\theta \cdot \frac{1}{3}\sin^3\theta + \sin\theta \cdot \frac{1}{3}\cos^3\theta \right) \\
&= \frac{2}{3}\gamma R^3 \sin\theta\cos\theta\, (\sin^2\theta + \cos^2\theta) = \frac{2}{3}\gamma R^3 \sin\theta\cos\theta \quad \cdots\cdots\cdots\cdots\cdots (A.3.18)
\end{aligned}
$$

A. 3. 4 Positioning of the center of hydrostatic pressure C_P for the semi-submerged circular cylinder

To locate the center of pressure C_P in o-$\eta\zeta$ coordinate system fixed to circular cylinder, the hydraulic method used in Sections 1.2.5 and 1.3.4 of Chapter 1 is applied. This method was used by Ohgushi [9-a] for an example problem of the rolling gate.

Since the forces $F_{-\eta}$ and $F_{-\zeta}$ due to the hydrostatic pressure obtained in Section A.3.1 act on the center of pressure $C_P\,(\eta_P, \zeta_P)$, the moments M_η and M_ζ due to the same pressure obtained in Section A.3.3 can be expressed respectively same as Eq. (1.27) in Chapter 1, as follows :

$$
\left.
\begin{aligned}
M_\eta &= F_{-\eta}\, \zeta_P \\
M_\zeta &= F_{-\zeta}\, \eta_P
\end{aligned}
\right\} \quad \cdots\cdots\cdots\cdots\cdots\cdots\cdots\cdots\cdots\cdots\cdots\cdots\cdots\cdots\cdots\cdots (A.3.19)
$$

Therefore, the unknown coordinate (η_P, ζ_P) of the center of hydrostatic pressure C_P can be determined by Eq. (A.3.19). Here, the η-coordinate, η_P, can be calculated by using Eq. (A.3.11) for $F_{-\zeta}$ and the Eq. (A.3.18) for M_ζ due to the hydrostatic pressure in the $-\zeta$ direction, as follows :

$$
\begin{aligned}
\eta_P &= \frac{M_\zeta}{F_{-\zeta}} \\
&= \frac{\frac{2}{3}\gamma R^3 \sin\theta\cos\theta}{\gamma \frac{\pi R^2}{2}\cos\theta} = \frac{4}{3\pi} R\sin\theta \quad \cdots\cdots\cdots\cdots\cdots\cdots\cdots\cdots\cdots\cdots (A.3.20)
\end{aligned}
$$

Similarly, the ζ - coordinate, ζ_P, can be calculated by using Eq. (A.3.10) for $F_{-\eta}$ and Eq. (A.3.18) for M_η due to the hydrostatic pressure in the $-\eta$ direction, as follows :

$$\zeta_P = \frac{M_\eta}{F_{-\eta}} = \frac{\frac{2}{3}\gamma R^3 \sin\theta\cos\theta}{\gamma\frac{\pi R^2}{2}\sin\theta} = \frac{4}{3\pi}R\cos\theta \quad \cdots\cdots (A.3.21)$$

Let us consider the above equations. For ζ_P in Eq. (A.3.21), if we assume the upright state $\theta = 0$ from the beginning, $\sin\theta$ in the denominator $F_{-\eta}$ and numerator M_η will be zero, so the fraction becomes indeterminate forms and ζ_P cannot be determined. The reason is why we were able to locate the vertical component ζ_P of the center of pressure, the semi-submerged cylinder was laterally inclined along with its $\eta\zeta$ - coordinate axes, even though the shape did not change when inclined.

On the other hand, for η_P in Eq. (A.3.20), even if the heel angle is $\theta = 0$ from the beginning, the denominator $F_{-\zeta}$ can take a finite value because of $\cos\theta = 1$, and horizontal component η_P can be determined.

From the results of both equations above, the coordinates (η_P, ζ_P) of the center of pressure C_P are determined as :

$$(\eta_P, \zeta_P) = \left(\frac{4}{3\pi}R\sin\theta,\ \frac{4}{3\pi}R\cos\theta\right) \quad \cdots\cdots (A.3.22)$$

The above (η_P, ζ_P) coordinates fixed to the inclined cylinder are transformed to (y_P, z_P) coordinates fixed to space, as follows :

$$\left.\begin{aligned} y_P &= \eta_P\cos\theta - \zeta_P\sin\theta \\ &= \frac{4}{3\pi}R(\sin\theta\cdot\cos\theta - \cos\theta\cdot\sin\theta) = 0 \\ z_P &= \zeta_P\cos\theta + \eta_P\sin\theta \\ &= \frac{4}{3\pi}R(\cos^2\theta + \sin^2\theta) = \frac{4}{3\pi}R \end{aligned}\right\} \quad \cdots\cdots (A.3.23)$$

Therefore, the center of hydrostatic pressure C_P in the space-fixed coordinate is located as :

$$(y_P, z_P) = \left(0,\ \frac{4}{3\pi}R\right) \quad \cdots\cdots (A.3.24)$$

This correctly indicates the figure centroid on the centerline (*i.e.* z-axis) of the semicircle below the water surface. Hence, it is proved that the center of hydrostatic pressure is equal to the well-known center of buoyancy, even for the shape of a semi-submerged circular cylinder.

A. 3. 5 Considerations

In the case of the semi-submerged circular cylinder in this appendix, the situation differs from that of a rectangle or an arbitrary cross-sectional shape in Chapter 1 and of a triangular prism in the previous Appendix A. 2. The reason is why its geometrical shape under the water surface does not change, even when the circular cylinder is inclined laterally. As a result, it is not necessary to determine the center of pressure in the upright position by setting the lateral inclination angle θ to zero. So, its position can be computed by coordinate transformation, as shown in Eq. (A.3.23) of the previous section.

Therefore, it was also found that the center of pressure can be positioned by tilting the coordinate system in a way that it is shifted from the vertical direction, without inclining the floating body as advocated by Yabushita *et al.*[27].

A. 4 Positioning of the Center of Hydrostatic Pressure C_p Acting on the Submerged Circular Cylinder

In Appendix A. 4, we apply to the submerged circular cylinder (32), 1st half of (36) and (79) the same method developed for floating bodies (*e.g.*, rectangular cross-section in Section 1.2, triangular prism in Appendix A.2, semi-submerged circular cylinder in Appendix A.3 and an arbitrary shaped cross-section in Section 1.3) by the authors already, in which the center of hydrostatic pressure is positioned by inclining the floating body laterally. It should be noted, however, in this submerged cylinder, as in the case of the semi-submerged cylinder, the cross-sectional shape does not change when it is laterally inclined.

Fig. A. 4. 1 shows that the cross-section of a circular cylinder with radius R is submerged at water depth f to the top, and is inclined laterally by heel angle θ to the starboard side. The origin o is placed at the center of circle, which depth is $f+R$. The coordinate system fixed in space with the z-axis pointing vertically downward is o-yz, and that fixed to the cylinder and tilted clockwise by θ is o-$\eta\zeta$. The following analysis is performed for the latter o-$\eta\zeta$ coordinate system, using the argument ϕ measured counterclockwise from the ζ-axis as a variable.

The water depth $Z(\phi)$, denoted by capital letter, from the still water surface is expressed as :

$$Z(\phi) = f + R + z(\phi) \quad \cdots\cdots (A.4.1)$$

Here, the small letter $z(\phi)$ on the right side is the water depth measured from the origin o downward, and is obtained on the cylinder surface $(\eta, \zeta) = (R\sin\phi, R\cos\phi)$, denoted by $c^{(\gamma)}$, as follows:

$$\begin{aligned} z(\phi) &= (\zeta + \eta\tan\theta)\cos\theta \\ &= R(\cos\phi\cos\theta + \sin\phi\sin\theta) \\ &= R\cos(\phi-\theta) \end{aligned} \quad \cdots\cdots (A.4.2)$$

The notation in the 3rd line of the above equation is also derived easily from Fig. A. 4. 1. And, note that $z(\phi)$ can also take negative values above the origin o.

Hydrostatic pressure $p(\phi)$ at the cylinder surface can be written as follows, using p_0 for the atmospheric pressure, γ for the specific weight of water, and Eq. (A.4.1) for the water depth $Z(\phi)$.

$$\begin{aligned} p(\phi) &= p_0 + \gamma Z(\phi) \\ &= p_0 + \gamma f + \gamma(R + z(\phi)) \\ &= p_0 + \gamma f + p'(\phi) \end{aligned} \quad \cdots\cdots (A.4.3)$$

Here, $p'(\phi)$ on the right-hand side of the above equation is the relative pressure to hydrostatic pressure $p_0 + \gamma f$ at the top of the cylinder and is defined as follows :

$$\begin{aligned} p'(\phi) &\equiv p(\phi) - (p_0 + \gamma f) \\ &= \gamma(R + z(\phi)) \end{aligned} \quad \cdots\cdots (A.4.4)$$

The pressure shown by vector in Fig. A. 4. 1 is this $p'(\phi)$. It acts in the $-\boldsymbol{n}$ direction perpendicular to the cylinder surface and is zero at the top of the cylinder.

And in the figure, the outward unit normal vector $\boldsymbol{n}$, standing on the cylinder surface, can be written using the argument ϕ, as follows :

$$\begin{aligned} \boldsymbol{n} &= n_\eta \boldsymbol{j} + n_\zeta \boldsymbol{k} \\ &= \sin\phi\, \boldsymbol{j} + \cos\phi\, \boldsymbol{k} \end{aligned} \qquad \cdots\cdots (A.4.5)$$

Here, n_η and n_ζ are the directional cosines in the η and ζ coordinates fixed to the cylinder, and $\boldsymbol{j}$ and $\boldsymbol{k}$ are the basic vectors in the η and ζ directions, similarly.

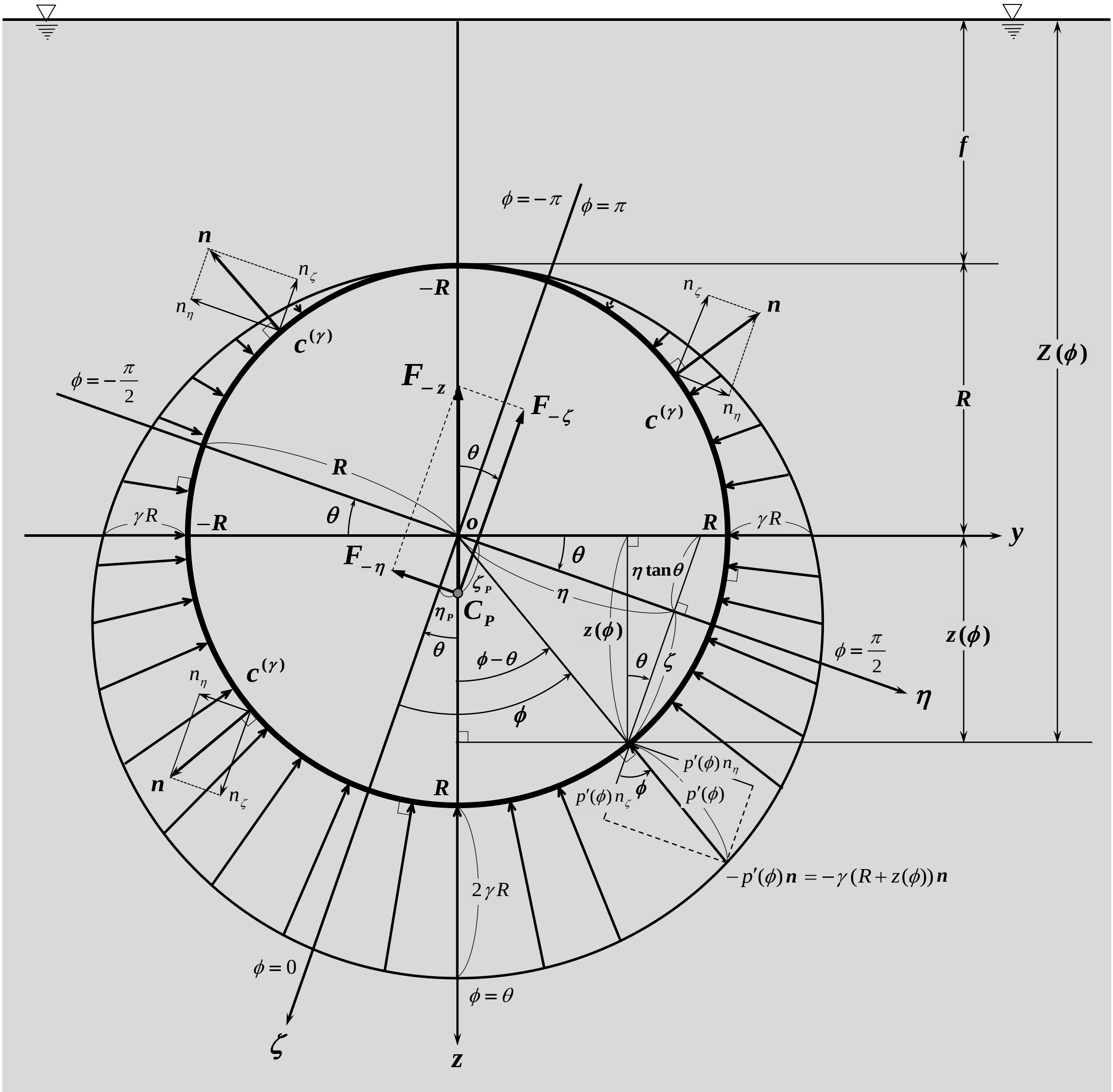

Fig. A. 4. 1 Hydrostatic pressure $p' = p - (p_0 + \gamma f)$ and the center of pressure C_P acting on the cross-section of an inclined submerged circular cylinder.

A.4.1 Forces $F_{-\eta}$ and $F_{-\zeta}$ due to pressure in the $-\eta$ and $-\zeta$ directions acting on the surface of submerged cylinder

The pressure $p(\phi)$ acting on the cylinder surface can be expressed by Eqs. (A.4.2), (A.4.3) and (A.4.4) in the previous section, as follows :

$$\begin{aligned} p(\phi) &= p_0 + \gamma f + p'(\phi) \\ &= p_0 + \gamma(f+R) + \gamma z(\phi) \\ &= p_C + \gamma R\cos(\phi-\theta) \end{aligned} \qquad \cdots\cdots\text{(A.4.6)}$$

In the above equation, p_C is defined as follows, and means the hydrostatic pressure on the y-axis, placed on water depth $f+R$, passing through the center O of circle.

$$p_C \equiv p_0 + \gamma(f+R) \qquad \cdots\cdots\text{(A.4.7)}$$

The total force $\boldsymbol{F}$ acting on the submerged cylinder is calculated by pressure integration over the cylinder surface $c^{(\gamma)}$, as follows :

$$\begin{aligned} \boldsymbol{F} &= -\oint_{c^{(\gamma)}} p(\phi)\,\boldsymbol{n}\,d\ell \\ &= F_{-\eta}(-\boldsymbol{j}) + F_{-\zeta}(-\boldsymbol{k}) \end{aligned} \qquad \cdots\cdots\text{(A.4.8)}$$

The $-\eta$ directional component $F_{-\eta}$ and the $-\zeta$ directional component $F_{-\zeta}$ of the above total force $\boldsymbol{F}$ are obtained by integrating the $-\eta$ and $-\zeta$ components of the hydrostatic pressure $p(\phi)$, as follows :

$$\left.\begin{aligned} F_{-\eta} &= \oint_{c^{(\gamma)}} p(\phi)\,n_\eta\,d\ell \\ F_{-\zeta} &= \oint_{c^{(\gamma)}} p(\phi)\,n_\zeta\,d\ell \end{aligned}\right\} \qquad \cdots\cdots\text{(A.4.9)}$$

Here, on the cylinder surface $c^{(\gamma)}$ ($\sqrt{\eta^2+\zeta^2}=R$), the line element is $d\ell = R\,d\phi$, and the directional cosines in the η and ζ directions of the normal vector $\boldsymbol{n}$ are $n_\eta = \sin\phi$ and $n_\zeta = \cos\phi$ according to Eq. (A.4.5), so that both $F_{-\eta}$ and $F_{-\zeta}$ can be written by integration with respect to the argument ϕ.

Therefore, $F_{-\eta}$ acting in the $-\eta$ direction is expressed by using Eq. (A.4.6) for $p(\phi)$, as follows :

$$\begin{aligned} F_{-\eta} &= \int_{-\pi}^{\pi} \left\{ p_C + \gamma R\cos(\phi-\theta) \right\} \sin\phi \cdot R\,d\phi \\ &= p_C R \int_{-\pi}^{\pi} \sin\phi\,d\phi + \gamma R^2\cos\theta \int_{-\pi}^{\pi} \sin\phi\cos\phi\,d\phi + \gamma R^2 \sin\theta \int_{-\pi}^{\pi} \sin^2\phi\,d\phi \\ &= p_C R \int_{-\pi}^{\pi} \sin\phi\,d\phi + \frac{1}{2}\gamma R^2\cos\theta \int_{-\pi}^{\pi} \sin 2\phi\,d\phi \\ &\qquad + \frac{1}{2}\gamma R^2 \sin\theta \left(\int_{-\pi}^{\pi} d\phi - \int_{-\pi}^{\pi} \cos 2\phi\,d\phi \right) \end{aligned} \qquad \cdots\cdots\text{(A.4.10)}$$

Similarly, $F_{-\zeta}$ acting in the $-\zeta$ direction is expressed as :

$$\begin{aligned} F_{-\zeta} &= \int_{-\pi}^{\pi} \left\{ p_C + \gamma R \cos(\phi - \theta) \right\} \cos\phi \cdot R d\phi \\ &= p_C R \int_{-\pi}^{\pi} \cos\phi d\phi + \gamma R^2 \sin\theta \int_{-\pi}^{\pi} \sin\phi \cos\phi \, d\phi + \gamma R^2 \cos\theta \int_{-\pi}^{\pi} \cos^2\phi d\phi \\ &= p_C R \int_{-\pi}^{\pi} \sin\phi d\phi + \frac{1}{2} \gamma R^2 \sin\theta \int_{-\pi}^{\pi} \sin 2\phi d\phi \\ &\quad + \frac{1}{2} \gamma R^2 \cos\theta \left(\int_{-\pi}^{\pi} d\phi + \int_{-\pi}^{\pi} \cos 2\phi d\phi \right) \end{aligned} \quad \cdots\cdots (A.4.11)$$

In both Eqs. (A.4.10) and (A.4.11) above, after expansion and integration by terms, the integrals of 1st, 2nd and 4th terms in the 3rd and 4th lines are zero, and the integral value 2π results from the 3rd term only. Thus, both $F_{-\eta}$ and $F_{-\zeta}$ are computed respectively, as follows :

$$\left. \begin{aligned} F_{-\eta} &= \gamma \cdot \pi R^2 \cdot \sin\theta \\ F_{-\zeta} &= \gamma \cdot \pi R^2 \cdot \cos\theta \end{aligned} \right\} \quad \cdots\cdots (A.4.12)$$

Therefore, it is indicated that the both forces acting on the submerged cylinder are not dependent of atmospheric pressure p_0 or submerged depth f, since the term on p_C is vanished. In addition, $F_{-\eta}$ and $F_{-\zeta}$ are obtained as the sine and cosine components of the buoyancy $\gamma \cdot \pi R^2$, as shown by F_{-z} of Eq. (A.4.13) in the next section, with respect to the heel angle θ.

A. 4. 2 Forces F_{-y} and F_{-z} converted in the $-y$ and $-z$ directions

In this section, let us find the horizontal and vertical components of the force acting on the submerged circular cylinder. By using $F_{-\eta}$ and $F_{-\zeta}$ obtained in Eq. (A.4.12) in the previous section, the horizontal component F_{-y} in the $-y$ direction and the vertical component F_{-z} in the $-z$ direction are converted as follows :

$$\left. \begin{aligned} F_{-y} &= F_{-\eta} \cos\theta - F_{-\zeta} \sin\theta \\ &= \gamma \cdot \pi R^2 (\sin\theta \cdot \cos\theta - \cos\theta \cdot \sin\theta) \\ &= 0 \\ F_{-z} &= F_{-\zeta} \cos\theta + F_{-\eta} \sin\theta \\ &= \gamma \cdot \pi R^2 (\cos^2\theta + \sin^2\theta) \\ &= \gamma \cdot \pi R^2 \;\; (= \textit{Buoyant Force}) \end{aligned} \right\} \quad \cdots\cdots (A.4.13)$$

The above results show that the horizontal component F_{-y} does not act as the combined force due to pressure integration. The vertical component F_{-z} is the product of the specific weight γ of water and the area πR^2 of submerged circle, and is indeed the buoyant force itself generated vertically upward, as Archimedes' principle (1) teaches.

A.4.3 Moments M_η and M_ζ due to pressure in the η and ζ directions acting on the surface of submerged cylinder

The clockwise moment M_η about the origin o due to the pressure $p(\phi)$ in the $-\eta$ direction acting on the cylinder surface $c^{(\gamma)}$ and the counterclockwise moment M_ζ due to the pressure in the $-\zeta$ direction can be computed by multiplying the integrand in Eq. (A.4.9) by ζ or η as the lever of moment respectively, as follows :

$$\left.\begin{aligned} M_\eta &= \oint_{c^{(\gamma)}} p(\phi)\,\zeta\cdot n_\eta\,d\ell \\ M_\zeta &= \oint_{c^{(\gamma)}} p(\phi)\,\eta\cdot n_\zeta\,d\ell \end{aligned}\right\} \quad \cdots\cdots (A.4.14)$$

Here, if the above moments are expressed by contour integrals with respect to the argument ϕ, as in Eqs. (A.4.10) and (A.4.11) for $F_{-\eta}$ and $F_{-\zeta}$ in the Section A.4.1, M_η becomes as :

$$\begin{aligned} M_\eta &= \int_{-\pi}^{\pi} \left\{ p_C + \gamma R\cos(\phi-\theta) \right\} R\cos\phi\cdot\sin\phi\cdot R d\phi \\ &= p_C R^2 \int_{-\pi}^{\pi} \sin\phi\cos\phi\, d\phi + \gamma R^3 \int_{-\pi}^{\pi} \cos(\phi-\theta)\sin\phi\cos\phi\, d\phi \end{aligned} \quad \cdots\cdots (A.4.15)$$

And, M_ζ becomes as :

$$\begin{aligned} M_\zeta &= \int_{-\pi}^{\pi} \left\{ p_C + \gamma R\cos(\phi-\theta) \right\} R\sin\phi\cdot\cos\phi\cdot R d\phi \\ &= p_C R^2 \int_{-\pi}^{\pi} \sin\phi\cos\phi\, d\phi + \gamma R^3 \int_{-\pi}^{\pi} \cos(\phi-\theta)\sin\phi\cos\phi\, d\phi \end{aligned} \quad \cdots\cdots (A.4.16)$$

The above results show that both equations for M_η and M_ζ are equivalent. Hence, the total counterclockwise moment M_o around the origin o due to pressure is zero, as follows :

$$M_o = M_\zeta - M_\eta = 0 \quad \cdots\cdots (A.4.17)$$

This is confirmed by the fact that the pressure acts perpendicular to the cylinder surface and is all directed toward the center o of the circle, as in the case of the semi-submerged circular cylinder in Eq. (A.3.16) of Appendix A.3.

Further expanding Eqs. (A.4.15) and (A.4.16) for both moments and proceeding with the calculation, we obtain as follows :

$$\begin{aligned} M_\eta &= M_\zeta \\ &= \frac{1}{2} p_C R^2 \int_{-\pi}^{\pi} \sin 2\phi\, d\phi + \gamma R^3\cos\theta \int_{-\pi}^{\pi} \sin\phi\cos^2\phi\, d\phi \\ &\qquad + \gamma R^3 \sin\theta \int_{-\pi}^{\pi} \sin^2\phi\cos\phi\, d\phi \\ &= 2\gamma R^3\sin\theta \int_0^{\pi} \sin^2\phi\cos\phi\, d\phi \end{aligned} \quad \cdots\cdots (A.4.18)$$

Here, in the above equation, the 1st and 2nd terms of 2nd and 3rd lines are zero, because the integrand is a odd function with respect to ϕ. And, the 3rd term is an even function, so it is written with the

integral interval folded in half.

Furthermore, by replacing the integral variable from ϕ to φ by $\varphi = \phi - \frac{\pi}{2}$, the above equation is computed as follows :

$$
\begin{aligned}
M_\eta &= M_\zeta \\
&= -2\gamma R^3 \sin\theta \int_{-\frac{\pi}{2}}^{\frac{\pi}{2}} \cos^2\varphi \sin\varphi \, d\varphi \\
&= 0 \qquad \cdots\cdots (A.4.19)
\end{aligned}
$$

This is because the integrand in the above equation is an odd function with respect to φ, so the integral value is zero. This result shows that the η and ζ components of the hydrostatic pressure do not cause moments around the center o of the circle in the case of the submerged cylinder, unlike the semi-submerged cylinder in Eq. (A.3.18) of the previous Appendix A. 3.

A. 4. 4 Positioning of the center of hydrostatic pressure C_P for the submerged circular cylinder

To locate the center of pressure C_P in o-$\eta\zeta$ coordinate system fixed to circular cylinder, the hydraulic method used in Chapter 1 for floating bodies is applied. This method was used by Ohgushi[(9-a)] for an example problem of the rolling gate.

Since the forces $F_{-\eta}$ and $F_{-\zeta}$ due to the hydrostatic pressure obtained in Section A. 4. 1 act on the center of pressure $C_P\ (\eta_P, \zeta_P)$, the moments M_η and M_ζ due to the corresponding pressure obtained in Section A. 4. 3 can be expressed respectively same as Eq. (1.27) in Chapter 1, as follows :

$$
\left.
\begin{aligned}
M_\eta &= F_{-\eta}\, \zeta_P \\
M_\zeta &= F_{-\zeta}\, \eta_P
\end{aligned}
\right\} \qquad \cdots\cdots (A.4.20)
$$

Therefore, the unknown coordinate (η_P, ζ_P) of the center of hydrostatic pressure C_P can be determined by Eq. (A.4.20). Hence, the η - coordinate, η_P, can be determined by the combined force $F_{-\zeta}$ and the moment M_ζ due to the hydrostatic pressure in the $-\zeta$ direction, and the ζ - coordinate, ζ_P, by $F_{-\eta}$ and M_η in the $-\eta$ direction, by using Eqs. (A.4.12) and (A.4.19) respectively, as follows :

$$
\left.
\begin{aligned}
\eta_P &= \frac{M_\zeta}{F_{-\zeta}} = \frac{0}{\gamma \cdot \pi R^2 \cdot \cos\theta} = 0 \\
\zeta_P &= \frac{M_\eta}{F_{-\eta}} = \frac{0}{\gamma \cdot \pi R^2 \cdot \sin\theta} = 0
\end{aligned}
\right\} \qquad \cdots\cdots (A.4.21)
$$

Let us consider the above equation. For the latter ζ_P of vertical component, if we assume the upright state $\theta = 0$ from the beginning, $\sin\theta$ in the denominator $F_{-\eta}$ will be zero, so the fraction becomes indeterminate forms and ζ_P cannot be determined. We were able to locate the vertical component ζ_P of the center of pressure, because the submerged cylinder was laterally inclined along with its $\eta\zeta$ - coordinate axes, even though the shape did not change when inclined.

On the other hand, for the former η_P, even if the heel angle is $\theta = 0$ from the beginning, the denominator $F_{-\zeta}$ can take a finite value because of $\cos\theta = 1$, and horizontal component η_P can be determined.

As a result, the center of pressure C_P of the submerged cylinder is obtained in the $o\text{-}\eta\zeta$ coordinate system fixed and inclined to the cylinder, as follows. It is found that the C_P is located at the origin o, which is the center of the submerged circle.

$$C_P(\eta_P, \zeta_P) = (0, 0) \quad \cdots\cdots (A.4.22)$$

Therefore, its C_P is also located at the following position o in the space-fixed $o\text{-}yz$ coordinate system and can be determined without any need for coordinate transformation, unlike the semi-submerged case in Eq. (A.3.23) of Appendix A.3.

$$C_P(y_P, z_P) = (0, 0) \quad \cdots\cdots (A.4.23)$$

The both Eqs. (A.4.22) and (A.4.23) above is correctly indicates the figure centroid of the submerged circle. Hence, we were able to prove that the center of hydrostatic pressure is equal to the well-known center of buoyancy even for submerged bodies, as in the case of floating bodies in Chapter 1, Appendices A.2 and A.3.

A. 5 Positioning of the Center of Hydrostatic Pressure C_P Acting on the Submerged Body with Arbitrary Shape

In Appendix A. 5, we apply the same method as used in the previous Appendix A. 4, in which the submerged circular cylinder is inclined laterally, to the submerged body with the arbitrary shape (37), 2nd half of (36) and (79). It is then proved that the center of hydrostatic pressure is equal to well-known center of buoyancy by using Gauss's integral theorem, which has already been applied to floating bodies with arbitrary form in Section 1. 3 of Chapter 1.

Fig. A. 5. 1 shows the cross-section of an arbitrary shaped body submerged at water depth f to the top, inclined laterally about its top by heel angle θ to the starboard side. The origin o is placed at the top of submerged body. The coordinate system fixed in space with the z-axis pointing vertically downward is o-yz, and that fixed to the body and tilted clockwise by θ is o-$\eta\zeta$. The following analysis is performed for the latter inclined o-$\eta\zeta$ coordinate system.

The water depth Z, denoted by capital letter, on the surface (η, ζ) of submerged body from the still water line is expressed as :

$$\begin{aligned} Z &= f + z(\eta, \zeta) \\ &= f + (\zeta + \eta \tan\theta)\cos\theta \\ &= f + (\zeta \cos\theta + \eta \sin\theta) \end{aligned} \quad \cdots\cdots (A.5.1)$$

Here, in the above equation, the small letter z on the right-hand represents the water depth measured from the top o.

Hydrostatic pressure p at the body surface, denoted by $c^{(\gamma)}$, can be written as follows, by using p_0 for the atmospheric pressure, γ for the specific weight of water, and the 1st line of Eq. (A.5.1) for the water depth Z.

$$\begin{aligned} p &= p_0 + \gamma Z \\ &= p_0 + \gamma f + \gamma z(\eta, \zeta) \\ &\equiv p_0 + \gamma f + p'(\eta, \zeta) \end{aligned} \quad \cdots\cdots (A.5.2)$$

Where, p' on the right-hand side of the above 3rd line is the relative pressure to hydrostatic pressure $p_0 + \gamma f$ at the top of submerged body and is defined by using Eq. (A.5.1), as follows :

$$\begin{aligned} p'(\eta, \zeta) &\equiv p - (p_0 + \gamma f) \\ &= \gamma z(\eta, \zeta) \\ &= \gamma(\zeta \cos\theta + \eta \sin\theta) \end{aligned} \quad \cdots\cdots (A.5.3)$$

Here, the pressure shown by vector in Fig. A. 5. 1 is the above relative pressure p'. It acts in the $-\boldsymbol{n}$ direction perpendicular to the body surface and is zero at the top of body.

Then, $\boldsymbol{n}$ is the outward unit normal vector standing on the body surface, and as in the case of circular cylinder in the previous Appendix A. 4, is written as follows :

$$\boldsymbol{n} = n_\eta \boldsymbol{j} + n_\zeta \boldsymbol{k} \quad \cdots\cdots (A.5.4)$$

Here, n_η and n_ζ are the directional cosines in the η and ζ coordinates fixed to the body, and $\boldsymbol{j}$ and $\boldsymbol{k}$ are the basic vectors in the η and ζ directions, similarly.

A.5.1 Components $F_{-\eta}$ and $F_{-\zeta}$ of the total force due to hydrostatic pressure in the $-\eta$ and $-\zeta$ directions acting on the submerged body

The total force $\boldsymbol{F}$ acting on the submerged body is calculated by pressure integration over the body surface $c^{(\gamma)}$ with the line element $d\ell$, as follows :

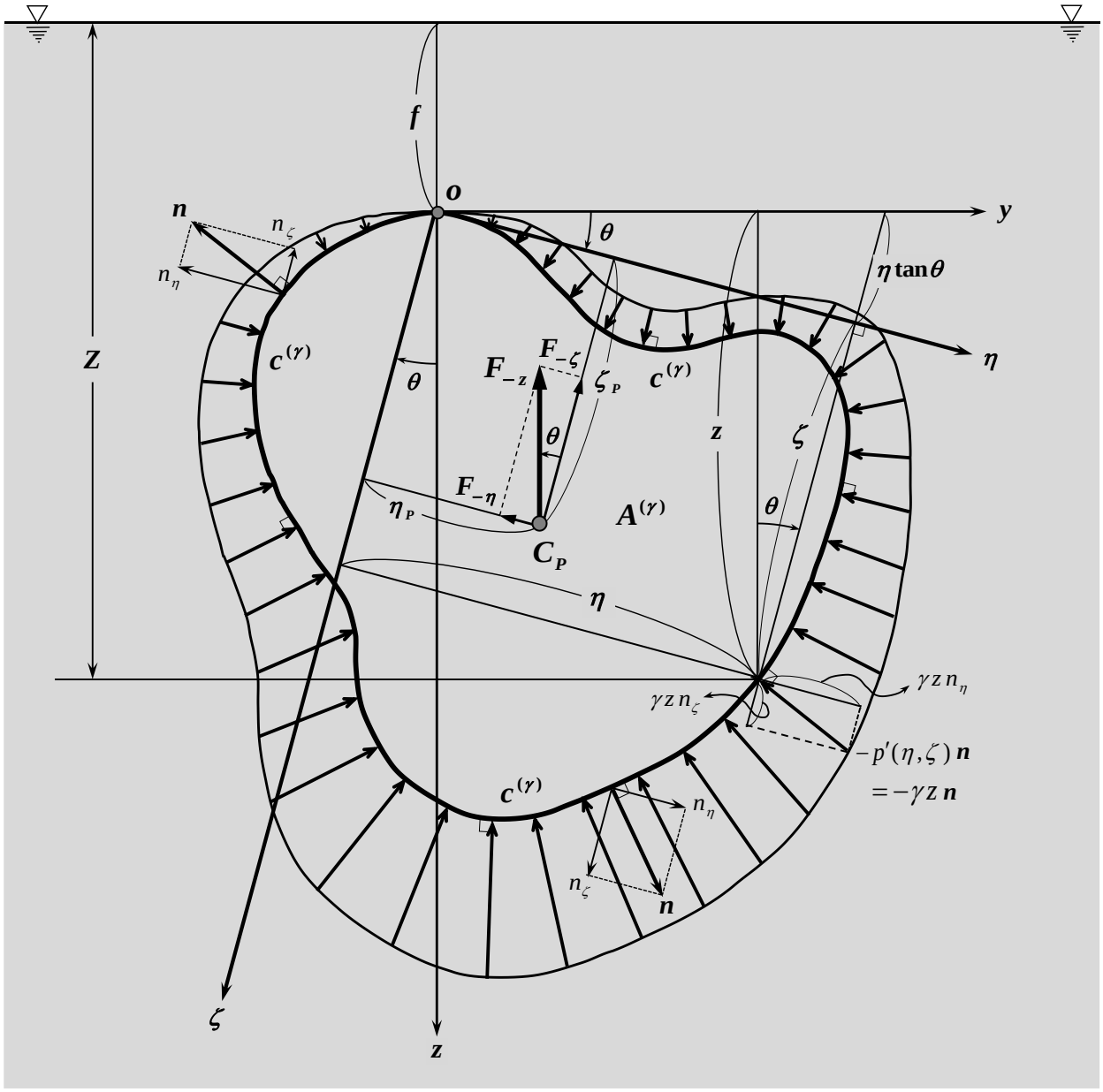

Fig. A.5.1 Hydrostatic pressure $p' = p - (p_0 + \gamma f)$ and the center of pressure C_P acting on the cross-section of an inclined submerged body with arbitrary shape.

$$\begin{aligned} \boldsymbol{F} &= -\oint_{c^{(\gamma)}} p(\eta,\zeta)\,\boldsymbol{n}\,d\ell \\ &= F_{-\eta}(-\boldsymbol{j}) + F_{-\zeta}(-\boldsymbol{k}) \end{aligned} \qquad \cdots\cdots (A.5.5)$$

The $-\eta$ directional component $F_{-\eta}$ and the $-\zeta$ directional component $F_{-\zeta}$ of the above total force $\boldsymbol{F}$ can be obtained by integrating the $-\eta$ and $-\zeta$ components of the hydrostatic pressure $p(\eta,\zeta)$ in Eq. (A.5.2), as follows :

$$\left.\begin{aligned} F_{-\eta} &= \oint_{c^{(\gamma)}} p(\eta,\zeta)\,n_\eta\,d\ell \\ &= \oint_{c^{(\gamma)}} \left\{ p_0 + \gamma f + p'(\eta,\zeta) \right\} n_\eta\,d\ell \\ F_{-\zeta} &= \oint_{c^{(\gamma)}} p(\eta,\zeta)\,n_\zeta\,d\ell \\ &= \oint_{c^{(\gamma)}} \left\{ p_0 + \gamma f + p'(\eta,\zeta) \right\} n_\zeta\,d\ell \end{aligned}\right\} \qquad \cdots\cdots (A.5.6)$$

In proceeding with the calculation, the 3rd line of Eq. (A.5.3) is used for the relative pressure p' and the termwise integration is performed respectively. Then, $F_{-\eta}$ is calculated as :

$$\begin{aligned} F_{-\eta} &= \oint_{c^{(\gamma)}} \left\{ p_0 + \gamma f + \gamma(\zeta\cos\theta + \eta\sin\theta) \right\} n_\eta\,d\ell \\ &= \oint_{c^{(\gamma)}} (p_0 + \gamma f)\,n_\eta\,d\ell + \gamma\cos\theta \oint_{c^{(\gamma)}} \zeta\,n_\eta\,d\ell + \gamma\sin\theta \oint_{c^{(\gamma)}} \eta\,n_\eta\,d\ell \end{aligned} \qquad \cdots\cdots (A.5.7)$$

Similarly, $F_{-\zeta}$ is calculated as :

$$\begin{aligned} F_{-\zeta} &= \oint_{c^{(\gamma)}} \left\{ p_0 + \gamma f + \gamma(\eta\sin\theta + \zeta\cos\theta) \right\} n_\zeta\,d\ell \\ &= \oint_{c^{(\gamma)}} (p_0 + \gamma f)\,n_\zeta\,d\ell + \gamma\sin\theta \oint_{c^{(\gamma)}} \eta\,n_\zeta\,d\ell + \gamma\cos\theta \oint_{c^{(\gamma)}} \zeta\,n_\zeta\,d\ell \end{aligned} \qquad \cdots\cdots (A.5.8)$$

Let us now apply the following two-dimensional ($\eta\zeta$ -plane) Gauss's integral theorem to the above contour integral in order to convert the line integral into an areal integral, same as Section 1.3.1 for floating body.

$$\left.\begin{aligned} \oint_c u(\eta,\zeta)\,n_\eta\,d\ell &= \iint_A \frac{\partial u}{\partial \eta}\,dA \\ \oint_c v(\eta,\zeta)\,n_\zeta\,d\ell &= \iint_A \frac{\partial v}{\partial \zeta}\,dA \end{aligned}\right\} \qquad \cdots\cdots (A.5.9)$$

In the above theorem, n_η and n_ζ are the directional cosines of the outward unit normal vector $\boldsymbol{n}$ in η and ζ directions, as shown in Eq. (A.5.4) and Fig. A. 5. 1.

Then, $F_{-\eta}$ in Eq. (A.5.7) can be converted to an areal integral and written as :

$$\begin{aligned} F_{-\eta} &= \iint_{A^{(\gamma)}} \frac{\partial(p_0 + \gamma f)}{\partial \eta}\,dA + \gamma\cos\theta \iint_{A^{(\gamma)}} \frac{\partial \zeta}{\partial \eta}\,dA + \gamma\sin\theta \iint_{A^{(\gamma)}} \frac{\partial \eta}{\partial \eta}\,dA \\ &= \gamma\sin\theta \iint_{A^{(\gamma)}} dA = \gamma A^{(\gamma)} \sin\theta \end{aligned} \qquad \cdots\cdots (A.5.10)$$

Similarly, $F_{-\zeta}$ in Eq. (A.5.8) can be written as :

$$F_{-\zeta} = \iint_{A^{(\gamma)}} \frac{\partial(p_0+\gamma f)}{\partial \zeta} dA + \gamma \sin\theta \iint_{A^{(\gamma)}} \frac{\partial \eta}{\partial \zeta} dA + \gamma \cos\theta \iint_{A^{(\gamma)}} \frac{\partial \zeta}{\partial \zeta} dA$$
$$= \gamma \cos\theta \iint_{A^{(\gamma)}} dA = \gamma A^{(\gamma)} \cos\theta \qquad \cdots\cdots (A.5.11)$$

From the results above, it can be seen that both forces are determined by the cross-sectional area $A^{(\gamma)}$ of the submerged body and the lateral inclination angle θ , and do not depend on the atmospheric pressure p_0 and the submerged depth f . The reason is why the integrands of 1st and 2nd terms in 1st line of both Eqs. (A.5.10) and (A.5.11) become zero and vanished.

In addition, $F_{-\eta}$ and $F_{-\zeta}$ are obtained as $-\eta$ and $-\zeta$ directional components of the buoyancy $\gamma A^{(\gamma)}$, as shown by F_{-z} of Eq. (A.5.12) in the next section, respectively.

A.5.2 Forces F_{-y} and F_{-z} converted in the $-y$ and $-z$ directions

In this section, let us find the horizontal and vertical components of the force acting on the submerged body. By using $F_{-\eta}$ and $F_{-\zeta}$ obtained in Eqs. (A.5.10) and (A.5.11) in the previous section, the horizontal component F_{-y} in the $-y$ direction and the vertical component F_{-z} in the $-z$ direction are converted as follows :

$$\left.\begin{aligned} F_{-y} &= F_{-\eta}\cos\theta - F_{-\zeta}\sin\theta \\ &= \gamma A^{(\gamma)}(\sin\theta\cdot\cos\theta - \cos\theta\cdot\sin\theta) \\ &= 0 \\ F_{-z} &= F_{-\zeta}\cos\theta + F_{-\eta}\sin\theta \\ &= \gamma A^{(\gamma)}(\cos^2\theta + \sin^2\theta) \\ &= \gamma A^{(\gamma)} \ (= \mathit{Buoyant\ Force}) \end{aligned}\right\} \qquad \cdots\cdots (A.5.12)$$

The above results show that the horizontal component F_{-y} does not act as the combined force due to pressure integration, even when the pressure field is left-right asymmetric. The vertical component F_{-z} is the product of the specific weight γ of water and the cross-sectional area $A^{(\gamma)}$ of submerged body, and is the buoyant force itself generated vertically upward, as Archimedes' principle[(1)] teaches. This situation is similar to Eq. (A.4.13) for the submerged circular cylinder in Section A.4.2.

A.5.3 Moments M_η and M_ζ due to hydrostatic pressure in the η and ζ directions acting on the submerged body

In this section, we shall calculate the total counterclockwise moment M_o around the origin o due to hydrostatic pressure acting on the surface of the submerged body. It can be calculated by superimposing the clockwise moment M_η due to the pressure component in the $-\eta$ direction and the counterclockwise moment M_ζ due to in the $-\zeta$ direction, as follows :

$$M_o = -M_\eta + M_\zeta \quad \cdots\cdots (A.5.13)$$

Here, M_η and M_ζ can be calculated by multiplying the integrand in Eq. (A.5.6) by ζ or η as the lever of moment respectively, in the following form :

$$\left.\begin{aligned} M_\eta &= \oint_{c^{(\gamma)}} p(\eta,\zeta)\,\zeta\cdot n_\eta\, d\ell \\ &= \oint_{c^{(\gamma)}} \left\{ p_0 + \gamma f + p'(\eta,\zeta)\right\}\zeta\cdot n_\eta\, d\ell \\ M_\zeta &= \oint_{c^{(\gamma)}} p(\eta,\zeta)\,\eta\cdot n_\zeta\, d\ell \\ &= \oint_{c^{(\gamma)}} \left\{ p_0 + \gamma f + p'(\eta,\zeta)\right\}\eta\cdot n_\zeta\, d\ell \end{aligned}\right\} \quad \cdots\cdots (A.5.14)$$

Now, as in the case of forces $F_{-\eta}$ and $F_{-\zeta}$ in Eqs. (A.5.7) and (A.5.8), M_η can be expressed as the superposition of the contour integrals along $c^{(\gamma)}$ by using Eq. (A.5.3) for the relative pressure p', as follows :

$$\begin{aligned} M_\eta &= \oint_{c^{(\gamma)}} \left\{ p_0 + \gamma f + \gamma(\zeta\cos\theta + \eta\sin\theta)\right\}\zeta\, n_\eta\, d\ell \\ &= (p_0 + \gamma f)\oint_{c^{(\gamma)}} \zeta\, n_\eta\, d\ell + \gamma\cos\theta\oint_{c^{(\gamma)}} \zeta^2\, n_\eta\, d\ell + \gamma\sin\theta\oint_{c^{(\gamma)}} \eta\zeta\, n_\eta\, d\ell \end{aligned} \quad \cdots\cdots (A.5.15)$$

Similarly, M_ζ can be expressed as :

$$\begin{aligned} M_\zeta &= \oint_{c^{(\gamma)}} \left\{ p_0 + \gamma f + \gamma(\eta\sin\theta + \zeta\cos\theta)\right\}\eta\, n_\zeta\, d\ell \\ &= (p_0 + \gamma f)\oint_{c^{(\gamma)}} \eta\, n_\zeta\, d\ell + \gamma\sin\theta\oint_{c^{(\gamma)}} \eta^2\, n_\zeta\, d\ell + \gamma\cos\theta\oint_{c^{(\gamma)}} \zeta\,\eta\, n_\zeta\, d\ell \end{aligned} \quad \cdots\cdots (A.5.16)$$

Therefore, we can apply Gauss's integral theorem in Eq. (A.5.9) to the above contour integrals, as in the case of forces $F_{-\eta}$ and $F_{-\zeta}$ in Section A.5.1, and convert them into areal integrals.

Then, the clockwise moment M_η in Eq. (A.5.15) can be converted to an areal integral and written as follows, and is consequently obtained in proportion to the areal moment about the η-axis.

$$\begin{aligned} M_\eta &= (p_0 + \gamma f)\iint_{A^{(\gamma)}} \frac{\partial\zeta}{\partial\eta}\, dA + \gamma\cos\theta\iint_{A^{(\gamma)}} \frac{\partial\zeta^2}{\partial\eta}\, dA + \gamma\sin\theta\iint_{A^{(\gamma)}} \frac{\partial(\eta\zeta)}{\partial\eta}\, dA \\ &= \gamma\sin\theta\iint_{A^{(\gamma)}} \zeta\, dA \end{aligned} \quad \cdots\cdots (A.5.17)$$

On the other hand, the counterclockwise moment M_ζ in Eq. (A.5.16) can be written as follows, and is consequently obtained in proportion to the areal moment about the ζ-axis.

$$\begin{aligned} M_\zeta &= (p_0 + \gamma f)\iint_{A^{(\gamma)}} \frac{\partial\eta}{\partial\zeta}\, dA + \gamma\sin\theta\iint_{A^{(\gamma)}} \frac{\partial\eta^2}{\partial\zeta}\, dA + \gamma\cos\theta\iint_{A^{(\gamma)}} \frac{\partial(\zeta\eta)}{\partial\zeta}\, dA \\ &= \gamma\cos\theta\iint_{A^{(\gamma)}} \eta\, dA \end{aligned} \quad \cdots\cdots (A.5.18)$$

From the both results above, it can be found that both moments do not depend on the atmospheric

pressure p_0 and the submerged depth f, as in the case of forces $F_{-\eta}$ and $F_{-\zeta}$ in Eqs. (A.5.10) and (A.5.11). The reason is why the integrands of 1st and 2nd terms in 1st line of both Eqs. (A.5.17) and (A.5.18) become zero and vanished.

A. 5. 4 Positioning of the center of hydrostatic pressure C_P for the submerged body with an arbitrary shape

For the positioning of the center of pressure of the submerged body, we will use the hydraulic method by Ohgushi[9-a], as in the case of the submerged circular cylinder in the previous appendix A. 4.

Since the forces $F_{-\eta}$ and $F_{-\zeta}$ due to the hydrostatic pressure obtained in Section A. 5. 1 act on the center of pressure $C_P\,(\eta_P, \zeta_P)$, the clockwise moment M_η and the counterclockwise moment M_ζ due to the corresponding pressure obtained in Section A. 5. 3 can be expressed exactly same as Eq. (1.27) in Chapter 1, as follows :

$$\left.\begin{aligned} M_\eta &= F_{-\eta}\,\zeta_P \\ M_\zeta &= F_{-\zeta}\,\eta_P \end{aligned}\right\} \quad \cdots\cdots (A.5.19)$$

Then, the total counterclockwise moment M_o around the origin o in Eq. (A.5.13) can be calculated as :

$$M_o = -F_{-\eta}\,\zeta_P + F_{-\zeta}\,\eta_P \quad \cdots\cdots (A.5.20)$$

On the other hand, the moment M_{C_P} around the point C_P, at which $F_{-\eta}$ and $F_{-\zeta}$ act, is computed as follows, and becomes zero.

$$M_{C_P} = -F_{-\eta} \times 0 + F_{-\zeta} \times 0 = 0 \quad \cdots\cdots (A.5.21)$$

This correctly indicates that C_P is the center of hydrostatic pressure for the submerged body.

Therefore, the unknown coordinate (η_P, ζ_P) of this center of pressure C_P can be determined by Eq. (A.5.18). First, the η - coordinate, η_P, can be determined by using Eq. (A.5.11) for $F_{-\zeta}$ and Eq. (A.5.18) for M_ζ, as follows :

$$\begin{aligned} \eta_P &= \frac{M_\zeta}{F_{-\zeta}} = \frac{\gamma \cos\theta \iint_{A^{(\gamma)}} \eta\, dA}{\gamma A^{(\gamma)} \cos\theta} \\ &= \frac{1}{A^{(\gamma)}} \iint_{A^{(\gamma)}} \eta\, dA \;\; \left(= \eta_G\right) \end{aligned} \quad \cdots\cdots (A.5.22)$$

Next, the ζ - coordinate, ζ_P, can be determined by using Eq. (A.5.10) for $F_{-\eta}$ and Eq. (A.5.17) for M_η, as follows :

$$\begin{aligned} \zeta_P &= \frac{M_\eta}{F_{-\eta}} = \frac{\gamma \sin\theta \iint_{A^{(\gamma)}} \zeta\, dA}{\gamma A^{(\gamma)} \sin\theta} \\ &= \frac{1}{A^{(\gamma)}} \iint_{A^{(\gamma)}} \zeta\, dA \;\; \left(= \zeta_G\right) \end{aligned} \quad \cdots\cdots (A.5.23)$$

Appendices

A. 5 Positioning of the Center of Hydrostatic Pressure C_P Acting on the Submerged Body with Arbitrary Shape

As a result, since the η_P and ζ_P are obtained with the form in which the areal moment about the ζ- and η- axis is divided by the cross-sectional area $A^{(\gamma)}$ respectively, it can be seen that they are the η_G and ζ_G of the figure centroid position for submerged body geometrically. And, in the both equations, the specific weight γ of water and the heel angle θ have been cancelled out in the denominator and numerator respectively, so that the both results are independent of θ. Furthermore, the geometric shape of a submerged body does not change when it is laterally inclined, unlike the case of a floating body. Therefore, this shows that the center of pressure (η_P, ζ_P) of the submerged body in the inclined state always coincides with the centroid (η_G, ζ_G) of the cross-sectional area $A^{(\gamma)}$, *i.e.*, the well-known center of buoyancy, regardless of whether it is laterally inclined or not.

Considering the above, ζ_P of vertical component can be obtained by offsetting the zero factor $\sin\theta$ at the heel angle $\theta \to 0$ with the denominator and numerator, as shown in Eq. (A.5.23). Here, if we start the calculation as the upright state $\theta = 0$, both the denominator $F_{-\eta}$ and the numerator M_η are in equilibrium and become zero, so the fraction becomes indeterminate forms and ζ_P cannot be determined. This is the reason why we were able to determine the position of the center of pressure in the ζ direction as $\zeta_P = \zeta_G$ by inclining the submerged body laterally.

On the other hand, in the calculation of η_P in Eq. (A.5.22), even if the heel angle is $\theta = 0$ from the beginning, the denominator $F_{-\zeta}$ takes a finite value as the cosine component of the buoyancy. Therefore, the horizontal component η_P can be determined as $\eta_P = \eta_G$, if we start the calculation as the upright state.

These situations described above are exactly the same as in Eq. (A.4.21) of Section A. 4. 4 for the submerged circular cylinder.

As a final step, let's find the center of pressure in the upright state by setting the heel angle to $\theta \to 0$, in order to make this result clearer. Then, since the $\eta\zeta$- coordinates tilted and fixed on the submerged body coincide with the yz- coordinates fixed in space and the cross-sectional area $A^{(\gamma)}$ is invariant regardless of θ, the Eqs. (A.5.22) and (A.5.23) become as :

$$\left.\begin{aligned} (y_P,\ z_P) &= \left(\frac{1}{A^{(\gamma)}} \iint_{A^{(\gamma)}} y\, dA\ ,\ \frac{1}{A^{(\gamma)}} \iint_{A^{(\gamma)}} z\, dA \right) = (y_G,\ z_G) \\ \therefore\ C_P &= B \end{aligned}\right\} \cdots\cdots\cdots\cdots \text{(A.5.24)}$$

Therefore, this proves that the center of hydrostatic pressure C_P coincides with the well-known "Center of Buoyancy, B" for the submerged body.

A. 6 Movement of the Centroid of Whole Area when a Partial Area Moves

In Appendix A. 6, we derive a dynamical law that shows how the centroid of the whole area moves when a partial area moves.

Fig. A. 6. 1 shows the case that a square $\square ABDC$ (area A, centroid G) transforms into an isosceles triangle $\triangle CBE$ (area A, centroid G'), when a right triangle $\triangle ABC$ (gray-filled area a, centroid g) is rotated 90° counterclockwise around point C and moved to a right triangle $\triangle CDE$ (gray-filled area a, centroid g').

In this appendix, let's consider the distance and direction of movement of the centroid of the whole area, *i.e.*, from G of the square $\square ABDC$ to G' of the isosceles triangle $\triangle CBE$. The right triangle $\triangle CBD$ (white-filled area A-a, centroid o) in Fig. A. 6. 1 is a fixed and common area before and after the movement. Here, the centroid G of the whole area is located geometrically on the line segment $\overline{og}$ connecting the respective centroids o and g, and G' is located on the line segment $\overline{og'}$ connecting o and g'.

A. 6. 1 General theory

Firstly, we will develop the general theory without setting a specific area *etc.*.

For the square $\square ABDC$ before the move, the following equation holds from the equilibrium of the areal moments of a and A around point o, which is the centroid of a fixed triangle $\triangle CBD$.

$$\left.\begin{aligned} a \cdot \overline{og} &= A \cdot \overline{oG} \\ \rightarrow a \cdot \ell_g &= A \cdot \ell_G \end{aligned}\right\} \quad \cdots\cdots (A.6.1)$$

Here, for simplicity's sake, we have written $\overline{og} = \ell_g$, $\overline{oG} = \ell_G$. By the above equation, the following relation is obtained as :

$$\frac{\ell_G}{\ell_g} = \frac{a}{A} \quad \cdots\cdots (A.6.2)$$

Next, for the isosceles triangle $\triangle CBE$ after the move, the following equation holds from the equilibrium of the areal moments of a and A around the point o as well.

$$\left.\begin{aligned} a \cdot \overline{og'} &= A \cdot \overline{oG'} \\ \rightarrow a \cdot \ell'_g &= A \cdot \ell'_G \end{aligned}\right\} \quad \cdots\cdots (A.6.3)$$

Here, we have abbreviated $\overline{og'} = \ell'_g$, $\overline{oG'} = \ell'_G$ in the same way. By the above equation, the following relation is obtained as well.

$$\frac{\ell'_G}{\ell'_g} = \frac{a}{A} \quad \cdots\cdots (A.6.4)$$

Let us now consider the trapezoid $\square ABEC$, which combines three right triangles, two before and after the move and one fixed. By Eqs. (A.6.2) and (A.6.4), the following relationship can be easily derived as :

Appendices

A. 6 Movement of the centroid of whole area when a partial area moves

$$\frac{\ell_G}{\ell_g} = \frac{\ell'_G}{\ell'_g} \left(= \frac{a}{A} \right) \quad \cdots\cdots (A.6.5)$$

This indicates that the scale ratio on the left side of the two triangles, small $\triangle GoG'$ and large $\triangle gog'$, is equal to that on the right side. By transforming the above equation, we can obtain the relational equation as follows :

$$\frac{\ell_G}{\ell'_G} = \frac{\ell_g}{\ell'_g} \quad \cdots\cdots (A.6.6)$$

It shows that the ratio of the left side to the right side is the same in the two triangles, small $\triangle GoG'$ and large $\triangle gog'$. Furthermore, the apex angles of both small and large triangles are clearly common as follows :

$$\angle GoG' = \angle gog' \quad \cdots\cdots (A.6.7)$$

Therefore, according to Eqs. (A.6.6) and (A.6.7) above, we can see that both small and large triangles are similar as follows :

$$\triangle GoG' \backsim \triangle gog' \quad \cdots\cdots (A.6.8)$$

As a result of the above discussion, it can be seen that the ratio of $\overline{GG'}$ to $\overline{gg'}$, which corresponds to the base of both triangles, is also the same as that in Eq. (A.6.5), and the two are parallel. It can be written as follows :

$$\left.\begin{array}{l} \dfrac{\overline{GG'}}{\overline{gg'}} = \dfrac{a}{A} \ (<1) \ \rightarrow \ \therefore \overline{GG'} = \dfrac{a}{A} \cdot \overline{gg'} \\ \overline{GG'} \ /\!/ \ \overline{gg'} \end{array}\right\} \quad \cdots\cdots (A.6.9)$$

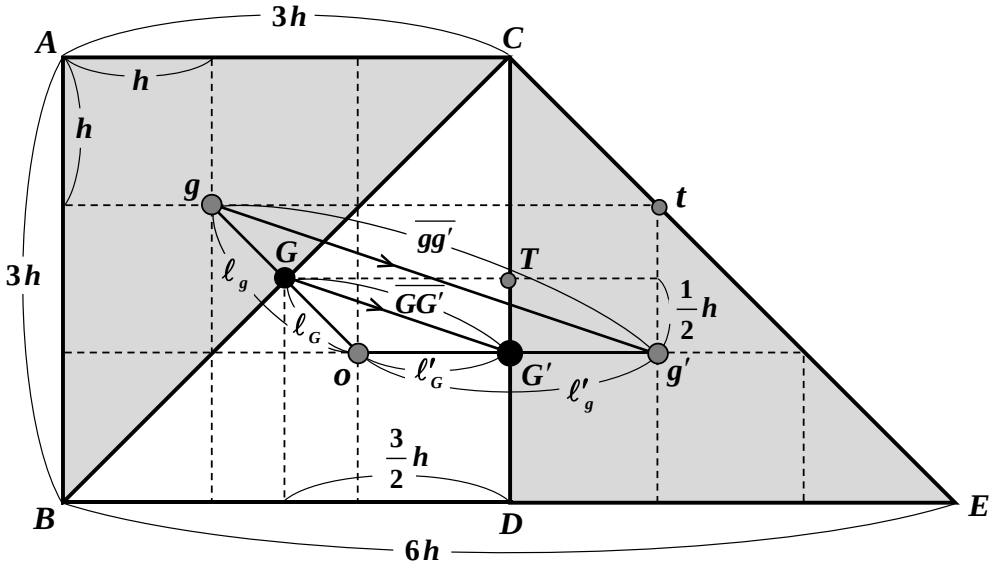

Fig. A. 6. 1 Movement of the centroid of whole area when a partial area moves.

The above equation is the law of dynamics as described in textbooks[(7-c),(8-b),(9-b),(12-b),(41),(42-a),(43)~(47)] on naval architecture and nautical mechanics. There is no restriction on the size of the area ratio a/A in the 1st line above, except that it is less than one. In this appendix, we have discussed the case where the area moves, which is the easiest to understand, but it can be applied by replacing a and A in the above Eq. (A.6.9) with v and V for volume and w and W for weight.

A. 6. 2 Numerical calculations for the verification of A. 6. 1

In this section, let's set numerical values for the area *etc.* and do some calculations. In that sense, the state of Fig. A. 6. 1 can be verified by the theory of Section A. 6. 1, because the position of the centroid G and G' before and after the move is geometrically known.

As shown in Fig. A. 6. 1, the square $\square ABDC$ has a side of $3h$ before the move and the isosceles triangle $\triangle CBE$ has a base of $6h$ and a height of $3h$ after the move, the two moving right triangles $\triangle ABC$ and $\triangle CDE$ have a base and a height of $3h$. Therefore, the whole area A, the moving area a and their ratio are written as follows :

$$\left.\begin{aligned} A &= 9h^2 \\ a &= \frac{9}{2}h^2 \end{aligned}\right\} \rightarrow \frac{a}{A} = \frac{1}{2} \qquad \cdots\cdots (\text{A.6.10})$$

Now, since the distance and direction of the movement $\overline{GG'}$ of centroid of the whole area A due to the movement $\overline{gg'}$ of a partial area a are determined by Eq. (A.6.9), we will consider the moving distance by breaking it down into its horizontal and vertical components.

As shown in Fig. A. 6. 1, each component in the moving distance $\overline{gg'}$ of centroid of a partial area a is geometrically measured via point t, as follows :

$$\left.\begin{aligned} &\textit{Horizontal} : \overline{gt} = 3h \\ &\textit{Vertical} \quad : \overline{tg'} = h \end{aligned}\right\} \qquad \cdots\cdots (\text{A.6.11})$$

Here, by the 2nd line of Eq. (A.6.9), line segments $\overline{GG'}$ and $\overline{gg'}$ are parallel, so if we place point T corresponding to point t, both right triangles $\Delta GTG'$ and $\Delta gtg'$ are similar as follows :

$$\Delta GTG' \backsim \Delta gtg' \qquad \cdots\cdots (\text{A.6.12})$$

Therefore, the moving distance $\overline{GG'}$ of centroid of the whole area A can be determined for horizontal and vertical direction via point T respectively, by adopting the value of Eqs. (A.6.10) and (A.6.11) into the 1st line of Eq. (A.6.9), as follows :

$$\left.\begin{aligned} &\textit{Horizontal} : \overline{GT} = \frac{1}{2}\overline{gt} = \frac{3}{2}h \\ &\textit{Vertical} \quad : \overline{TG'} = \frac{1}{2}\overline{tg'} = \frac{1}{2}h \end{aligned}\right\} \qquad \cdots\cdots (\text{A.6.13})$$

Then, the result of the above equation places the point G' at one-third of the height $\overline{DC}$ of the isosceles triangle $\triangle CBE$, and just above the midpoint D of the base $\overline{BE}$. This point G' is correctly the centroid of the isosceles triangle $\triangle CBE$. Since this fact is consistent with what geometry teaches, we were able to verify that Eq. (A.6.9), which is derived in the general theory of Section A.6.1, is correct.

A. 7 Lecture Videos Uploaded to YouTube on the Hydrostatics of Floating Bodies

In Appendix A. 7, we present seven lecture videos uploaded to YouTube on *the New Developments in the Fundamental Theory for Hydrostatics of Floating Bodies*.

The content of Chapter 1, which proves that "Center of Buoyancy = Center of Pressure" by inclining a floating body with rectangular cross-section laterally, is lectured to 2nd year students of the naval architectural engineering course[53),54)] in the "*Hydrostatics of Floating Bodies*" of the university where the 1st author[52)] works.

And the content of Chapter 2, in which a new derivation process for metacentric radius $\overline{BM}$ is developed, is lectured to 2nd year students of the same course as a subject of "*Hydrostatics of Floating Bodies*" at the same university.

With the recent trend of remote lectures, the situation of the two cntents above is filmed in two parts, the 1st half[66),68)] and the 2nd half[67),69)] respectively, and on-demand teaching materials are created and uploaded as four YouTube videos.

Furthermore, one of the authors[52)] teaches the theory of ship's hydrostatic stability, which is developed in Chapter 3, to 2nd year students of the above course in a lecture entitled "*Theory of Ship Stability*" at the author's university[53),54)]. We have also uploaded the three recorded videos of the lecture to YouTube as on-demand materials, following the same trend as above.

The 1st video[70)] is a theory for determining the condition of breadth β for a columnar ship with a rectangular cross-section, whose specific weight is half that of water $\alpha = \frac{1}{2}$, to float stably in an upright position, which is explained in Section 3. 3. 1 of Chapter 3.

The 2nd video[80)] shows that the above theory was confirmed experimentally in a small water tank for the inquiry learning online of high school students.

The 3rd video[71)] explains that a theory for determining the conditions of specific weight α (*i.e.* lightness or heaviness of the material) for a columnar ship with square cross-section $\beta = 1$, to float stably in an upright position, which is described in Section 3. 3. 2 of the same Chapter 3.

The above seven lecture videos are explained in Japanese, but if you are interested, please have a look.